รายงานฉบับสมบูรณ์

โครงการ **การศึกษาโครงสร้างและหน้าที่ของโปรตีนสารพิษฆ่าลูกน้ำยุงจากแบคทีเรีย *Bacillus sphaericus***

Elucidating the structure and function of the binary toxin from *Bacillus sphaericus*

โดย

ผู้ช่วยศาสตราจารย์ ดร.ปนัดดา บุญเสริม

มิถุนายน 2556

สัญญาเลขที่ RMU5380002

รายงานฉบับสมบูรณ์

โครงการ **การศึกษาโครงสร้างและหน้าที่ของโปรตีนสารพิษฆ่าลูกน้ำยุงจากแบคทีเรีย *Bacillus sphaericus***

Elucidating the structure and function of the binary toxin from *Bacillus sphaericus*

ผู้วิจัย

ผศ.ดร.ปนัดดา บุญเสริม

สังกัด

สถาบันชีววิทยาศาสตร์โมเลกุล

มหาวิทยาลัยมหิดล

สนับสนุนโดยสำนักงานคณะกรรมการการอุดมศึกษา

และสำนักงานกองทุนสนับสนุนการวิจัย

Acknowledgements

This work was supported the Thailand Research Fund, the Commission on Higher Education, Thailand, the Mahidol University Research Grant and the National Center for Genetic Engineering and Biotechnology, National Science and Technology Development Agency, Thailand. We are also grateful to Ms. Chanikarn Boonchoy and Ms. Monruedee Srisaisup for technical assistance.

บทคัดย่อ

รหัสโครงการ RMU5380002

ชื่อโครงการ การศึกษาโครงสร้างและหน้าที่ของโปรตีนสารพิษฆ่าลูกน้ำยุงจากแบคทีเรีย *Bacillus sphaericus*

ชื่อนักวิจัย ผู้ช่วยศาสตราจารย์ปนัดดา บุญเสริม
สถาบันชีววิทยาศาสตร์โมเลกุล มหาวิทยาลัยมหิดล

E-mail Address panadda.boo@mahidol.ac.th

ระยะเวลาโครงการ 3 ปี

แบคทีเรีย *Bacillus sphaericus* สร้างโปรตีน binary toxin ที่ประกอบด้วยโปรตีน BinA และ BinB ที่มีขนาด 42 และ 51 กิโลดาลตันตามลำดับ โปรตีนทั้งสองนี้ต้องทำงานร่วมกันในการออกฤทธิ์ฆ่าลูกน้ำยุง โดย BinB ทำหน้าที่จับกับตัวรับจำเพาะบนเยื่อหุ้มเซลล์ และ BinA ทำหน้าที่ทำลายเซลล์ อย่างไรก็ตามกลไกการทำงานของโปรตีน binary toxin ในระดับโมเลกุลยังไม่เป็นที่เข้าใจลึกซึ้ง เนื่องจากยังขาดข้อมูลเชิงโครงสร้างของโปรตีน ในช่วงที่ยังไม่มีข้อมูลโครงสร้างของโปรตีน เราได้ทำการศึกษากลไกการทำงานของโปรตีน BinB โดยเฉพาะอย่างยิ่งทางด้านปลายอะมิโน โดยทำการเปลี่ยนแปลงลำดับกรดอะมิโนในช่วง 35-37 และ 41-43 ผลการทดสอบการฆ่าลูกน้ำยุงรำคาญ การจับกับตัวรับจำเพาะ และการทำลายเยื่อหุ้มเซลล์จำลองพบว่า กรดอะมิโนตำแหน่ง P35, F41 และ Y42 มีความสำคัญต่อกลไกการฆ่าลูกน้ำยุง โดยเฉพาะอย่างยิ่งในขั้นตอนการจับกับตัวรับจำเพาะ และการทำลายเยื่อหุ้มเซลล์ นอกจากนี้เราได้ศึกษาการทำงานของโปรตีน BinA โดยเฉพาะในกลไกการเกิดปฏิสัมพันธ์ระหว่างกรดอะมิโนชนิดอะโรมาติกกับเยื่อหุ้มเซลล์ โดยการแทนที่กรดอะมิโนชนิดอะโรมาติกในตำแหน่ง Y213, Y214, Y215, W222 และ W226 ด้วยกรดอะมิโนลิวซีน ผลการทดลองพบว่าโปรตีนกลายพันธุ์ดังกล่าวมีความสามารถในการรบกวนเยื่อหุ้มเซลล์จำลองได้เช่นเดียวกับโปรตีนต้นแบบ และผลการศึกษาการแทรกตัวเข้าสู่ชั้นไขมันที่สร้างเป็นแผ่นฟิล์มชั้นเดียว (monolayer) โดยอาศัยวิธี Langmuir–Blodgett trough พบว่าโปรตีนกลายพันธุ์ทั้งหมดสามารถแทรกตัวในชั้นไขมันได้เช่นเดียวกับโปรตีนต้นแบบ แต่จากการทดสอบการออกฤทธิ์ฆ่าลูกน้ำยุงพบว่าประสิทธิภาพในการฆ่าลูกน้ำยุงรำคาญของโปรตีนกลายพันธุ์ W222L W226L ลดลงอย่างชัดเจน ซึ่งประสิทธิภาพในการฆ่าลูกน้ำยุงที่ลดลงนี้ อาจเกี่ยวข้องกับกลไกการทำงานในกระบวนการอื่นๆที่เกิดขึ้นภายในเซลล์ของลูกน้ำยุง

เพื่อเข้าใจกลไกการทำงานของโปรตีน binary toxin ในเชิงลึกถึงระดับโมเลกุลมากยิ่งขึ้น เราได้ศึกษาโครงสร้างสามมิติของโปรตีน binary toxin โดยใช้เทคนิค X-ray crystallography ผลการศึกษาพบว่าโปรตีนชนิด BinB สามารถตกผลึกได้และกระเจิงรังสีเอ็กซ์ได้ถึงระดับความละเอียดที่ 1.75 อังสตรอม หลังจากนั้นได้นำเทคนิค Single-wavelength anomalous dispersion (SAD) มาใช้วิเคราะห์โครงสร้างสามมิติของโปรตีน BinB พบว่าโครงสร้างสามมิติของ BinB ประกอบไปด้วยสองส่วนที่แตกต่างกัน คือทางด้านปลายอะมิโนมีโครงสร้างคล้ายกับโปรตีนที่จับกับน้ำตาล หรือ lectin ส่วนทางด้านปลายคาร์บอกซิลมีรูปร่างยาวและมีโครงสร้างหลักเป็น β-strands ซึ่งมีลักษณะคล้ายกับโปรตีนสร้างรูรั่วชนิด aerolysin จากข้อมูลเบื้องต้นของโครงสร้างสามมิติของ BinB แสดงให้เห็นว่าโปรตีน BinB ทำหน้าที่จับกับกับตัวรับจำเพาะ และอาจช่วยส่งผ่านโปรตีน BinA หรือ BinA-BinB complex เข้าสู่เซลล์และทำลายเซลล์ต่อไป

Abstract

Project Code: RMU5380002

Project Title: Elucidating the structure and function of the binary toxin from *Bacillus sphaericus*

Investigator: Assistant Professor Panadda Boonserm
Institute of Molecular Biosciences, Mahidol University

E-mail Address: panadda.boo@mahidol.ac.th

Project Period: 3 years

The binary toxin produced from *Bacillus sphaericus* is highly toxic against mosquito larvae. The two major components of the binary toxin are 42-kDa BinA and 51-kDa BinB. BinA is proposed to function as a toxic subunit, whereas BinB is responsible for receptor binding. So far, there is no detailed knowledge of the molecular mechanism of the binary toxin, mainly due to the lack of structural information. In the absence of the structural information, we investigated the role of amino acids at the N-terminal region of BinB in governing the larvicidal activity via amino acid substitutions at residues spanning positions 35-37 and 41-43. Bioassays, receptor and membrane binding analyses demonstrated that residues P35, F41 and Y42 of BinB are crucial for the larvicidal activity, especially during the steps of membrane and receptor binding. In order to identify functional sites of BinA, aromatic cluster in BinA at positions Y213, Y214, Y215, W222 and W226 were substituted by leucine. All mutants were able to insert into lipid monolayers as observed by Langmuir–Blodgett trough and could permeabilize the liposomes in a similar manner as the wild type. However, mosquito-larvicidal activity was abolished for W222L and W226L mutants suggesting that tryptophan residues at both positions play an important role in the toxicity of BinA, possibly involved in the cytopathological process after toxin entry into the cells.

In order to gain more insight into the molecular mechanism of the binary toxin, the X-ray crystallographic analysis was performed. Only the crystal of activated BinB could diffract to 1.75 Å resolution. The structure of activated BinB has been determined by single-wavelength anomalous dispersion (SAD) method. The structure of activated BinB is composed of two domains: an N-terminal β-trefoil lectin-like domain and an elongated C-terminal domain. The N-terminal domain shares similar features to the sugar binding proteins or lectins. The C-terminal domain resembles the pore-forming domain of the aerolysin-type β-pore forming toxins. Taken together, the crystal structure of the BinB subunit confirms the important role of BinB for receptor binding and possibly facilitating the internalization of the BinA or BinA-BinB complex into the cells to exert its cytotoxicity. However, the functional detail of BinB protein requires further elucidation.

Keywords: binary toxin, immunohistochemistry, receptor binding, site-directed mutagenesis, larvicidal activity, X-ray crystallography

1. Introduction

Bacillus sphaericus (Bs) is a Gram-positive, spore-forming aerobic bacterium (Charles, et al., 1996). During the sporulation phase, a number of highly toxic strains of Bs synthesize a binary toxin which is a crystalline mosquito-larvicidal protein composed of 42 kDa (BinA) and 51 kDa (BinB) subunits. The larvicidal activity against *Culex* and *Anopheles* mosquito larvae is dependent on the presence of both BinA and BinB subunits (Oei, et al., 1990, Baumann, et al., 1991, Nicolas, et al., 1993). This toxin, however, is weakly toxic or non-toxic to *Aedes* larvae (Berry, et al., 1993).

Upon larval ingestion of protein inclusions, crystalline inclusions are dissolved in alkaline conditions of the larval midgut. Thereafter, BinA and BinB protoxins are activated by midgut proteases to generate the active proteins of approximately 39 and 43 kDa, respectively (Broadwell & Baumann, 1987, Nicolas, et al., 1990). The activated binary toxin, especially the BinB component, then binds to a specific receptor located on the surface of midgut epithelium cell of susceptible larvae (Davidson, 1988, Silva-Filha, et al., 1997). The binary toxin receptor has been identified as 60-kDa α-glucosidase (Cpm1) which is attached to the cell membrane via a glycosyl-phosphatidyl inositol (GPI) anchor (Silva-Filha, et al., 1999, Darboux, et al., 2001). Nevertheless, detailed mechanism of action of the binary toxin remains elusive, mainly due to the lack of the structural information. Analysis of the amino acid sequences of BinA and BinB reveals a negligible level of similarity with any protein with established crystal structure, however, they are homologous to each other, with a 25% amino acid identity and a 40% similarity (Promdonkoy, et al., 2008). Despite their similarity, these two proteins have distinct functions, i.e., BinB is responsible for receptor binding, whereas BinA presumably acts as a toxic component (Oei, et al., 1992, Charles, et al., 1997, Shanmugavelu, et al., 1998, Elangovan, et al., 2000).

The binary toxin genes have been cloned and expressed in several host cells such as *Escherichai coli*, *Bacillus thuringiensis* and *Bacillus subtilis* (Baumann & Baumann, 1989, Bourgouin, et al., 1990, Promdonkoy, et al., 2003, Promdonkoy, et al., 2008), however, in most cases their expressed proteins are accumulated in inclusion bodies. Consequently, several subsequent steps of protein preparation, i.e., inclusion solubilization in highly alkaline condition, dialysis against a normal alkaline buffer, and soluble protein purification are required for further structural and functional analyses. Moreover, both binary toxin components tend to be easily

degraded and form large oligomer in solution after being solubilized in alkaline condition (Baumann, et al., 1985, Promdonkoy, et al., 2008), causing the difficulty in achieving the high protein purity and homogeneity for structural studies.

Although the structural basis of the binary toxin is unavailable, some amino acids residues have been subjected to mutagenesis to investigate their roles on the mosquitocidal activity. In addition, the deletions of some amino acids at the N- and C-terminal ends of the BinA and BinB proteins abolished the toxicity. The effects of these deletions on the biological activity of the binary toxin are not completely understood. In particular, BinB has been shown to confer the specificity by binding to a specific receptor. However, its binding mechanism is still unknown. Earlier studies with the binary toxin suggested that the N-terminal region of BinB is crucial for receptor binding in gut epithelial cells (Oei, et al., 1992). Consistent with the above data, recent studies showed that multiple elements within the N-terminal half of BinB are required for the receptor binding (Romao, et al., 2011, Tangsongcharoen, et al., 2011). Nevertheless, the C-terminal half of BinB, as well as its N-terminal half, also has been shown to participate in the larval gut membrane binding (Tangsongcharoen, et al., 2011). Examination of the toxin deletion derivatives BinB revealed that 34 amino acids could be removed from the N-terminus without affecting the toxicity and regional binding to the larval gut. However, a further deletion of 41 amino acids from the N-terminal region rendered the toxin inactive (Clark & Baumann, 1990). Moreover, replacements of amino acids located at the N-terminus of BinB revealed the crucial importance of residues $_{32}$YNL$_{34}$ and $_{38}$SKK$_{40}$ for the toxicity (Elangovan, et al., 2000). On the basis of the deletion and mutagenic data described earlier, it is conceivable that amino acids at positions around 30-40 in the N-terminal region of BinB may play an important role, either structurally or functionally, for the toxicity of the binary toxin.

Since the interaction of the binary toxin with target lipid membrane is one of the key steps in eliciting cytopathological effects on mosquito larvae, molecular insights into the interaction of the binary toxin with lipid membranes is required to gain a better understanding of the mechanism of toxicity. The binary toxin has been shown to induce channel and pore formation in cultured *C. quinquefasciatus* cells and in a mammalian epithelial cell line (MDCK) expressing the binary toxin Cpm1 receptor (Cokmus, et al., 1997, Pauchet, et al., 2005). The ability of the binary toxin to insert into receptor-free lipid membranes and permeabilize phospholipid vesicles has also been reported (Schwartz, et al., 2001, Boonserm, et al., 2006,

Kunthic, et al., 2011). Moreover, several cytopathological alterations were observed on intoxicated *C. quinquefasciatus* larvae including the formation of cytoplasm vacuoles, mitochondria swelling, and microvilli destruction (Silva-Filha & Peixoto, 2003). The above evidence seems to indicate a complex mechanism for binary toxin activity.

In this study, we have investigated the role of amino acids at the N-terminal region of BinB in governing the larvicidal activity by performing amino acid substitutions at residues spanning positions 35-37 and 41-43. Bioassays, receptor and membrane binding analyses demonstrated that residues P35, F41 and Y42 of BinB are crucial for the larvicidal activity, especially during the steps of membrane and receptor binding. Besides, aromatic residues, particularly tyrosine and tryptophan of BinA were selected for site-directed mutagenesis in search of crucial residues for the membrane interaction and biological activity. Within this region, tryptophan residues at positions 222 and 226 are found to have functional significance towards *C. quinquefasciatus* larvae. To facilitate the structural analysis of the binary toxin components, we expressed the individual BinA and BinB proteins with a hexahistidine tag at their N-termini and modified the conditions to express them as the soluble proteins. These recombinant soluble proteins, when fed together to *Culex quinquefasciatus* mosquito larvae, confer high larvicidal activity, indicating that their active-protein conformations are maintained. We also report the crystallization and X-ray crystallographic analysis of the functional form of BinB protein. This structural data is tremendously useful by providing insights into the structure-function correlation and guidelines for engineering the protein in the future.

2. Materials and Methods

2.1 Bacterial strains, plasmids, and oligonucleotides

The binary toxin genes, *binA* and *binB*, were isolated from *Bacillus sphaericus* strain 2297 as previously described (Promdonkoy, et al., 2003, Promdonkoy, et al., 2008). The plasmid pRSET C (Invitrogen) was used as a cloning vector for *binA* gene, whereas the plasmid pET-28b (+) (Novagen) was used as a cloning vector for *binB* gene. Both plasmids contain the N-terminal tag coding sequences. *Escherichia coli* K-12 JM109 and *E. coli* BL21 (DE3) pLysS (Novagen, USA) were used as host strains for mutagenesis and for protein expression of the recombinant plasmids, respectively. A recombinant plasmid pGEX-BinA encoding the GST-BinA fusion protein was used as a template for BinA mutagenesis, while a recombinant plasmid pET-tbinB expressing the truncated BinB as previously described (Boonyos, et al., 2010) was used as a template for BinB mutagenesis. Mutagenic oligonucleotide primers were purchased from Sigma Proligo (Singapore). Each primer was designed to introduce or abolish a restriction endonuclease recognition site in order to differentiate between the wild-type and mutant plasmids (Table 1).

2.2 Construction of BinA and BinB mutant plasmids

All mutant plasmids were generated based on polymerase chain reaction using a high fidelity *Pfu* DNA polymerase following the procedure of the QuikChange™ site-directed mutagenesis method (Stratagene). PCR products were treated with *Dpn*I to get rid of the DNA templates and then transformed into *E. coli* JM109 competent cells. The recombinant plasmids were extracted and the desired mutations were selected by restriction endonuclease digestion, and further confirmed by automated DNA sequencing at Macrogen Inc, Korea.

Table 1. Oligonucleotide primers for generation of BinA and BinB mutants

Primer	Sequence (5´-3´)	Enzyme
BinA Mutants		
Y213Lf	AAAACGACT**CCGCTC**TATTATGTAAAGCAC	*Bsr*BI
Y213Lr	CTTTACATAATA**GAGCGG**AGTCGTTTTCAT	
Y214Lf	CGACTCCATAT**CTGTACGTA**AAGCACACTC	*Sna*BI
Y214Lr	TGTGCTTTAC**G**TA**CAG**ATATGGAGTCGTTT	
Y215Lf	ACTCCATATTA**CCTG**GTAAAGCACACTCAA	*Bst*NI
Y215Lr	AGTGTGCTTTAC**CAGG**TAATATGGAGTCGT	
W222Lf	CACACTCA**ATATCT**GCAAAGCATGTGGTCC	*Ssp*I
W222Lr	CCACATGCTTTGC**AGATAT**TGAGTGTGCTT	
W226Lf	TGGCAAA**GCATGC**TGTCCGCGCTCTTTCCA	*Sph*I
W226Lr	AAAGAGCGCGGACA**GCATGC**TTTGCCAATA	
BinB Mutants		
35PEI37f	TAGCAACCTT**G**CGG**CCG**CATCAAAAAAATTTTATA	*Eae*I
35PEI37r	AAAATTTTTTTGAT**GCGG**CCG**C**AAGGTTGCTAGCC	
41FYN43f	TATCAAAAAAA**GCAGCTGC**CCTTAAGAATAAATAT	*Pvu*II
41FYN43r	ATTCTTAAGG**GCAGCTGC**TTTTTTTGATATTTCTG	
P35Af	GCTAGCAACCT**GGCCG**AAATATCAAAAAAA	*Cfr*I
P35Ar	TTTTTTGATATTTC**GGCCA**GGTTGCTAGCC	
E36Af	AGCAACCTTCC**GGCCA**TATCAAAAAAATTT	*Cfr*I
E36Ar	ATTTTTTTGATAT**GGCCG**GAAGGTTGCTAG	
I37Af	AACCTTCCAGAA**GCTT**CAAAAAAATTTTAT	*Hind*III
I37Ar	TAAAATTTTTTTGA**AGCTT**CTGGAAGGTTG	
F41Af	ATATCAAAAAA**GGCCT**ATAACCTTAAGAAT	*Stu*I
F41Ar	CCTAAGGTTAT**AGGCCT**TTTTTGATATTTC	
Y42Af	TCAAAAAAATT**CGCGA**ACCTTAAGAATAAA	*Nru*I
Y42Ar	TCTTAAGGT**TCGCGA**ATTTTTTTGATATTT	
N43Af	ATATCAAAAAAA**TTTTA**TGCCCTTAAGAAT	-
N43Ar	CTTAAGGGC**ATAAA**ATTTTTTTGATATTTC	

*Recognition sites introduced in the primers for restriction endonuclease analysis are underlined. Mutated nucleotides are shown in bold; f and r represent forward and reverse primers, respectively.

2.3 Protein preparation

To express the BinB or its mutant proteins, the *E. coli* JM109 containing pET-tbinB wild type or its mutants was re-transformed into *E. coli* BL21(DE3) pLysS and grown at 37 ºC in a Luria-Bertani medium containing ampicillin 100 µg/ml and chloramphenicol 34 µg/ml until OD_{600} of the culture reached 0.4. For the BinA protein or its mutants, the *E. coli* JM109 harbouring GST-BinA wild type and its mutants were grown in LB broth containing 100 µg/ml ampicillin at 37 °C until OD_{600} of the culture reached 0.5. Then 0.1 mM isopropyl-β-D-

thiogalactopyranoside (IPTG) was added to induce protein expression. Cell cultures were then induced with 0.1 mM isopropyl-β-D-thiogalactopyranoside (IPTG) and further incubated at 37 ºC for 5 h. Cells were collected by centrifugation and then lysed using a French Pressure Cell. Protein inclusions were collected after centrifugation and partially purified using differential centrifugation as described previously (Singkhamanan, et al., 2010). The identity of mutant proteins were further confirmed by Western-blot analysis using polyclonal anti-BinA or anti-BinB as described previously (Singkhamanan, et al., 2010).

Protein inclusions at a concentration about 2-3 mg/ml were solubilized in 25 mM NaOH, 5 mM DTT at 37 ºC for 15 min. Solubilized protein was subjected to stepwise dialysis against 50 mM Na_2CO_3, pH 10.0 at 4 ºC overnight and further purified by gel filtration using a superdex 200HR 10/300 column (Amersham Pharmacia Biotech). Protein concentration was determined by the method of Bradford using Bio-Rad protein assay reagent with bovine serum albumin as a standard.

2.4 Construction of recombinant plasmids to express histidine-tagged BinA and BinB proteins

The *binA* and *binB* genes were separately cloned in-frame with the hexahistidine tags at their 5′ ends. The genes encoding BinA and BinB were amplified by polymerase chain reaction from the recombinant plasmid pET42f and pET51f, respectively (Promdonkoy, et al., 2003, Promdonkoy, et al., 2008). The forward and reverse primers for *binA* amplification were 5′-CCG TGG ATC CGA AAT TTG GAT TTT ATT GAT TCT-3′ and 5′-GCG AAG CTT TTA GTT TTG ATC ATC TGT AAT AAT-3′, respectively. The forward and reverse primers for *binB* amplification were 5′-GCG CCA TAT GTG CGA TTC AAA AGA CAA TTT C-3′ and 5′-GCG CGG ATC CTC ACT GGT TAA TTT TAG GTA ATT C-3′, respectively (BioDesign, Thailand). The PCR product of *binA* gene was digested with *Bam*HI and *Hind*III and ligated in-frame into pRSET C vector between the same restriction sites to create the recombinant vector pRSETC-BinA with a hexahistidine tag at the 5′ end of the cloned gene. While, the PCR product of *binB* gene was digested with *Nde*I and *Bam*HI and ligated in-frame into pET28b (+) vector between the same restriction sites to create the recombinant vector pET28b-BinB with a hexahistidine tag at the 5′ end of the cloned gene.

2.5 Histidine-tagged BinA and BinB protein expression and purification

E.coli BL21(DE3)pLysS cells harboring pRSETC-BinA or pET28b-BinB were grown in Luria-Bertani (LB) medium containing appropriate antibiotics (100 µg/ml ampicillin and 34 µg/ml chloramphenicol for BinA and 50 µg/ml kanamycin and 34 µg/ml chloramphenicol for BinB). The culture cells were induced with 0.2 mM isopropyl β-D thiogalactopyranoside (IPTG) when OD_{600} reached 0.7 and further grown at 18°C for five hours. The culture cells were harvested by centrifugation at 7000g for 10 minutes. The cell pellets were suspended in buffer A (50 mM Tris-HCl pH8.0 and 200 mM NaCl), and subsequently subjected to ultra-sonication to completely break the cells. Crude extracts were separated by centrifugation in order to collect supernatant containing the expressed $(His)_6$-tagged BinA and $(His)_6$-tagged BinB for further purification step. The supernatant fraction was loaded into a HiTrap™ Chelating HP 5-ml column prepacked with a precharged Ni^{2+} (GE Healthcare Life Sciences) that had been pre-equilibrated with buffer A. Non-specific bound proteins were washed twice with buffer A containing 25 mM imidazole and 50 mM imidazole, respectively. The bound $(His)_6$-tagged BinA was eluted with buffer A containing 100 mM imidazole, whereas the bound $(His)_6$- tagged-BinB was eluted with buffer A containing 250 mM imidazole. The protein-containing fractions were pooled and concentrated by ultrafiltration at 4 ^{o}C using a Centriprep column (30-kDa cutoff, Amicon), followed by applying the concentrated fraction into a Superdex 200 HR 10/30 column (GE Healthcare Life Sciences) which was equilibrated with 50 mM Tris-HCl pH 9.0 and 1mM DTT. The BinA and BinB proteins eluted from the size exclusion column were examined their molecular sizes and homogeneity by comparing with standard proteins (gel filtration LMW calibration kit, GE Healthcare Life Sciences).

2.6 Trypsin activation of BinA and BinB

Purified BinA and BinB recombinant protoxins were mixed with trypsin (L-1-tosylamide-2-phenylethyl chloromethyl ketone treated, Sigma) at a trypsin:protoxin ratio of 1:20 (w/w) and incubated at 37 ^{o}C for 2 hours. The proteolytic reaction was stopped by adding 10 mM Phenylmathylsulfonyl fluoride (PMSF, Sigma). Trypsin-activated BinA (40 kDa) and BinB (45 kDa) were purified by size exclusion chromatography using the Superdex 200 HR 10/30 column,

which was equilibrated with 50 mM Tris-HCl pH 9.0 and 1mM DTT. Eluted fractions were concentrated by ultrafiltration as described above.

2.7 Secondary structure analysis

The secondary structures of the recombinant BinA and BinB, both protoxins and activated forms, were determined by using a Jasco J-715 CD spectropolarimeter (Jasco Inc., USA). The purified protein of 1 mg/ml in a quartz cuvette (0.2 mm optical path length) was measured the CD spectra from 200 to 260 nm with scanning speed of 50 nm/min. Each spectrum was averaged from three scans and subtracted from a baseline.

2.8 Mosquito-larvicidal activity assay

Toxicity assays against the second–instar *Culex quinquefasciatus* larvae were conducted following the protocol as previously described (Promdonkoy, et al., 2008). Mixtures of equal amounts of BinA wild-type inclusions and BinB wild-type or mutant inclusions were diluted in 1 ml of water to make a series of two-fold serial dilutions, from 64 µg/ml to 0.125 µg/ml. The toxicity was also tested with the soluble proteins by mixing the purified BinA and BinB, either $(His)_6$-tagged protoxins or trypsin activated forms, at 1:1 molar ratio, followed by 2-fold serially diluted with distilled water in different concentrations. Then, 1 ml of each protein dilution was added to each well of a 24-well tissue culture plate containing 10 larvae/well in 1 ml water. The BinB alone was used as a negative control. Mortality was recorded after incubation at room temperature for 48 hours. All of the data from three independent experiments were used to calculate median lethal concentration (LC_{50}) by using GWbasic program Probit analysis.

2.9 Far-Western dot blot analysis

Various amounts of purified truncated BinA were immobilized on strips of nitrocellulose membrane which were soaked in phosphate buffered saline (PBS) by using a Bio-Dot Microfiltration Apparatus (Bio-RAD) (Limpanawat, et al., 2009). The protein-bound membranes were blocked in 5% skimmed milk at 4 ºC overnight. Then, 20 µg/ml of purified wild-type BinB or its mutants in 5% skimmed milk was overlaid on each strip for 1 hour and subsequently washed with 0.1% Tween-20 in PBS (PBS-T20) 3 times, for 5 min each time. Bound BinB was detected by probing with polyclonal rabbit anti-BinB (1:20,000) for 1 hour. Unbound antibody was removed by washing 3 times with PBS-T20, 5 min each time. The membranes were

incubated with goat anti-rabbit IgG alkaline phosphatase conjugate (1:5,000) as a secondary antibody. Excess antibody was removed by washing twice with PBS-T20, 5 min each, followed by washing with PBS for 5 min. The immunoreactive signals were detected by using the ECL plus kit (GE healthcare).

2.10 In vitro binding assays via immunohistochemistry

Histological sections of the 4th-instar *C. quinquefasciatus* larval gut tissue were prepared and immunohistochemical detection was performed following protocols described previously (Chayaratanasin, et al., 2007, Moonsom, et al., 2007, Singkhamanan, et al., 2010). Briefly, endogenous peroxidase activity in the gut tissue was blocked by incubating the sections in PBS containing 0.1% TritonX-100 and 3% H_2O_2 for 30 min, followed by washing 3 times with 0.1% TritonX-100 in PBS (T-PBS), 15 min each. After blocking non-specific binding sites with normal goat serum (1:200) (Vector) for 45 min and washing excess serum, the sections were incubated with the purified wild-type or mutant BinB at a concentration of 20 µg/ml for 45 min. After washing 3 times with T-PBS, the sections were incubated with polyclonal rabbit anti-BinB (1:10,000) for 45 min. After washing with T-PBS, biotin-Goat anti-rabbit IgG (1:200) (Invitrogen) was added and further incubated for 45 min. The slides containing sections were then washed 3 times with T-PBS and incubated with HRP-Streptavidin conjugate (1:500) (Invitrogen) for 45 min. After washing with T-PBS, immunocomplexes were detected by incubation with 3,3'-diaminobenzidine (DAB, SK-400, Vector) for 2 min and the reaction was stopped by rinsing with distilled water. The apparent brown color observed under a light microscope indicated positive staining of the bound toxin.

2.11 Membrane insertion assay by Langmuir-Blodgett method

The interaction of BinA, BinB and their mutants with 2-Dimyristoylrac-glycero-3-phosphocholine (DMPC) monolayer was monitored by using a KSV 2,000 Langmuir-Blodgett trough (KSV, Finland). First, 15 nmol of DMPC in chloroform was spread on 50 mM Na_2CO_3 buffer, pH 10 which was used as an aqueous subphase. After lipid monolayer was rested for 15-20 min to allow the complete evaporation of the solvent, it was compressed at the speed of 10 mm/min until the surface pressure reached 10 mN/m and the monolayer was kept constant at this surface pressure by using the constant surface pressure mode. After that, the sample containing

the protein (5 nmol) was injected at 1,000 s by L-shaped syringe right underneath the monolayer forming area. Protein insertion was monitored by an increase of the mean molecule area as a function of time. All experiments were performed at room temperature and each experiment was repeated at least three times. Only buffer was injected into the subphase as a control.

2.12 Membrane perturbation assay by calcein release method

Large unilamellar vesicles (LUVs) were prepared from 2 mg/ml of a lipid mixture of phosphatidylcholine (PC)/ phosphatidic acid (PA) in ratio 1:1 (w/w) dissolved in chloroform. The lipid mixture was evaporated under a nitrogen stream and the lipid film was resuspended in 200 µl of 60 mM calcein (pre-dissolved in 500 mM Na_2CO_3, pH 10) in 50 mM Na_2CO_3, pH 10. The mixture was subjected to 5 repeated cycles of freezing and thawing. Then the suspension was passed through a polycarbonate membrane (0.1-µm pore size, Avanti Polar Lipid) for at least 20 passes using a two-syringe extruder (Avanti Polar Lipid). The untrapped calceins were removed by using a HiTrap^{TM} desalting column (GE Healthcare). Liposome concentrations were estimated by measuring the lipid phosphorus content (Mrsny, et al., 1986). The calcein-encapsulated lipid vesicle solution was placed into a 0.5-cm light-path quartz SUPRASIL cell at a final concentration of 1.25 µM. Protein at concentration of 0.016-0.25 µM was added at time 250 s and then incubated for 10 min. The fluorescence signals were detected by using the Jasco FP-6300 spectrofluorometer at the emission and excitation wavelengths of 520 and 485 nm, respectively, with a slit width of 5 nm. Finally, 0.1% (v/v) Triton X-100 was added at time 900 s to totally release entrapped calceins. The degree of LUVs perturbation was determined as the percentage of calcein release as described previously (Schwartz, et al., 2001).

2.13 Preparation of selenomethionine-substituted BinB for structural analysis

The activated BinB is composed of 390 amino acids with 7 methionine residues, therefore, the selenomethionine substituted BinB (SeMetBinB) was prepared for phasing. The recombinant plasmid, pET 28b-BinB, was introduced into *E.coli* B834 (DE3) methionine (Met) auxotrophic strain (Wood, 1966, Leahy, et al., 1992). The transformant was pre-cultured in 100 ml Luria-Bertani (LB) broth containing 50 µg/ml kanamycin at 310 K for 18 hours and cultured cells were harvested by centrifugation. The cell pellets were washed twice with PBS buffer before being resuspended in 1 liter of M9 medium containing 40 µg of each amino acid except

methionine, 1 μg of each vitamin mixture supplement (riboflavin, pyridoxine monohydrochloride, thiamine and nicotinamide) and 40 μg of SeMet (SIGMA). Expression was induced by the addition of 1 mM isopropyl β-D thiogalactopyranoside (IPTG) when the culture reached an OD_{600} of 0.6 and cultured cells were further grown at 303 K for 24 hours. SeMetBinB was purified and activated following the same protocols as those for the native protein.

2.14 Crystallization and X-ray diffraction data collection

Crystallization was performed by hanging- and sitting-drop vapour-diffusion methods in 96 and 24-well plates at 295 K (Molecular Dimensions, UK and QIAGEN, Germany). Initial screening was performed using Hampton Research Crystal Screen kits (Hampton Research, USA) and positive hits were then optimized. Drops were prepared by mixing 1 μl of 5 mg/ml protein solution (50 mM Tris-HCl pH 9.0, 1 mM DTT) with an equivalent volume of reservoir solution and were equilibrated against 500 μl of reservoir solution. For the SeMetBinB, initial screening was done using PEGs suite crystallization screening kit (QIAGEN, Germany). Both native and SeMetBinB crystals were briefly soaked in a cryo-protecting solution consisting of 25% (v/v) glycerol dissolved in their corresponding mother liquors before being cryocooled in nitrogen steam at 100 K.

Preliminary diffraction data were collected in-house (Thailand) using a Cu rotating-anode generator (λ=1.54 Å, MICROSTAR^{TM}, BRUKER). Higher resolution data were collected at the beamline BL41XU of the SPring-8 synchrotron (Hyogo, Japan). The diffraction data set of native crystal was collected at 1 Å wavelength. The single-wavelength anomalous dispersion (SAD) data of SeMetBinB crystal was collected at 0.979 Å based on the fluorescence spectrum of the Se K absorption edge (Rice, et al., 2000). A total of 180 frames of native and SAD data were collected with an oscillation angle of 0.5° and an exposure time of 0.3 second for each image. The diffraction images of both crystals were recorded on the Rayonix MX-225HE CCD detector. All diffraction data were indexed and integrated using iMOSFLM software (Leslie, 1992), and scaled and merged with SCALA in the CCP4 program suite (Winn, et al., 2011). Anomalous difference Patterson maps for SeMetBinB were calculated by the CCP4 program package. After scaling, SHELX C and SHELX D were then used for data preparation and selenium atom searching. The selenium sites were used for phasing and density modification carried by SHELX E. The atomic model was built by using ARP/ wARP program. The

refinement was carried by LAFIRE and Refmac5. The model was manual checked by COOT program. The quality of protein structure was determined by BAVERAGE and PROCHECK.

3. Results and Discussion

3.1 Investigation of the role of BinA aromatic residues in toxicity

3.1.1 Replacements of Y213, Y214, Y215, W222 and W226 and their effects on toxicity

The mechanism by which the binary toxin kills the mosquito larvae remains unclear, however, it has been shown that the binary toxin is internalized in both mosquito midgut cells and MDCK cells expressing the Cpm1 receptor, possibly via endocytosis (Oei, et al., 1992, Opota, et al., 2011). Hence, interaction of the binary toxin with the lipid membrane is a key step during the intoxication process. Previous study has shown that the aromaticity of F149 and Y150 of BinB is a prerequisite for larvicidal activity, possibly by playing a crucial role in membrane interaction and receptor binding (Singkhamanan, et al., 2010). According to amino acid sequence of BinA protein, the aromatic residues especially tryptophan and tyrosine are clustered at the positions 213 to 226. We expected that this region could be essential for membrane interaction. To investigate the functional importance of aromatic amino acids of BinA, site-directed mutagenesis was performed by replacements of aromatic amino acids (Y213, Y214, Y215, W222, and W226) in this region by leucine residues. After obtaining the mutant plasmids, automated DNA sequencing analysis revealed that all selected aromatic residues were replaced by leucines (data not shown). Upon IPTG induction, all mutant proteins were expressed as inclusions with expression levels comparable to that of the wild type (Fig. 1), suggesting that the mutations of these aromatic residues did not affect protein production and inclusion formation of the BinA. Any change of protein conformation as a result of point mutations was monitored by using the Circular Dichroism (CD) spectroscopy. CD spectra in a far UV region (190-260 nm) of all mutants were apparently similar to that of the wild-type protein, suggesting that the mutations at these selected positions did not affect the structural folding of the BinA protein (data not shown).

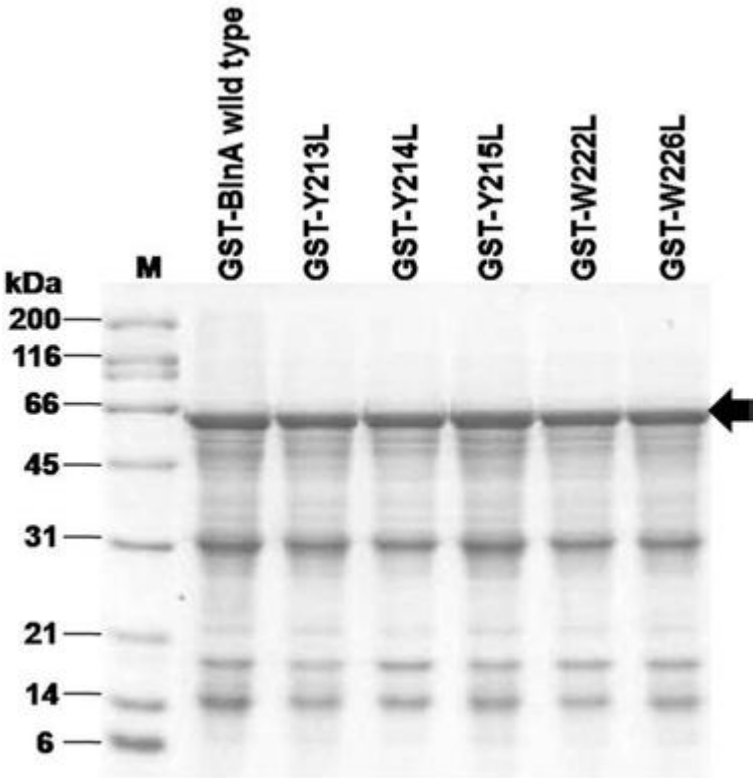

Figure 1. Partially purified inclusions of GST-BinA and its mutants were analyzed on 12% SDS-PAGE. M represents the molecular mass standards. Position of GST-BinA fusion protein is indicated by an arrow.

All mutants were tested the mosquito-larvicidal activity and results showed that the single mutations of three consecutive tyrosines (Y213L, Y214L and Y215L) conferred the comparable toxicity to that of the wild type, whereas the mutations of two tryptophans, W222L and W226L, rendered toxin inactive even using the concentration of inclusions up to 32 µg/ml (Table 2). These data suggest that tryptophan residues at positions 222 and 226 play a crucial role in larvicidal activity. The considerably reduced toxicity of W222L and W226L mutants, however, was not associated with the structural alterations as described earlier. Both W222 and W226 of BinA, therefore, seem to have functional significance in the toxication process of the binary toxin.

Table 2. Mosquito-larvicidal activity of the wild-type and mutant toxins against *Culex quinquefasciatus* larvae. The mortality was recorded after feeding the mixture of GST-BinB and GST-BinA or its mutant inclusions at a 1:1 molar ratio for 48 h. The LC_{50} (median lethal concentration) was calculated from three independent experiments by using Probit analysis. Numbers in parenthesis indicate the fiducial limits at 95% confidence. Mortality was not detected for W222L and W226L mutants when used the toxin up to 32 μg/ml.

Protein	**LC_{50} (μg/ml)**
GST-BinB + GST-BinA wild type	0.20 (0.14 – 0.32)
GST-BinB + GST-Y213L	0.45 (0.31 – 0.76)
GST-BinB + GST-Y214L	0.57 (0.41 – 0.89)
GST-BinB + GST-Y215L	0.45 (0.33 – 0.94)
GST-BinB + GST-W222L	not toxic
GST-BinB + GST-W226L	not toxic

3.1.2 Effects of W222 and W226 mutations on membrane insertion and permeability

In order to study the membrane insertion ability of BinA and its mutants, the DMPC lipid monolayers were generated and the Langmuir-Blodgett (LB) trough technique was used. These DMPC lipid monolayers were previously used as model lipid monolayers for the study of interaction of BinA and BinB with receptor-free lipid membranes (Boonserm, et al., 2006). Upon injection of the protein sample in the subphase of the trough, the degree of membrane insertion was monitored by the mean molecular area expansion. The results showed an increase in area expansion as a function of time in all protein samples, indicating the ability of these proteins to insert into DMPC monolayer. Therefore, the insertion of protein molecule into lipid monolayers was calculated and shown in term of area per molecule protein versus time (Fig. 2). No insertion was observed in the GST alone, indicating that the membrane insertion was only mediated by BinA molecules. Among the BinA mutants, the extents of membrane insertion were somewhat different. Three active mutant proteins; GST-Y213L, GST-Y214L and GST-Y215L, were able to insert into the DMPC monolayer to the same extent as that of the wild-type BinA which also correlated well with their larvicidal activity. For the tryptophan mutations; GST-

W222L and GST-W226L, however, less extent of membrane insertion was observed compared with that of the wild type (Fig. 2). Although the larvicidal activity of the GST-W222L and GST-W226L mutants was abolished, membrane insertion was only slightly compromised, suggesting that these two tryptophans may not directly involve in the membrane insertion.

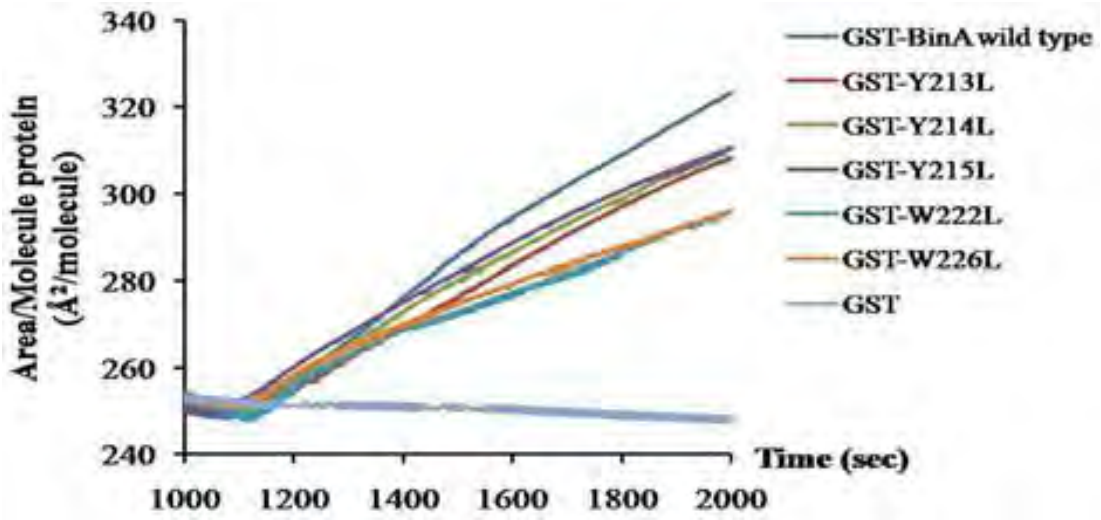

Figure 2. The insertion ability of wild-type GST-BinA and its mutant proteins into DMPC monolayer. The data were obtained by measuring the change of lipid surface area under a constant surface pressure. Only GST protein was used as a negative control. Upon the injection, the increase of area per molecule protein was observed in all mutant proteins.

Calcein release assay was used to investigate the effect of BinA mutations on LUV permeability. The fluorescence intensity was observed after adding the wild-type GST-BinA and its mutants, indicating that all these proteins could perturb the lipid vesicles, resulting in the leakage of encapsulated calceins to the solution. In contrast, no leakage of calceins was observed in GST alone, suggesting that calcein release was solely induced by BinA protein. By comparing the degree of membrane permeability among BinA mutants, interestingly, both W222L and W226L showed less membrane permeability than that of tyrosine mutations (Fig. 3). This result is in agreement with the membrane insertion assay, providing a clue that these tryptophans may partially participate in the membrane perturbation. Since the localization of W222 and W226 in BinA molecule cannot be easily predicted with the absence of structural information of the

binary toxin, it is hard to make a conclusive assumption of how these tryptophans participate in the membrane insertion and permeability. Moreover, conformational changes of the BinA/BinB complex accompanying the receptor binding to transform the water-soluble form into the membrane-traslocation structure may take place inside the larval midgut. Therefore, upon the receptor-mediated conformational changes, the membrane insertion and permeability of W222L and W226L mutants may be severely affected, leading to the loss of larvicidal activity.

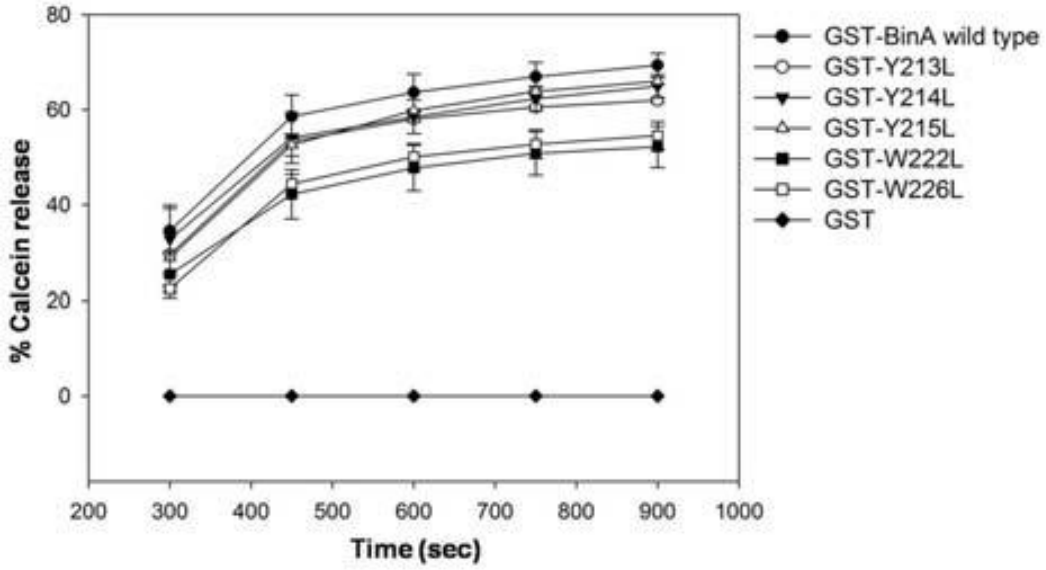

Figure 3. The calcein release from LUVs treated with wild-type GST-BinA and its mutant proteins. Only GST protein was used as a negative control. The error bars represent the standard deviation of the measurements from three independent experiments.

3.2 Investigation of the role of the amino acids at the N-terminal region of BinB in toxicity

3.2.1 Effects of alanine substitutions at positions 35-37 and 41-43 on protein production and larvicidal activity

Earlier studies have shown that the deletion of 34 amino acids from the N-terminus of BinB did not affect the toxicity and regional binding to the larval gut, while further deletion up to 41 amino acids from the N-terminal end totally abolished the toxicity (Oei, et al., 1992). The functional importance of the N-terminus of BinB was further revealed from the loss of toxicity when amino acids at positions $_{32}$YNL$_{34}$ and $_{38}$SKK$_{40}$ from *B. sphaericus* 1593M were substituted by AAA (Elangovan, et al., 2000). Based upon the secondary structure prediction,

amino acid residues 1-34 and 35-45 have been proposed to adopt a random coil and a helical structure, respectively (Elangovan, et al., 2000). Thus, certain mutations at these N-terminal regions may disturb the structural folding or functional sites of BinB protein. In this study, two additional block mutations ($_{35}PEI_{37}\rightarrow_{35}AAA_{37}$ and $_{41}FYN_{43}\rightarrow_{41}AAA_{43}$) of the amino acid residues flanking those N-terminal regions were initially performed to test the possible functional significance of these selected BinB regions.

Both block mutants were expressed in *E. coli* BL21(DE3) pLysS as inclusions upon IPTG induction, with expression levels similar to that of the wild-type BinB (Fig. 4A), suggesting that the mutations do not affect the protein expression of BinB. Upon immunological detection with polyclonal-anti BinB by Western blot analysis, a major band at 43 kDa reacted specifically with anti-BinB was observed in both block mutants (data not shown), confirming the immunological identity of the BinB mutant proteins.

Mosquito-larvicidal activity of each block mutant was tested by feeding the mutant inclusions to *Culex quinquefasciatus* larvae together with the wild type-BinA inclusions. Both block mutations, $_{35}PEI_{37}\rightarrow_{35}AAA_{37}$ and $_{41}FYN_{43}\rightarrow_{41}AAA_{43}$ were inactive (Table 3). Thereafter, the residues in these two regions were individually substituted with alanine (P35A, E36A, I37A, F41A, Y42A, N43A) to define amino acids important for the larvicidal activity. All these mutants were produced as inclusion bodies at comparable levels to that of the wild-type BinB (Fig. 4B). Of these alanine substitutions, mosquito-larvicidal activity was significantly reduced for P35A, E36A, F41A, and Y42A mutants (Table 3). Further analyses were therefore focused on these mutants, while N43A was used as a representative of the active mutants.

Any major structural change induced by the mutations was explored by using the intrinsic fluorescence spectroscopy. Tryptophan emission spectra of the mutants were not significantly different from that of the BinB wild type (data not shown), suggesting that alanine substitutions at P35, E36, F41 and Y42 are unlikely to perturb the overall conformation of the toxin.

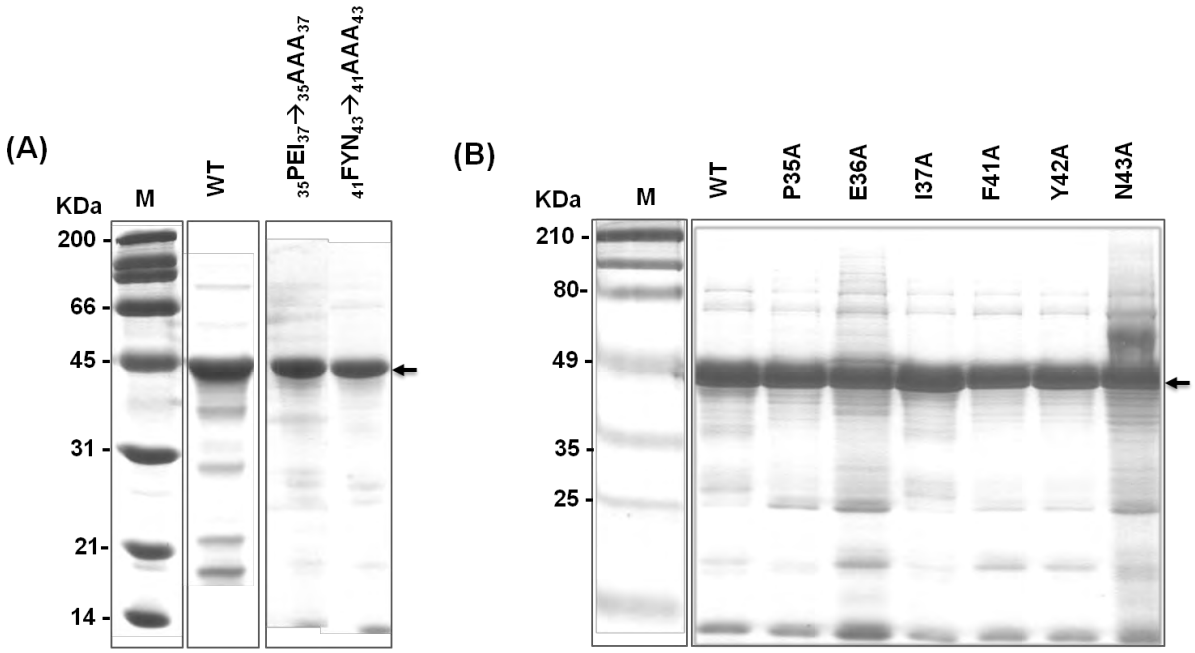

Figure 4. 12% SDS-polyacrylamide gel of BinB wild-type and mutant proteins. *E. coli* cells harbouring the 43-kDa truncated *binB* gene (WT) or mutated plasmids were induced by 0.1 mM IPTG for 5 hours. Cells were lysed using a French Pressure cell and protein inclusions were partially purified by repeated washing and centrifugation. Panel A represents partially purified inclusion bodies of block mutants, $_{35}PEI_{37}\rightarrow_{35}AAA_{37}$, $_{41}FYN_{43}\rightarrow_{41}AAA_{43}$ and panel B represents partially purified inclusion bodies of single-point mutants, P35A, E36A, I37A, F41A, Y42A, and N43A. M represents protein standard markers. Arrows indicate the BinB protein bands.

Table 3. Mosquito larvicidal activity of the wild-type and mutant toxins against the 2nd-instar *C. quinquefasciatus* larvae

Protein	LC_{50} (µg/ml)
BinB	Inactive
BinA + BinB wild type	0.36 (0.31-0.42)
BinA+ $_{35}PEI_{37} \rightarrow {}_{35}AAA_{37}$	Inactive
BinA+ $_{41}FYN_{43} \rightarrow {}_{41}AAA_{43}$	Inactive
BinA + P35A	1.45 (1.24-1.68)
BinA + E36A	1.75 (1.51-2.02)
BinA + I37A	0.51 (0.43-0.60)
BinA + F41A	3.38 (2.92-3.90)
BinA + Y42A	2.43 (2.10-2.84)
BinA + N43A	0.49 (0.42-0.56)

3.2.2 Single alanine substitutions at positions 35-37 and 41-43 in BinB did not affect BinA-BinB interaction

As the full activity of the binary toxin is achieved only when both BinA and BinB components are present together, the interaction between BinA and BinB supposedly is one of the critical steps during the pathological process. In this study, the effect of single mutations at positions 35-37 and 41-43 on the *in vitro* interaction between BinB mutants and the wild-type BinA was assessed by Far-Western dot blot analysis. The BinA protein was immobilized on the membrane which was then incubated with the purified wild-type BinB or one of the mutant proteins. The BinA-BinB bound complexes were further detected by probing with anti-BinB. The results showed that all BinB mutants could interact with the immobilized BinA, giving comparable intensity to that of the wild-type protein (Fig. 5). These results indicated that none of these mutations disrupted inter-molecular BinA-BinB interaction. Therefore, the dramatic

decrease in toxicity of mutants P35A, E36A, F41A and Y42A may be caused by another defect in the pathological process.

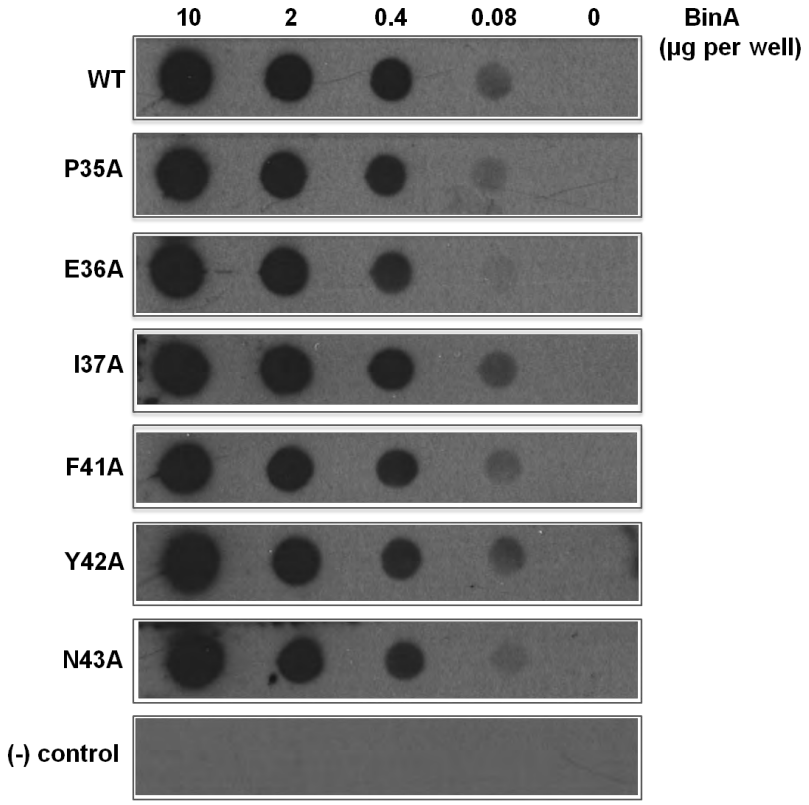

Figure 5. BinA-BinB interaction detected by Far-Western dot blot analysis. Various amounts of BinA protein were immobilized on a membrane and then overlaid with BinB wild-type or its mutant protein at a concentration of 20 µg/ml. Negative control was BinA alone without overlaid BinB protein. BinA-BinB complexes were detected by incubating the membrane with rabbit anti-BinB followed by goat anti-rabbit IgG conjugated with alkaline phosphatase.

3.2.3 Single alanine substitution at position Y42 in BinB affects receptor binding

Evidence has been provided that BinB is the binding component of the binary toxin by interacting with a specific receptor on the surface of midgut epithelium cells (Davidson, 1988, Silva-Filha, et al., 1997). Immunohistochemistry assay was used to test the effect of BinB mutations on the binding to the midgut of susceptible *C. quinquefasciatus* larvae. The localization of the BinB wild-type protein on the midgut section was demonstrated as an intense brown staining after probing with anti-BinB, while a faint signal was observed in the negative

control (without BinB overlay) (Fig. 6). An intense staining was also observed from the section incubated with mutants P35A, F41A and N43A, whereas a very weak signal was detected in the Y42A mutant. These results suggest that P35A, F41A and N43A mutants still retain the ability to bind to the apical microvilli of larval midgut. Despite the preserved receptor binding activity, the larvicidal activity of P35A and F41A was significantly reduced. These data suggest that, after the BinB- receptor interaction, P35 and F41 residues may contribute to a subsequent step of cytotoxic process. Of these mutants, the receptor binding activity was greatly reduced by the mutation of Y42 which correlates well with its loss of toxicity. Previously, we reported the crucial role of Y150, particularly its aromaticity, in receptor binding of BinB (Singkhamanan, et al., 2010). Herein, Y42 was also found to be crucial for the binding to apical brush border microvilli of susceptible larvae. Taken together, data suggest that BinB receptor binding could be mediated by Y42 and Y150.

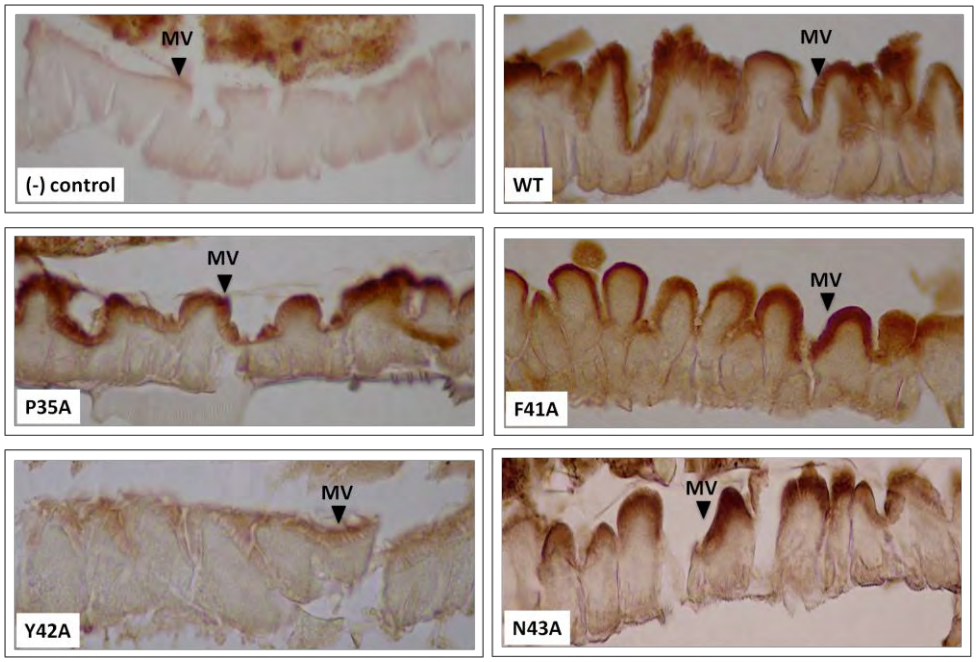

Figure 6. Immunohistrochemical staining of the 4th-instar *C. quinquefasciatus* larval midgut tissues. Slides were incubated with either BinB wild type (WT) or P35A, F41A, Y42A, and N43A mutants at a concentration of 20 µg/ml. Negative control was done by incubating with carbonate buffer. MV represents microvilli.

3.2.4 Single alanine subsitutons at positions 35-37 and 41-43 in BinB affect membrane insertion

Membrane-protein interaction generally promotes a cascade of events leading to pathological effects of most bacterial toxins. To explore the effect of BinB mutations on the protein penetration into the phospholipid membrane, a Langmuir membrane system was used. When the protein sample was injected into the aqueous subphase with a given time to interact with the lipid monolayer, the degree of membrane penetration was measured as a time-dependent increase of the mean molecular area. The results demonstrated three distinct groups of membrane penetration behaviors of BinB mutants (Fig. 7). The first group (F41A and N43A) showed a greater extent of membrane penetration when compared with that of the BinB wild type, whereas a lower extent of membrane penetration was found in the second group (E36A, I37A and Y42A) and the lowest extent of membrane penetration was observed in the third group (P35A and BinA) (Fig. 7). The fact that the F41A efficiently penetrated the lipid monolayer despite its reduced larvicidal activity suggests that the compromised biological activity of the F41A was not due to the impaired lipid-membrane interaction. In contrast, the reduced membrane penetration ability of P35A, E36A and Y42A was correlated with the decrease of larvicidal activity of these mutants. It is noteworthy that P35A and BinA showed a much lower rate of membrane penetration when compared with BinB and other BinB mutants. Previously, an incapability of BinA to insert into the artificial lipid monolayer was reported (Boonserm, et al., 2006). These data thus indicate, albeit using a model membrane, that P35 plays a key role in the lipid membrane penetration, while E36 and Y42 may be partly involved in this step. According to the secondary structure prediction, P35 and E36 have been proposed to locate at the end of a loop preceding a helical structure at the N-terminal region of BinB (Elangovan, et al., 2000). Particularly, P35 seems to confer the structural integrity of the loop which may be required for the lipid membrane insertion. In agreement with our finding, the necessity of the structural integrity of the loop joining the α4-α5 transmembrane hairpin for an efficient membrane insertion of the Cry4Aa mosquito-larvicidal toxin has also been reported (Tapaneeyakorn, et al., 2005). However, herein the precise structural role of the P35 and E36 residues await further confirmation by the crystal structure of the BinB protein. Although previous evidence has provided an important clue of the N-terminal region of BinB for the receptor recognition, here we demonstrate that the N-terminus of BinB is also involved in the membrane interaction.

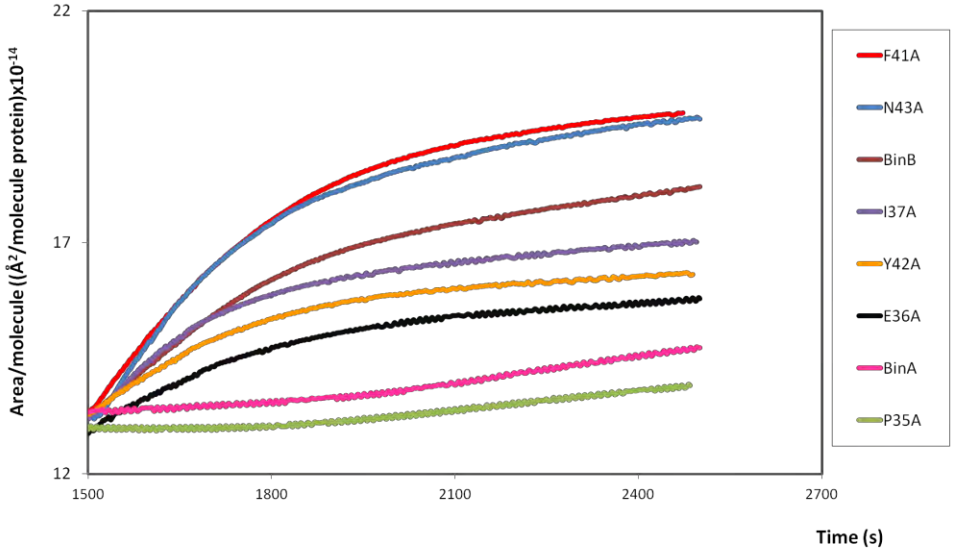

Figure 7. The insertion ability of BinB wild-type and its mutant proteins into DMPC monolayer using the Langmuir-Blodgett Trough. The degree of membrane insertion was monitored by an increase of the mean molecule area as a function of time under a constant surface pressure. All data were subtracted from the negative control (buffer only).

3.3 Structural determination of the binary toxin

3.3.1 Expression and purification of BinA and BinB soluble proteins

As described above, both BinA and BinB have been cloned and expressed in various host strains, but expressed proteins tended to accumulate as inclusion bodies. Although those expressed proteins are in a similar form as the native binary toxin, solubilization in highly alkaline pH results in several additional steps of protein preparation. To facilitate the soluble protein expression and protein purification, both *binA* and *binB* genes from *Bs* strain 2297 were independently cloned and expressed with $(His)_6$-tags at their N-termini. The recombinant BinA and BinB proteins were expressed in *E.coli* BL21 (DE3)pLysS with modified conditions to provide an optimum yield of soluble products. Both recombinant BinA and BinB fused with polyhistidine tags at their N-termini were expressed mainly in soluble form after induction with 0.2 mM IPTG at lower temperature of 18°C for 5 h. Crude extract was released by sonication and the supernatant fraction containing either expressed BinA or BinB was initially loaded into the

Ni-NTA affinity chromatography. The collected BinA and BinB proteins after elution from the Ni-NTA column were subsequently loaded to a size exclusion column to improve purity. Purified proteins were analysed by SDS-PAGE (Fig. 8). The BinA and BinB proteins appeared as bands with apparent molecular masses of 42 and 51 kDa, and showed high purity.

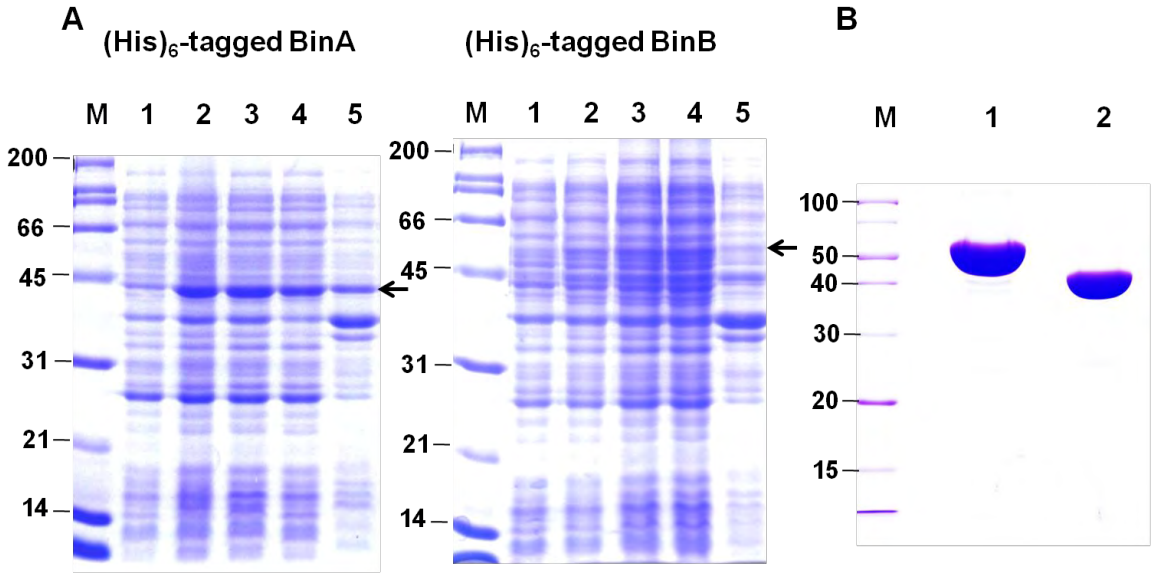

Figure 8. Coomassie-stained SDS-PAGE (12 % gel) showing the protein expression and purification of the recombinant BinA and BinB. (A) Expression profiles of $(His)_6$-tagged BinA and $(His)_6$-tagged BinB. Lanes 1 and 2, uninduced and IPTG-induced cell cultures, respectively; lanes 3, 4, and 5 Cell lysate, supernatant and pellet fractions after ultrasonication, respectively; M, molecular mass standards. Arrows indicate the expressed proteins at their predicted MW. (B) Purity assessment of $(His)_6$-tagged BinB (lane 1) and $(His)_6$-tagged BinA (lane 2) after Ni-NTA affinity and size exclusion chromatography.

3.3.2 BinA and BinB toxin activation and their complex formation in solution

The native BinA and BinB proteins are produced as protoxins that are subsequently digested by larval proteases and converted to active toxins (Broadwell & Baumann, 1987). Here, *in-vitro* toxin activation was performed by incubating $(His)_6$-tagged BinA and BinB with trypsin, followed by purification of the native proteins by size exclusion chromatography. The molecular sizes of the trypsin-activated BinA and BinB were checked by SDS-PAGE and MALDI-TOF mass spectrometry. As observed by SDS-PAGE, digestion with trypsin appeared to generate a resistant-fragment of about 40 kDa and 45 kDa for BinA and BinB, respectively (Fig. 9). MALDI-TOF mass spectra of trypsin-digested BinA and BinB showed peaks at 40,823

Da and 45,028 Da for BinA and BinB, respectively (data not shown) that agree well with the predicted molecular masses from their deduced amino acid sequences (40,985 Da for BinA and 44,884 Da for BinB).

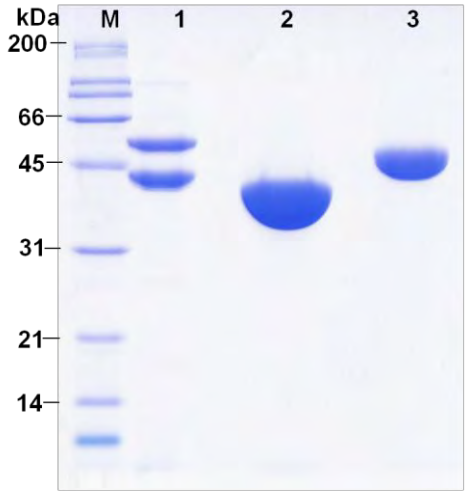

Figure 9. Coomassie-stained SDS-PAGE (12 % gel) showing proteolytic activation of recombinant BinA and BinB. Lane 1, mixture of undigested BinA (lower band) and undigested BinB (upper band); lane 2, trypsin-activated BinA (40 kDa); lane 3, trypsin-activated BinB (45 kDa); M, molecular mass standards.

To demonstrate a complex formation of activated BinA and BinB in solution, their trypsin-activated products were mixed at a 1:1 molar ratio before applying size exclusion chromatography (HiLoad 16/60 Superdex 200). Both trypsin-activated BinA and BinB co-eluted before the individual proteins, indicating formation of a BinA-BinB complex in solution after trypsin activation (Fig. 10). The gel-filtration elution volume of the binary toxin complex was between IgG (158 kDa) and albumin (66 kDa). According to the estimation based on this elution volume, the molecular mass of the binary toxin complex was about 140 kDa. MALDI-TOF mass spectra of the binary toxin complex showed peaks corresponding to the 40,823 Da BinA and 45,028 Da BinB (data not shown), confirming the presence of both activated components in the complex. It has been demonstrated that native BinA and BinB protoxins form an oligomer in solution that contains two copies of each BinA and BinB (Smith, et al., 2005). However, in that report, the trypsin-digested binary toxin was not found in an oligomeric form. Our result, in contrast, provides evidence of the formation of a BinA-BinB complex in solution after trypsin

activation. This oligomeric complex may play a role in toxin insertion into the membranes of the target cells, probably via pore formation, causing pathological effects inside the cells.

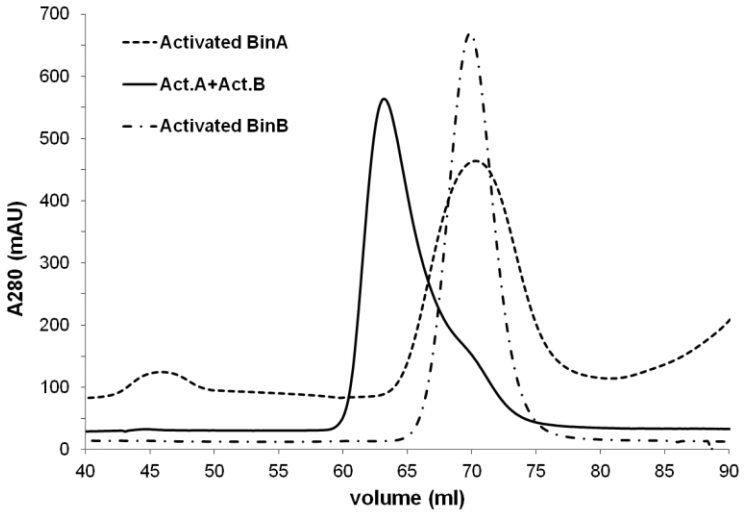

Figure 10. Elution profile from a size-exclusion chromatographic column (Hiload Superdex 200 16/600) of the 40-kDa trypsin-activated BinA, 45-kDa trypsin-activated BinB and their mixture at equal concentration.

Larvicidal activity of recombinant BinA and BinB against *C. quinquefasciatus* larvae was tested, either as protoxins or as trypsin-activated proteins. Neither BinA nor BinB alone was toxic to *C. quinquefasciatus* larvae, even using a concentration of 50 µg/ml. However, high toxicity was achieved when BinA and BinB were combined at 1:1 molar ratio (Table 4). Both protoxin and trypsin-activated BinA-BinB mixtures showed comparable toxicity, indicating that both larval gut proteases and trypsin could convert the protoxins into their active forms.

Table 4. Mosquito-larvicidal activity of the purified BinA and BinB with histidine tag and after trypsin activation against *Culex quinquefasciatus* larvae.

Sample	LC_{50} (ng/ml)
$(His)_6$-tagged BinA	Not toxic
$(His)_6$-tagged BinB	Not toxic
$(His)_6$-tagged BinA + $(His)_6$-tagged BinB	8.0 (5.7 -10.4)
Activated BinA + Activated BinB	10.0 (7.4-14.6)

3.3.3 Protein crystallisation of the binary toxin in solution

In order to gain insights into the mechanism of toxicity of the binary toxin, structural analysis of the binary toxin has been carried out using X-ray crystallographic technique. Protein crystallization screening of His-BinA, His-BinB and their activated proteins was performed by using sitting drop vapour diffusion method and reservoir conditions obtained from Hampton research, the crystal screening kits.

Upon initial crystallization screening, microcrystals appeared in conditions containing PEG 4000 and some divalent cation salts such as magnesium chloride, lithium sulfate and calcium chloride. All favorable conditions were further optimized by slightly adjusting the protein concentration, precipitant concentration, salts concentration and the pH of buffer from 6.5 to 10. In this study, crystallization screening of BinA and BinB protein was performed separately. Both BinA and BinB proteins appeared to form crystals, however, only the crystal of activated BinB could diffract to high resolution of about 1.75 Å. Therefore, in this report, only the structure of BinB in its active form was described.

The best native BinB crystals appeared in a condition containing of 0.1 M Tris-HCl pH 8.0, 0.2 M Lithium sulfate and 12% (*w*/*v*) PEG 4000. The crystals grew to their maximal dimensions of 250µm × 250µm × 50 µm within one week (Fig. 11). Since a limited sequence identity is observed between BinB and other proteins with known structures, the single-wavelength anomalous dispersion (SAD) method has been used for experimental phasing. The Selenomethionine (SeMet)-substituted BinB was prepared, activated by trypsin digestion and purified by the same procedure as that of the native BinB. Furthermore, the SeMet-substituted BinB still retained the toxicity against the *C. quinquefasciatus* larvae (data not shown). The SeMet-substituted BinB crystals were obtained from a condition consisting of 0.1 M Tris-HCl pH 8.0, 0.2 M Magnesium acetate and 16% (*w*/*v*) PEG 3350 which is closely similar to that of the native crystals. The crystals grew to their maximal dimensions of 100µm × 50µm × 50 µm after four days (Fig. 11).

X-ray diffraction data of the native BinB crystal were collected to 1.75 Å resolution using 25% glycerol as a cryo-protectant. The crystal belongs to space group $P6_222$ with unit-cell parameters a = 95.21, b = 95.21, c = 154.89 Å. The single-wavelength anomalous dispersion (SAD) data of a SeMet-substituted BinB crystal was collected to 1.85 Å resolution at the Se K-absorption edge (wavelength: 0.979 Å). The SeMet-substituted crystal was found isomorphous

with the native crystal with unit-cell parameters a = 95.03, b = 95.03, c = 154.54 Å and space group $P6_222$. The Matthews coefficient (V_M) is 2.35 $Å^3Da^{-1}$ for one molecule, corresponding to a solvent content of 48% (Matthews, 1968). Anomalous difference Patterson Harker sections for SeMet derivative of BinB revealed seven selenium sites (data not shown), suggesting the usefulness of these data for phasing using the SAD method. Details of the data-collection statistics are summarized in Table 5.

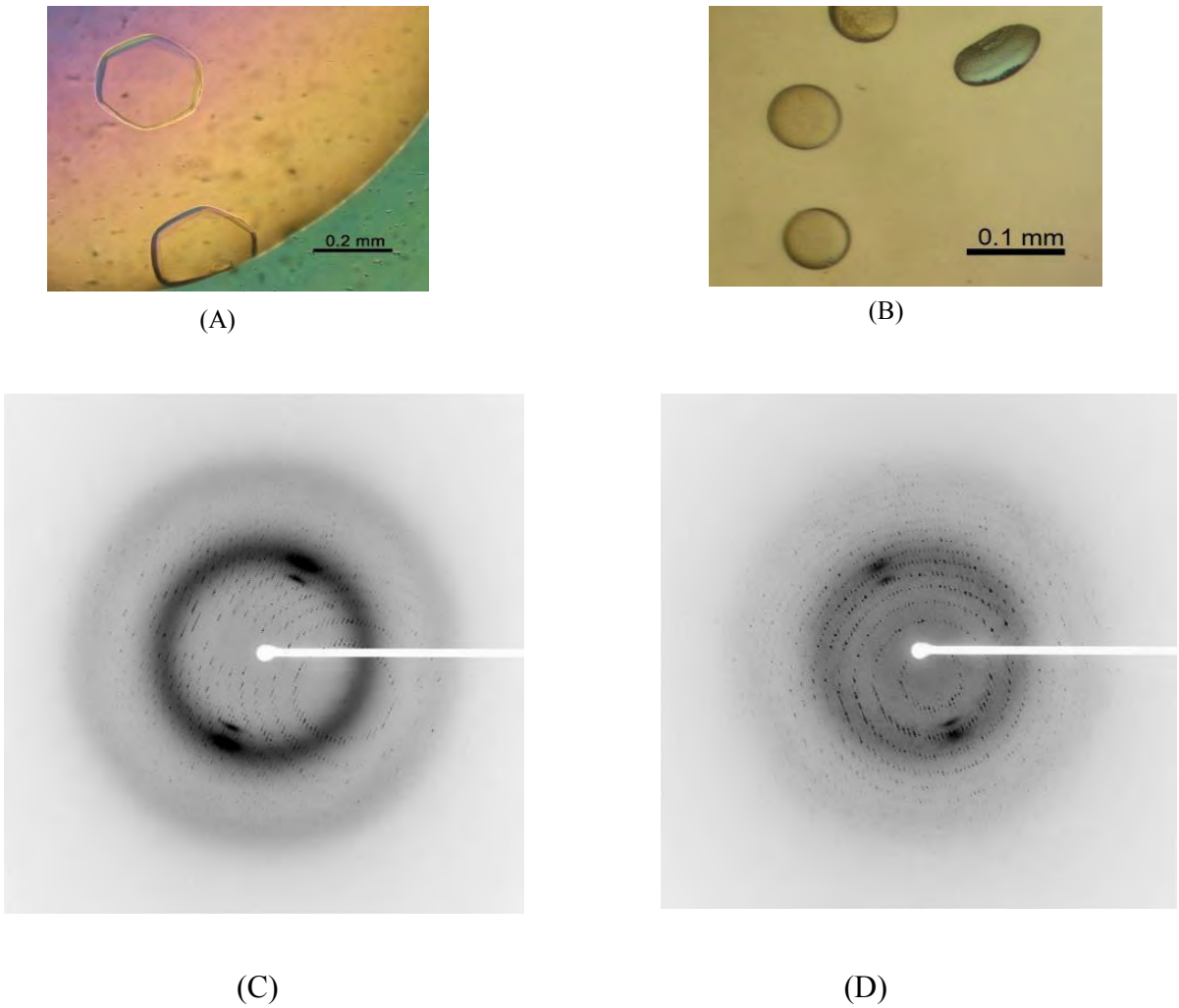

(A) (B)

(C) (D)

Figure 11. Crystals of native (A) and SeMet-substituted BinB (B) used for X-ray diffraction and their diffraction patterns are shown in C and D, respectively.

Table 5. Summary of crystallographic data. Values in parentheses are for the highest resolution shell.

	Native	**SeMet**
Wavelength (Å)	1 Å	0.979 Å
Space group	*$P6_222$*	*$P6_222$*
Unit-cell parameters		
***a* (Å)**	95.2	95.0
***b* (Å)**	95.2	95.0
***c* (Å)**	154.9	154.5
Resolution range (Å)	28.99-1.75 (1.84-1.75)	28.99-1.85 (1.95-1.85)
No. of unique reflections	42536 (6069)	35916 (5127)
Average redundancy	10.6 (10.7)	15 (15)
Completeness (%)	100 (100)	100 (100)
<I/s (I)>	4.4 (1.8)	4.7 (2.4)
Rmeas† (%)	12.6 (45.5)	11.9 (32.9)

† Rmeas $=\sum_h \sqrt{\left(\frac{m_h}{m_h-1}\right)} \sum_j \left|\langle I_h\rangle - I_{h,j}\right| / \sum_h \sum_j \langle I_{h,j}\rangle$, where $\langle I_h\rangle$ is the mean intensity of symmetry-equivalent reflection h and m is redundancy.

3.3.4 The overall structure of activated BinB

The structure of activated BinB molecule has been determined at 1.75 Å resolution by the single-wavelength anomalous dispersion (SAD) method and refined to R-factor and R-free of 17.2% and 21.1%, respectively. The refinement statistics are summarized in Table 6. The Ramachandran map generated by PROCHECK shows 90.8%, residues in favoured regions, 9% in additional allowed regions and 0.3% in disallowed regions.

Table 6. Refinement Statistics of activated BinB structure

	Native Activated BinB
Resolution range (Å)	28.91-1.75 (1.84-1.75)
Number of used reflections	42392 (6069)
Completeness (%)	99.7 (99.9)
[a]R-factor (%)	17.4
[b]R_{free}-factor (%)	21.0
Number of non-hydrogen atoms	
Protein	3159
Water	440
Averaged B factors (Å^2)	21.8
Protein	19.3
Water	36.8
RMS deviatioins	
Bond length (Å)	0.010
Bond angle (°)	1.08
[c]Ramachandran plot (%)	
Favored regions	90.8
Additional allowed regions	9.0
Disallowed regions	0.3

[a]R-factor = $\sum |F_{obs}-F_{cal}|/\sum F_{obs}$, where F_{obs} and F_{cal} are observed and calculated structure factor amplitudes, respectively. [b]R_{free}-factor value was calculated as R-factor but using a subset (10%) of reflections that were not used for refinement. [c]Ramachandran plot was calculated using PROCHECK.

Activated BinB structure is composed of 389 amino acid residues which can be divided into two domains, N-terminal (NTD) and C-terminal domains (CTD). The overall structure is in an elongated shape with approximately dimensions of 97Å × 56Å × 56Å and mainly contains β-structure as shown in a topology diagram (Fig. 12). The N-terminal domain covering amino acids threonine 19 to alanine 200 is a globular structure (Fig. 13). This domain adopts a β-trefoil fold with a pseudo 3-fold rotation axis and is subdivided into α (P35-D90), β (D91-I141) and γ (T142-A200) subunits. Two loops of α and γ-subunits are connected by a disulfide bridge formed between C67 and C161, thereby restraining their flexibility.

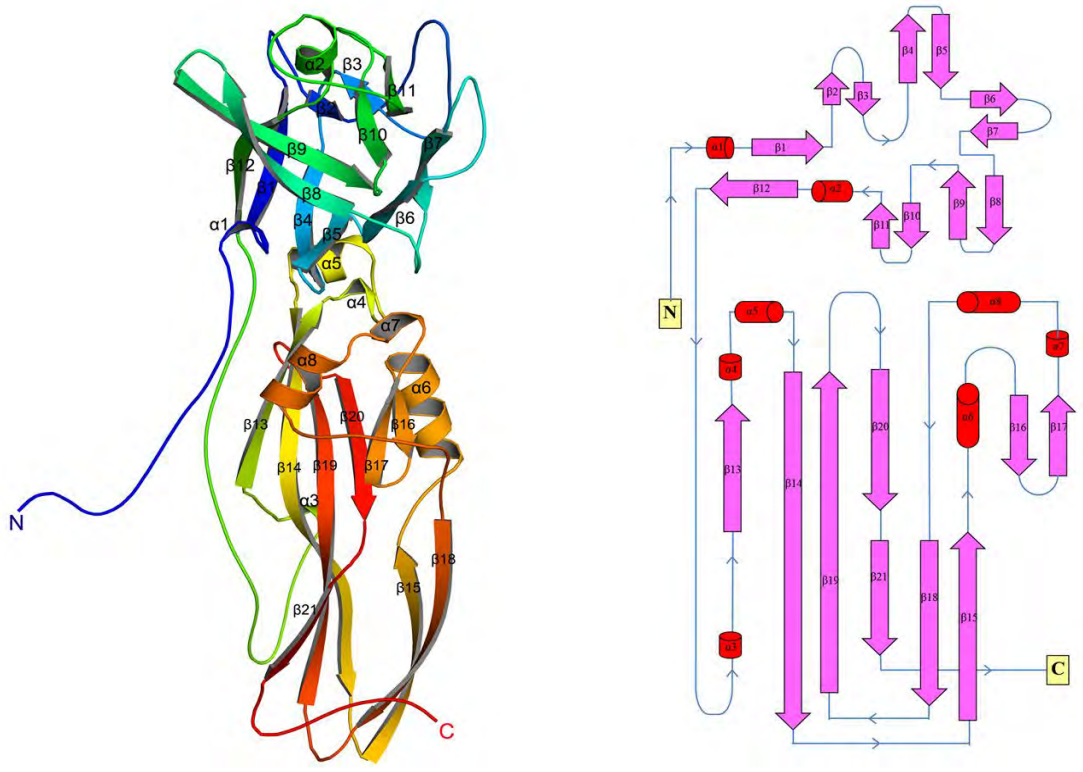

(A) (B)

Figure 12. Structure of the activated BinB. (A) Cartoon represents the structure of activated BinB which is composed of 389 amino acid residues. The polypeptide chain is represented in a rainbow pattern from blue at the N-terminus to red at the C-terminus. (B) The topology diagram represents the secondary structures of the activated BinB including 21 β-strands and 10 α-helices as shown in pink and red colors, respectively.

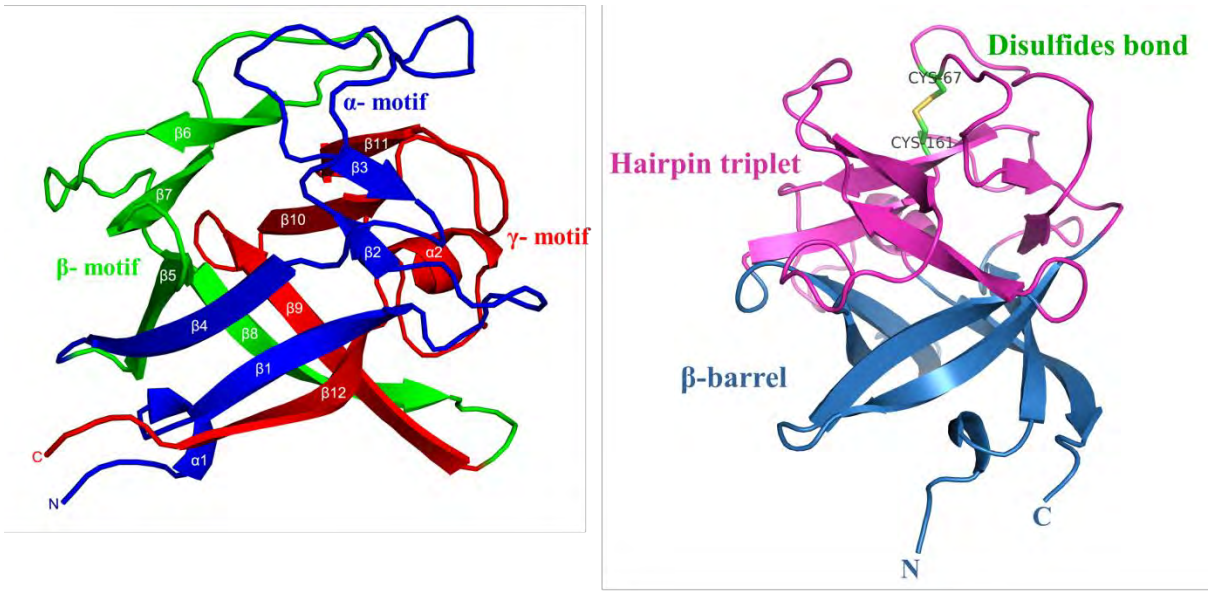

(A) (B)

Figure 13. The N-terminal domain of activated BinB structure**.** (A) The N-terminal domain of activated BinB structure is composed of β-trefoil fold which is characteristic of the sugar-binding proteins. The α, β and γ-motifs are represented in blue, green and red colors, respectively. This domain is proposed to function as a receptor binding domain. The blue and pink colors represent β-barrel and hairpin triplet, respectively, which are features of the lectin-like domain. (B) The disulfide bond is formed between C67 and C161 connecting the long loops in the α and γ-motifs.

Structural homology searching by DALI server found that the overall structure of BinB displays no obvious structural similarity to other established crystal structures (Holm & Rosenstrom, 2010). However, the N-terminal domain shares similar organization to several sugar binding proteins such as sugar binding domain of hemagglutinin component (HA) from *Clostridium botulinum* (3AH1; Z score 17.3) and ricin B-like domain of mosquitocidal toxin from *Bacillus sphaericus* (2VSA; Z score 15.9). The N- and C-terminal domains are connected by a long loop spanning residues A201-L225. The C-terminal domain encompassing residues P226-T407 has an elongated shape and is predominated with β-structure, mainly anti-parallel β-sheet and β-sandwich (Fig.14). Structural comparison of C-terminal domain using DALI server

shows some common structural features with some pore-forming toxins such as parasporin-2 from *Bacillus thuringiensis* (2ZTB; Z score 4.4) and epsilon toxin from *Clostridium perfringens* (1UYJ; Z score 3.9), both of which belong to aerolysin-type β-pore forming toxins. However, amino acid sequences of those toxins in this group show very low levels of similarity.

The final refined model was deposited in the Protein Data Bank (PDB) with the PDB accession code of 3WA1.

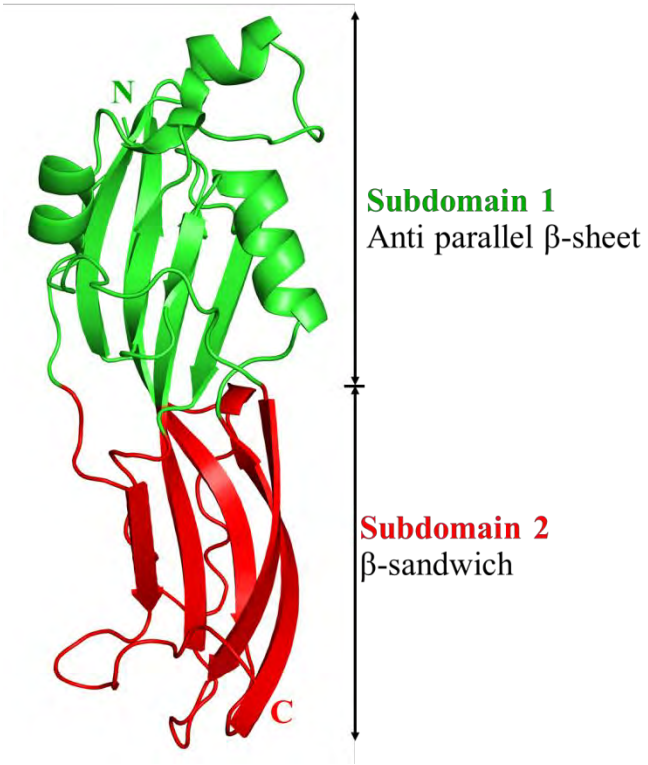

Figure 14. Cartoon representation of C-terminal domain. The C-terminal pore forming domain is composed of two subdomains, subdomains 1 and 2. Subdomain 1 (green) is an anti-parallel β-sheet and subdomain 2 (red) is a β-sandwich.

4. References

Baumann L & Baumann P (1989) Expression in *Bacillus subtilis* of the 51- and 42-kilodalton mosquitocidal toxin genes of Bacillus sphaericus. *Appl Environ Microbiol* **55**: 252-253.

Baumann P, Clark MA, Baumann L & Broadwell AH (1991) *Bacillus sphaericus* as a mosquito pathogen: properties of the organism and its toxins. *Microbiol Rev* **55**: 425-436.

Baumann P, Unterman BM, Baumann L, Broadwell AH, Abbene SJ & Bowditch RD (1985) Purification of the larvicidal toxin of *Bacillus sphaericus* and evidence for high-molecular-weight precursors. *J Bacteriol* **163**: 738-747.

Berry C, Hindley J, Ehrhardt AF, Grounds T, de Souza I & Davidson EW (1993) Genetic determinants of host ranges of *Bacillus sphaericus* mosquito larvicidal toxins. *J Bacteriol* **175**: 510-518.

Boonserm P, Moonsom S, Boonchoy C, Promdonkoy B, Parthasarathy K & Torres J (2006) Association of the components of the binary toxin from *Bacillus sphaericus* in solution and with model lipid bilayers. *Biochem Biophys Res Commun* **342**: 1273-1278.

Boonyos P, Soonsanga S, Boonserm P & Promdonkoy B (2010) Role of cysteine at positions 67, 161 and 241 of a *Bacillus sphaericus* binary toxin BinB. *BMB Rep* **43**: 23-28.

Bourgouin C, Delecluse A, de la Torre F & Szulmajster J (1990) Transfer of the toxin protein genes of *Bacillus sphaericus* into *Bacillus thuringiensis* subsp. *israelensis* and their expression. *Appl Environ Microbiol* **56**: 340-344.

Broadwell AH & Baumann P (1987) Proteolysis in the gut of mosquito larvae results in further activation of the *Bacillus sphaericus* toxin. *Appl Environ Microbiol* **53**: 1333-1337.

Charles JF, Nielson-LeRoux C & Delecluse A (1996) *Bacillus sphaericus* toxins: molecular biology and mode of action. *Annu. Rev. Entomol.* **41**: 451-472.

Charles JF, Silva-Filha MH, Nielsen-LeRoux C, Humphreys MJ & Berry C (1997) Binding of the 51- and 42-kDa individual components from the *Bacillus sphaericus* crystal toxin to mosquito larval midgut membranes from *Culex* and *Anopheles* sp. (Diptera: Culicidae). *FEMS Microbiol Lett* **156**: 153-159.

Chayaratanasin P, Moonsom S, Sakdee S, Chaisri U, Katzenmeier G & Angsuthanasombat C (2007) High level of soluble expression in *Escherichia coli* and characterisation of the cloned *Bacillus thuringiensis* Cry4Ba domain III fragment. *J Biochem Mol Biol* **40**: 58-64.

Clark MA & Baumann P (1990) Deletion analysis of the 51-kilodalton protein of the *Bacillus sphaericus* 2362 binary mosquitocidal toxin: construction of derivatives equivalent to the larva-processed toxin. *J. Bacteriol.* **172**: 6759-6763.

Cokmus C, Davidson EW & Cooper K (1997) Electrophysiological effects of *Bacillus sphaericus* binary toxin on cultured mosquito cells. *J. Invertebr. Pathol.* **69**: 197-204.

Darboux I, Nielsen-LeRoux C, Charles JF & Pauron D (2001) The receptor of *Bacillus sphaericus* binary toxin in *Culex pipiens* (Diptera: Culicidae) midgut: molecular cloning and expression. *Insect Biochem Mol Biol* **31**: 981-990.

Davidson EW (1988) Binding of the *Bacillus sphaericus* (Eubacteriales: Bacillaceae) toxin to midgut cells of mosquito (Diptera: Culicidae) larvae: relationship to host range. *J Med Entomol* **25**: 151-157.

Elangovan G, Shanmugavelu M, Rajamohan F, Dean DH & Jayaraman K (2000) Identification of the functional site in the mosquito larvicidal binary toxin of *Bacillus sphaericus* 1593M by site-directed mutagenesis. *Biochem. Biophys. Res. Commun.* **276**: 1048-1055.

Holm L & Rosenstrom P (2010) Dali server: conservation mapping in 3D. *Nucleic Acids Res* **38**: W545-549.

Kunthic T, Promdonkoy B, Srikhirin T & Boonserm P (2011) Essential role of tryptophan residues in toxicity of binary toxin from *Bacillus sphaericus. BMB Rep* **44**: 674-679.

Leahy DJ, Hendrickson WA, Aukhil I & Erickson HP (1992) Structure of a fibronectin type III domain from tenascin phased by MAD analysis of the selenomethionyl protein. *Science* **258**: 987-991.

Leslie AGW (1992) Recent changes to the MOSFLM package for processing film and image plate data. *Joint CCP4 + ESF-EAMCB Newsletter on Protein Crystallography* **No. 26**.

Limpanawat S, Promdonkoy B & Boonserm P (2009) The C-terminal domain of BinA is responsible for *Bacillus sphaericus* binary toxin BinA-BinB interaction. *Curr Microbiol* **59**: 509-513.

Matthews BW (1968) Solvent content of protein crystals. *J Mol Biol* **33**: 491-497.

Moonsom S, Chaisri U, Kasinrerk W & Angsuthanasombat C (2007) Binding characteristics to mosquito-larval midgut proteins of the cloned domain II-III fragment from the *Bacillus thuringiensis* Cry4Ba toxin. *J Biochem Mol Biol* **40**: 783-790.

Mrsny RJ, Volwerk JJ & Griffith OH (1986) Chem. Phys. Lipids. **39**: pp. 185-191.

Nicolas L, Lecroisey A & Charles JF (1990) Role of the gut proteinases from mosquito larvae in the mechanism of action and the specificity of the *Bacillus sphaericus* toxin. *Can J Microbiol* **36**: 804-807.

Nicolas L, Nielsen-Leroux C, Charles JF & Delecluse A (1993) Respective role of the 42- and 51-kDa components of the *Bacillus sphaericus* toxin overexpressed in *Bacillus thuringiensis*. *FEMS Microbiol Lett* **106**: 275-280.

Oei C, Hindley J & Berry C (1990) An analysis of the genes encoding the 51.4- and 41.9-kDa toxins of *Bacillus sphaericus* 2297 by deletion mutagenesis: the construction of fusion proteins. *FEMS Microbiol Lett* **60**: 265-273.

Oei C, Hindley J & Berry C (1992) Binding of purified *Bacillus sphaericus* binary toxin and its deletion derivatives to Culex quinquefasciatus gut: elucidation of functional binding domains. *J. Gen. Microbiol.* **138**: 1515-1526.

Opota O, Gauthier NC, Doye A, Berry C, Gounon P, Lemichez E & Pauron D (2011) *Bacillus sphaericus* binary toxin elicits host cell autophagy as a response to intoxication. *PLoS One* **6**: e14682.

Pauchet Y, Luton F, Castella C, Charles JF, Romey G & Pauron D (2005) Effects of a mosquitocidal toxin on a mammalian epithelial cell line expressing its target receptor. *Cell. Microbiol.* **7**: 1335-1344.

Promdonkoy B, Promdonkoy P & Panyim S (2008) High-level expression in *Escherichia coli,* purification and mosquito-larvicidal activity of the binary toxin from *Bacillus sphaericus*. *Curr Microbiol* **57**: 626-630.

Promdonkoy B, Promdonkoy P, Wongtawan B, Boonserm P & Panyim S (2008) Cys31, Cys47, and Cys195 in BinA are essential for toxicity of a binary toxin from *Bacillus sphaericus*. *Curr Microbiol* **56**: 334-338.

Promdonkoy B, Promdonkoy P, Audtho M, Tanapongpipat S, Chewawiwat N, Luxananil P & Panyim S (2003) Efficient expression of the mosquito larvicidal binary toxin gene from *Bacillus sphaericus* in *Escherichia coli. Curr Microbiol* **47**: 383-387.

Rice LM, Earnest TN & Brunger AT (2000) Single-wavelength anomalous diffraction phasing revisited. *Acta Crystallogr D Biol Crystallogr* **56**: 1413-1420.

Romao TP, de-Melo-Neto OP & Silva-Filha MH (2011) The N-terminal third of the BinB subunit from the *Bacillus sphaericus* binary toxin is sufficient for its interaction with midgut receptors in *Culex quinquefasciatus*. *FEMS Microbiol Lett* **321**: 167-174.

Schwartz JL, Potvin L, Coux F*, et al.* (2001) Permeabilization of model lipid membranes by *Bacillus sphaericus* mosquitocidal binary toxin and its individual components. *J. Membr. Biol.* **184**: 171-183.

Shanmugavelu M, Rajamohan F, Kathirvel M, Elangovan G, Dean DH & Jayaraman K (1998) Functional complementation of nontoxic mutant binary toxins of *Bacillus sphaericus* 1593M generated by site-directed mutagenesis. *Appl. Environ. Microbiol.* **64**: 756-759.

Silva-Filha MH & Peixoto CA (2003) Immunocytochemical localization of the *Bacillus sphaericus* binary toxin components in Culex quinquefasciatus (Diptera:Culicidae) larvae midgut. *Pestic. Biochem. Physiol.* **77**: 138-146.

Silva-Filha MH, Nielsen-Leroux C & Charles JF (1997) Binding kinetics of *Bacillus sphaericus* binary toxin to midgut brush-border membranes of *Anopheles* and *Culex* sp. mosquito larvae. *Eur J Biochem* **247**: 754-761.

Silva-Filha MH, Nielsen-LeRoux C & Charles JF (1999) Identification of the receptor for *Bacillus sphaericus* crystal toxin in the brush border membrane of the mosquito *Culex pipiens* (Diptera: Culicidae). *Insect Biochem Mol Biol* **29**: 711-721.

Singkhamanan K, Promdonkoy B, Chaisri U & Boonserm P (2010) Identification of amino acids required for receptor binding and toxicity of the *Bacillus sphaericus* binary toxin. *FEMS Microbiol Lett* **303**: 84-91.

Smith AW, Camara-Artigas A, Brune DC & Allen JP (2005) Implications of high-molecular-weight oligomers of the binary toxin from *Bacillus sphaericus*. *J. Invertebr. Pathol.* **88**: 27-33.

Tangsongcharoen C, Boonserm P & Promdonkoy B (2011) Functional characterization of truncated fragments of *Bacillus sphaericus* binary toxin BinB. *J Invertebr Pathol* **106**: 230-235.

Tapaneeyakorn S, Pornwiroon W, Katzenmeier G & Angsuthanasombat C (2005) Structural requirements of the unique disulphide bond and the proline-rich motif within the alpha4-alpha5 loop for larvicidal activity of the *Bacillus thuringiensis* Cry4Aa delta-endotoxin. *Biochem Biophys Res Commun* **330**: 519-525.

Winn MD, Ballard CC, Cowtan KD*, et al.* (2011) Overview of the CCP4 suite and current developments. *Acta Crystallogr D Biol Crystallogr* **67**: 235-242.

Wood WB (1966) Host specificity of DNA produced by *Escherichia coli*: bacterial mutations affecting the restriction and modification of DNA. *J. Mol. Biol.* **16**: 118-133.

5. Outputs:

5.1 Five publications have been produced during the three-year period grant as follows:

1. Singkhamanan, K., Promdonkoy, B,. Srikhirin, T. and **Boonserm, P.** (2013) Amino acid residues in the N-terminal region of the BinB subunit of *Lysinibacillus sphaericus* binary toxin play a critical role during receptor binding and membrane insertion. Accepted for publication on 28 May 2013, Impact Factor 2.064

2. Srisucharitpanit, K., Yao, M., Chimnaronk, S., Promdonkoy, B,. Tanaka, I. and **Boonserm, P.** (2013) Crystallization and preliminary X-ray crystallographic analysis of the functional form of BinB binary toxin from *Bacillus sphaericus*. *Acta Crystallogr Sect F Struct Biol Cryst Commun* **69(2)**, 170-173. Impact Factor 0.506

3. Srisucharitpanit, K., Inchana, P., Rungrod, A., Promdonkoy, B. and **Boonserm P.** (2012) Expression and purification of the active soluble form of *Bacillus sphaericus* binary toxin for structural analysis. *Protein Express Purif.* **82(2)**, 368-72. Impact Factor 1.587

4. Kunthic, T., Promdonkoy, B. Srikhirin, T. and **Boonserm, P.** (2011) Essential role of tryptophan residues in toxicity of binary toxin from *Bacillus sphaericus*. *BMB Reports*, **44(10)**, 674-9. Impact Factor 1.718

5. Tangsongcharoen, C., **Boonserm, P**. and Promdonkoy, B. (2011). Functional characterization of truncated fragments of *Bacillus sphaericus* binary toxin BinB. *J. Invert. Pathol.* **106(2)**, 230-5. Impact Factor 2.064

5.2 Five students working on this project were graduated during the three-year period as follows:

Ph.D. students

1. Miss Kamonnut Singkhamanan, Thesis title "Identification of the receptor binding motif of the binary toxin from *Bacillus sphaericus*"

2. Miss Kanokporn Srisucharitpanit, Thesis title "Structural determination of the mosquito-larvicidal binary toxin from *Bacillus sphaericus*"

M.Sc. students

1. Miss Chontida Tangsongcharoen, Thesis title "Functional characterization of truncated BinB fragments from *Bacillus sphaericus*"

2. Miss Thittaya Kunthic, Thesis title "Functional role of aromatic residues at the selected positions in BinA protein from *Bacillus sphaericus*"

3. Mr. Patarapong Inchana, Thesis title "Identification of domains important for membrane association of the *Bacillus sphaericus* binary toxin"

Appendix

Accepted Manuscript

Amino acid residues in the N-terminal region of the BinB subunit of *Lysinibacillus sphaericus* binary toxin play a critical role during receptor binding and membrane insertion

Kamonnut Singkhamanan, Boonhiang Promdonkoy, Toemsak Srikhirin, Panadda Boonserm

PII: S0022-2011(13)00086-4
DOI: http://dx.doi.org/10.1016/j.jip.2013.05.008
Reference: YJIPA 6444

To appear in: *Journal of Invertebrate Pathology*

Received Date: 5 May 2013
Accepted Date: 28 May 2013

Please cite this article as: Singkhamanan, K., Promdonkoy, B., Srikhirin, T., Boonserm, P., Amino acid residues in the N-terminal region of the BinB subunit of *Lysinibacillus sphaericus* binary toxin play a critical role during receptor binding and membrane insertion, *Journal of Invertebrate Pathology* (2013), doi: http://dx.doi.org/10.1016/j.jip.2013.05.008

Amino acid residues in the N-terminal region of the BinB subunit of *Lysinibacillus sphaericus* binary toxin play a critical role during receptor binding and membrane insertion

Kamonnut Singkhamanan[a,b], Boonhiang Promdonkoy[c], Toemsak Srikhirin[d], Panadda Boonserm[a,*]

[a]Institute of Molecular Biosciences, Mahidol University, Salaya Campus, 25/25 Putthamonthon 4 Road, Nakhon Pathom 73170, Thailand

[b]Department of Biomedical Sciences, Faculty of Medicine, Prince of Songkla University, 15 Kanchanawanich road, Hat Yai, Songkhla, 90110, Thailand

[c]National Center for Genetic Engineering and Biotechnology, National Science and Technology Development Agency, 113 Phahonyothin Road, Khlong Nueng, Khlong Luang, Pathum Thani 12120, Thailand

[d]Department of Physics, Faculty of Sciences, Mahidol University, Rama 6 Road, Bangkok 10400, Thailand

[*] Corresponding author: P. Boonserm, Phone: +662 4419003-7, Fax: +662 441 9906

E-mail: panadda.boo@mahidol.ac.th

Abstract

The binary toxin produced by *Lysinibacillus sphaericus* is composed of BinA and BinB subunits that work together in governing toxicity against mosquito larvae. BinA is proposed to be important for toxicity, whereas BinB has been shown to act as a specific receptor-binding component. The precise function of both subunits, however, is not well established. Here, we investigated the function of the N-terminal region of BinB subunit initially by introducing triple alanine substitutions at positions $_{35}$PEI$_{37}$ and $_{41}$FYN$_{43}$. Both block mutations abolished the larvicidal activity. Single point mutations (P35A, E36A, I37A, F41A, Y42A, N43A) were generated in order to identify amino acids that are critical for the toxin activity. Mosquito-larvicidal activity was significantly reduced in P35A, E36A, F41A and Y42A mutants. However, these mutants retained ability to form *in vitro* interaction with the BinA counterpart. Immunohistochemistry analysis revealed that P35A, F41A and N43A bind to the larval midgut membrane at comparable levels to that of the wild type BinB. In contrast, greatly reduced binding activity was observed in the Y42A, suggesting an important role of this residue in receptor binding. Alanine substitution at P35 resulted in a marked decrease in membrane penetration, indicating its functional importance for the membrane insertion. These results suggest the important roles of the N-terminal region of BinB in both the receptor recognition and the membrane interaction.

Keywords: *Lysinibacillus sphaericus*; binary toxin; BinB; mutagenesis; receptor binding; membrane penetration

1. Introduction

Lysinibacillus sphaericus (Ls) is a Gram-positive, spore-forming aerobic bacterium (Charles, et al., 1996). During the sporulation phase, a number of highly toxic strains of Ls synthesize a binary toxin which is a crystalline mosquito-larvicidal protein composed of 42 kDa (BinA) and 51 kDa (BinB) subunits. The larvicidal activity against *Culex* and *Anopheles* mosquito larvae is dependent on the presence of both BinA and BinB subunits (Oei, et al., 1990, Baumann, et al., 1991, Nicolas, et al., 1993). This toxin, however, is weakly toxic or non-toxic to *Aedes* larvae (Berry, et al., 1993).

Following larval ingestion of protein inclusions, crystalline inclusions are dissolved in alkaline conditions of the larval midgut. Subsequently, BinA and BinB protoxins are activated by midgut proteases to generate the active proteins of approximately 39 and 43 kDa, respectively (Broadwell & Baumann, 1987, Nicolas, et al., 1990). The activated binary toxin, especially the BinB component, then binds to a specific receptor located on the surface of midgut epithelium cell of susceptible larvae (Davidson, 1988, Silva-Filha, et al., 1997). The binary toxin receptor has been identified as 60-kDa α-glucosidase (Cpm1) which is attached to the cell membrane via a glycosyl-phosphatidyl inositol (GPI) anchor (Silva-Filha, et al., 1999, Darboux, et al., 2001). Nevertheless, detailed mechanism of action of the binary toxin remains elusive, mainly due to the lack of the structural information. Analysis of the amino acid sequences of BinA and BinB reveals a negligible level of similarity with any protein with established crystal structure, however, they are homologous to each other, with a 25% amino acid identity and a 40% similarity (Promdonkoy, et al., 2008). Despite their similarity, these two proteins have distinct functions, i.e., BinB is responsible for receptor binding, whereas BinA presumably acts as a toxic component (Oei, et al., 1992, Charles, et al., 1997, Shanmugavelu, et al., 1998, Elangovan, et al., 2000).

Although the structural basis of the binary toxin is unavailable, some amino acids residues have been subjected to mutagenesis to investigate their roles on the mosquitocidal activity. Examples of those are some amino acids located in the N- and C-terminal ends of both binary toxin components (Shanmugavelu, et al., 1998). In addition, it has been shown that the deletions of some amino acids at the N- and C-terminal ends of the BinA and BinB proteins abolished the toxicity. The effects of these mutations on the biological activity of the binary toxin are not completely understood. Particularly, BinB has been shown to confer the specificity by binding to a specific receptor. However, its binding mechanism is still unknown. Earlier studies with the binary toxin suggested that the N-terminal region of BinB is crucial for receptor binding in gut epithelial cells (Oei, et al., 1992). Consistent with the above data, recent studies showed that multiple elements within the N-terminal half of BinB are required for the receptor binding (Romao, et al., 2011, Tangsongcharoen, et al., 2011). Nevertheless, the C-terminal half of BinB, as well as its N-terminal half, also has been shown to participate in the larval gut membrane binding (Tangsongcharoen, et al., 2011).

Examination of the toxin deletion derivatives BinB revealed that 34 amino acids could be removed from the N-terminus without affecting the toxicity and regional binding to the larval gut. However, a further deletion of 41 amino acids from the N-terminal region rendered the toxin inactive (Clark & Baumann, 1990). Moreover, replacements of amino acids located at the N-terminus of BinB revealed the crucial importance of residues $_{32}$YNL$_{34}$ and $_{38}$SKK$_{40}$ for the toxicity (Elangovan, et al., 2000). On the basis of the deletion and mutagenic data described earlier, it is conceivable that that amino acids at positions around 30-40 in the N-terminal region of BinB may play an important role, either structurally or functionally, for the toxicity of the binary toxin.

To further investigate the role of amino acids at the N-terminal region of BinB in governing the larvicidal activity, here we performed amino acid substitutions at residues

spanning positions 35-37 and 41-43. Bioassays, receptor and membrane binding analyses demonstrated that residues P35, F41 and Y42 of BinB are crucial for the larvicidal activity, especially during the steps of membrane and receptor binding.

2. Materials and Methods

2.1 Bacterial strains, plasmids, and oligonucleotides

Escherichia coli K-12 JM109 and *E. coli* BL21 (DE3) pLysS (Novagen, USA) were used as host strains for mutagenesis and for protein expression of the recombinant plasmid containing truncated *binB* gene, respectively. A recombinant plasmid pET-tbinB expressing the 43-kDa truncated BinB as previously described (Boonyos, et al., 2010) was used as a template for mutagenesis. Mutagenic oligonucleotide primers were purchased from Sigma Proligo (Singapore). Each primer was designed to introduce or abolish a restriction endonuclease recognition site in order to differentiate between the wild-type and mutant plasmids (Table 1).

2.2 Construction of BinB mutant plasmids

All mutant plasmids were generated based on polymerase chain reaction using a high fidelity *Pfu* DNA polymerase following the procedure of the QuikChange™ site-directed mutagenesis method (Stratagene). PCR products were treated with *Dpn*I to get rid of the DNA templates and then transformed into *E. coli* JM109 competent cells. The recombinant plasmids were extracted and the desired mutations were selected by restriction endonuclease digestion, and further confirmed by automated DNA sequencing at Macrogen Inc, Korea.

2.3 Protein preparation

To express the proteins, each recombinant plasmid from *E. coli* JM109 was re-transformed into *E. coli* BL21(DE3) pLysS and grown at 37 ºC in a Luria-Bertani medium containing ampicillin 100 µg/ml and chloramphenicol 34 µg/ml until OD_{600} of the culture reached 0.4. Cell cultures were then induced with 0.1 mM isopropyl-β-D-thiogalactopyranoside (IPTG) and further incubated at 37 ºC for 5 h. Cells were collected by centrifugation and then lysed using a French Pressure Cell. Protein inclusions were collected after centrifugation and partially purified using differential centrifugation as described previously (Singkhamanan, et al., 2010). The identity of mutant BinB inclusions was further confirmed by Western-blot analysis using polyclonal anti-BinB as described previously (Singkhamanan, et al., 2010).

Protein inclusions at a concentration about 2-3 mg/ml were solubilized in 25 mM NaOH, 5 mM DTT at 37 ºC for 15 min. Solubilized protein was subjected to stepwise dialysis against 50 mM Na_2CO_3, pH 10.0 at 4 ºC overnight and further purified by gel filtration using a superdex 200HR 10/300 column (Amersham Pharmacia Biotech). Protein concentration was determined by the method of Bradford using Bio-Rad protein assay reagent with bovine serum albumin as a standard.

2.4 Larvicidal activity assay

Larvicidal activity assays were tested against the 2nd-instar *Culex quinquefasciatus* mosquito larvae in duplicate and at least three independent experiments were performed. Mixtures of equal amounts of BinA wild-type inclusions and BinB wild-type or mutant inclusions were diluted in 1 ml of water to make a series of two-fold serial dilutions, from 64 µg/ml to 0.125 µg/ml. Then 1 ml of each dilution was added to a well of a 24-well tissue culture plate containing 10 larvae in 1 ml water. The BinA-BinB wild-type inclusion mixture

was used as a positive control, while BinB wild-type inclusions were used as a negative control. After 48 hours of incubation, the mortality of the larvae was recorded and the LC_{50} was analyzed by Probit analysis (Finney, 1971).

2.5 Far-Western dot blot analysis

Various amounts of purified truncated BinA (0.08 – 10 µg) were immobilized on strips of nitrocellulose membrane which were soaked in phosphate buffered saline (PBS) by using a Bio-Dot Microfiltration Apparatus (Bio-RAD) (Limpanawat, et al., 2009). The protein-bound membranes were blocked in 5% skimmed milk at 4 ºC overnight. Then, 20 µg/ml of purified wild-type BinB or its mutants in 5% skimmed milk was overlaid on each strip for 1 hour and subsequently washed with 0.1% Tween-20 in PBS (PBS-T20) 3 times, for 5 min each time. Bound BinB was detected by probing with polyclonal rabbit anti-BinB (1:20,000) for 1 hour. Unbound antibody was removed by washing 3 times with PBS-T20, 5 min each time. The membranes were incubated with goat anti-rabbit IgG alkaline phosphatase conjugate (1:5,000) as a secondary antibody. Excess antibody was removed by washing twice with PBS-T20, 5 min each, followed by washing with PBS for 5 min. The immunoreactive signals were detected by using the ECL plus kit (GE healthcare).

2.6 In vitro binding assays via immunohistochemistry

Histological sections of the 4th-instar *C. quinquefasciatus* larval gut tissue were prepared and immunohistochemical detection was performed following protocols described previously (Chayaratanasin, et al., 2007, Moonsom, et al., 2007, Singkhamanan, et al., 2010). Briefly, endogenous peroxidase activity in the gut tissue was blocked by incubating the sections in PBS containing 0.1% TritonX-100 and 3% H_2O_2 for 30 min, followed by washing 3 times with 0.1% TritonX-100 in PBS (T-PBS), 15 min each. After blocking non-specific

binding sites with normal goat serum (1:200) (Vector) for 45 min and washing excess serum, the sections were incubated with the purified wild-type or mutant BinB at a concentration of 20 µg/ml for 45 min. After washing 3 times with T-PBS, the sections were incubated with polyclonal rabbit anti-BinB (1:10,000) for 45 min. After washing with T-PBS, biotin-Goat anti-rabbit IgG (1:200) (Invitrogen) was added and further incubated for 45 min. The slides containing sections were then washed 3 times with T-PBS and incubated with HRP-Streptavidin conjugate (1:500) (Invitrogen) for 45 min. After washing with T-PBS, immunocomplexes were detected by incubation with 3,3'-diaminobenzidine (DAB, SK-400, Vector) for 2 min and the reaction was stopped by rinsing with distilled water. The apparent brown color observed under a light microscope indicated positive staining of the bound toxin.

2.7 Membrane insertion assay by Langmuir-Blodgett method

The interaction of BinB and its mutants with 2-Dimyristoylrac-glycero-3-phosphocholine (DMPC) monolayer was monitored by using a KSV 2,000 Langmuir-Blodgett trough (KSV, Finland) following protocols described previously (Kunthic, et al., 2011). Briefly, 15 nmol of DMPC in chloroform was spread on 50 mM Na_2CO_3 buffer, pH 10 which was used as an aqueous subphase. After lipid monolayer was rested for 15-20 min to allow the complete evaporation of the solvent, it was compressed at the speed of 10 mm/min until the surface pressure reached 10 mN/m and the monolayer was kept constant at this surface pressure by using the constant surface pressure mode. After that, the sample containing the protein (5 nmol) was injected at 1,000 s by L-shaped syringe right underneath the monolayer forming area. Protein insertion was monitored by an increase of the mean molecule area as a function of time. All experiments were performed at room temperature and each experiment was repeated at least three times. Only buffer was injected into the subphase as a control

3. Results and discussion

3.1 Effects of alanine substitutions at positions 35-37 and 41-43 on protein production and larvicidal activity

Earlier studies have shown that the deletion of 34 amino acids from the N-terminus of BinB did not affect the toxicity and regional binding to the larval gut, while further deletion up to 41 amino acids from the N-terminal end totally abolished the toxicity (Oei, et al., 1992). The functional importance of the N-terminus of BinB was further revealed from the loss of toxicity when amino acids at positions $_{32}$YNL$_{34}$ and $_{38}$SKK$_{40}$ from *B. sphaericus* 1593M were substituted by AAA (Elangovan, et al., 2000). Based upon the secondary structure prediction, amino acid residues 1-34 and 35-45 have been proposed to adopt a random coil and a helical structure, respectively (Elangovan, et al., 2000). Thus, certain mutations at these N-terminal regions may disturb the structural folding or functional sites of BinB protein. In this study, two additional block mutations ($_{35}$PEI$_{37}$→$_{35}$AAA$_{37}$ and $_{41}$FYN$_{43}$→$_{41}$AAA$_{43}$) of the amino acid residues flanking those N-terminal regions were initially performed to test the possible functional significance of these selected BinB regions.

Both block mutants were expressed in *E. coli* BL21(DE3) pLysS as inclusions upon IPTG induction, with expression levels similar to that of the wild-type BinB (Fig. 1A), suggesting that the mutations do not affect the protein expression of BinB. Upon immunological detection with polyclonal-anti BinB by Western blot analysis, a major band at 43 kDa reacted specifically with anti-BinB was observed in both block mutants (data not shown), confirming the immunological identity of the BinB mutant proteins.

Mosquito-larvicidal activity of each block mutant was tested by feeding the mutant inclusions to *Culex quinquefasciatus* larvae together with the wild type-BinA inclusions. Both block mutations, $_{35}$PEI$_{37}$→$_{35}$AAA$_{37}$ and $_{41}$FYN$_{43}$→$_{41}$AAA$_{43}$ were inactive (Table 2). Thereafter, the residues in these two regions were individually substituted with alanine

(P35A, E36A, I37A, F41A, Y42A, N43A) to define amino acids important for the larvicidal activity. All these mutants were produced as inclusion bodies at comparable levels to that of the wild-type BinB (Fig. 1B). Of these alanine substitutions, mosquito-larvicidal activity was significantly reduced for P35A, E36A, F41A, and Y42A mutants (Table 2). Further analyses were therefore focused on these mutants, while N43A was used as a representative of the active mutants.

Any major structural change induced by the mutations was explored by using the intrinsic fluorescence spectroscopy. Tryptophan emission spectra of the mutants were not significantly different from that of the BinB wild type (data not shown), suggesting that alanine substitutions at P35, E36, F41 and Y42 are unlikely to perturb the overall conformation of the toxin.

3.2 Single alanine substitutions at positions 35-37 and 41-43 in BinB did not affect BinA-BinB interaction

As the full activity of the binary toxin is achieved only when both BinA and BinB components are present together, the interaction between BinA and BinB supposedly is one of the critical steps during the pathological process. In this study, the effect of single mutations at positions 35-37 and 41-43 on the *in vitro* interaction between BinB mutants and the wild-type BinA was assessed by Far-Western dot blot analysis. The BinA protein was immobilized on the membrane which was then incubated with the purified wild-type BinB or one of the mutant proteins. The BinA-BinB bound complexes were further detected by probing with anti-BinB. The results showed that all BinB mutants could interact with the immobilized BinA, giving comparable intensity to that of the wild-type protein (Fig. 2). These results indicated that none of these mutations disrupted inter-molecular BinA-BinB

interaction. Therefore, the dramatic decrease in toxicity of mutants P35A, E36A, F41A and Y42A may be caused by another defect in the pathological process.

3.3 Single alanine substitution at position Y42 in BinB affects receptor binding

Evidence has been provided that BinB is the binding component of the binary toxin by interacting with a specific receptor on the surface of midgut epithelium cells (Davidson, 1988, Silva-Filha, et al., 1997). Immunohistochemistry assay was used to test the effect of BinB mutations on the binding to the midgut of susceptible *C. quinquefasciatus* larvae. The localization of the BinB wild-type protein on the midgut section was demonstrated as an intense brown staining after probing with anti-BinB, while a faint signal was observed in the negative control (without BinB overlay) (Fig. 3). An intense staining was also observed from the section incubated with mutants P35A, F41A and N43A, whereas a very weak signal was detected in the Y42A mutant. These results suggest that P35A, F41A and N43A mutants still retain the ability to bind to the apical microvilli of larval midgut. Despite the preserved receptor binding activity, the larvicidal activity of P35A and F41A was significantly reduced. These data suggest that, after the BinB- receptor interaction, P35 and F41 residues may contribute to a subsequent step of cytotoxic process. Of these mutants, the receptor binding activity was greatly reduced by the mutation of Y42 which correlates well with its loss of toxicity. Previously, we reported the crucial role of Y150, particularly its aromaticity, in receptor binding of BinB (Singkhamanan, et al., 2010). Herein, Y42 was also found to be crucial for the binding to apical brush border microvilli of susceptible larvae. Taken together, data suggest that BinB receptor binding could be mediated by Y42 and Y150.

Although we have demonstrated previously that the receptor-binding sites of BinB may encompass several segments as observed from the ability of both N- and C-terminally truncated BinB fragments to bind to the susceptible larval gut membrane (Tangsongcharoen,

et al., 2011), single point mutations at Y42 and Y150 appeared to be sufficient to severely reduce and abolish the toxicity, respectively. These observations thus seem to indicate that these two tyrosine residues may provide the critical interaction, presumably via high affinity binding, with the receptor that may trigger the subsequent steps of the intoxication process. It also remains possible that these two aromatic residues could participate in the membrane interaction of the BinB component.

3.4 Single alanine subsitutons at positions 35-37 and 41-43 in BinB affect membrane insertion

Membrane-protein interaction generally promotes a cascade of events leading to pathological effects of most bacterial toxins. To explore the effect of BinB mutations on the protein penetration into the phospholipid membrane, a Langmuir membrane system was used. The Langmuir membrane system used here is composed of a 2-dimyristoyl-rac-glycero-3-phosphocholine (DMPC) monolayer generated on top of a buffered aqueous subphase. Although this phospholipid monolayer model may not represent the real biological membrane of mosquito-larval midgut, it has been effectively used as a receptor-free lipid membrane for monitoring protein-membrane interaction of the binary toxin subunits (Boonserm, et al., 2006, Kunthic, et al., 2011). As the liquid condensed phase was observed, which is a fluid stage of DMPC monolayer being relevant to biological membranes, the surface pressure was subsequently kept constant at 10 mN/m throughout this experiment. When the protein sample was injected into the aqueous subphase with a given time to interact with the lipid monolayer, the degree of membrane penetration was measured as a time-dependent increase of the mean molecular area. The results demonstrated three distinct groups of membrane penetration behaviors of BinB mutants (Fig. 4). The first group (F41A and N43A) showed a greater extent of membrane penetration when compared with that of the BinB wild type, whereas a

lower extent of membrane penetration was found in the second group (E36A, I37A and Y42A) and the lowest extent of membrane penetration was observed in the third group (P35A and BinA) (Fig. 4). The fact that the F41A efficiently penetrated the lipid monolayer despite its reduced larvicidal activity suggests that the compromised biological activity of the F41A was not due to the impaired lipid-membrane interaction. In contrast, the reduced membrane penetration ability of P35A, E36A and Y42A was correlated with the decrease of larvicidal activity of these mutants. It is noteworthy that P35A and BinA showed a much lower rate of membrane penetration when compared with BinB and other BinB mutants. Previously, an incapability of BinA to insert into the artificial lipid monolayer was reported (Boonserm, et al., 2006). These data thus indicate, albeit using a model membrane, that P35 plays a key role in the lipid membrane penetration, while E36 and Y42 may be partly involved in this step. According to the secondary structure prediction, P35 and E36 have been proposed to locate at the end of a loop preceding a helical structure at the N-terminal region of BinB (Elangovan, et al., 2000). Particularly, P35 seems to confer the structural integrity of the loop which may be required for the lipid membrane insertion. In agreement with our finding, the necessity of the structural integrity of the loop joining the α4-α5 transmembrane hairpin for an efficient membrane insertion of the Cry4Aa mosquito-larvicidal toxin has also been reported (Tapaneeyakorn, et al., 2005). However, herein the precise structural role of the P35 and E36 residues await further confirmation by the crystal structure of the BinB protein. Although previous evidence has provided an important clue of the N-terminal region of BinB for the receptor recognition, here we demonstrate that the N-terminus of BinB is also involved in the membrane interaction.

Acknowledgements

We would like to thank Dr. Urai Chaisri for assistance with immunohistochemistry technique, Ms. Chanikarn Boonchoy and Ms. Monruedee Srisaisup for technical assistance.

This work was supported by the Thailand Research Fund and the National Center for Genetic Engineering and Biotechnology, National Science and Technology Development Agency, Thailand. K.S. was supported by the Development and Promotion of Science and Technology Talent (DPST) scholarship.

References

Baumann, P., Clark, M.A., Baumann, L., Broadwell, A.H., 1991. *Bacillus sphaericus* as a mosquito pathogen: properties of the organism and its toxins. Microbiol. Rev. 55**,** 425-436.

Berry, C., Hindley, J., Ehrhardt, A.F., Grounds, T., de, S., I, Davidson, E.W., 1993. Genetic determinants of host ranges of *Bacillus sphaericus* mosquito larvicidal toxins. J. Bacteriol. 175**,** 510-518.

Boonserm, P., Moonsom, S., Boonchoy, C., Promdonkoy, B., Parthasarathy, K., Torres, J., 2006. Association of the components of the binary toxin from *Bacillus sphaericus* in solution and with model lipid bilayers. Biochem. Biophys. Res. Commun. 342**,** 1273-1278.

Boonyos, P., Soonsanga, S., Boonserm, P., Promdonkoy, B., 2010. Role of cysteine at positions 67, 161 and 241 of a *Bacillus sphaericus* binary toxin BinB. BMB Rep. 43**,** 23-28.

Broadwell, A.H., Baumann, P., 1987. Proteolysis in the gut of mosquito larvae results in further activation of the *Bacillus sphaericus* toxin. Appl. Environ. Microbiol. 53, 1333-1337.

Charles, J.F., Nielson-LeRoux, C., Delecluse, A., 1996. *Bacillus sphaericus* toxins: molecular biology and mode of action. Annu. Rev. Entomol. 41, 451-472.

Charles, J.F., Silva-Filha, M.H., Nielsen-LeRoux, C., Humphreys, M.J., Berry, C., 1997. Binding of the 51- and 42-kDa individual components from the *Bacillus sphaericus* crystal toxin to mosquito larval midgut membranes from *Culex* and *Anopheles* sp. (Diptera: Culicidae). FEMS Microbiol. Lett. 156, 153-159.

Chayaratanasin, P., Moonsom, S., Sakdee, S., Chaisri, U., Katzenmeier, G., Angsuthanasombat, C., 2007. High level of soluble expression in *Escherichia coli* and characterisation of the cloned *Bacillus thuringiensis* Cry4Ba domain III fragment. J. Biochem. Mol. Biol. 40**,** 58-64.

Clark, M.A., Baumann, P., 1990. Deletion analysis of the 51-kilodalton protein of the *Bacillus sphaericus* 2362 binary mosquitocidal toxin: construction of derivatives equivalent to the larva-processed toxin. J. Bacteriol. 172**,** 6759-6763.

Darboux, I., Nielsen-LeRoux, C., Charles, J.F., Pauron, D. 2001. The receptor of *Bacillus sphaericus* binary toxin in *Culex pipiens* (Diptera: Culicidae) midgut: molecular cloning and expression. Insect Biochem. Mol. Biol. 31, 981-990.

Davidson, E.W., 1988. Binding of the *Bacillus sphaericus* (Eubacteriales: Bacillaceae) toxin to midgut cells of mosquito (Diptera: Culicidae) larvae: relationship to host range. J. Med. Entomol. 25**,** 151-157.

Elangovan, G., Shanmugavelu, M., Rajamohan, F., Dean, D.H., Jayaraman, K., 2000. Identification of the functional site in the mosquito larvicidal binary toxin of *Bacillus sphaericus* 1593M by site-directed mutagenesis. Biochem. Biophys. Res. Commun. 276**,** 1048-1055.

Finney, D., 1971. Probit Analysis. 3 edn.Cambridge University Press, London, UK.

Kunthic, T., Promdonkoy, B., Srikhirin, T., Boonserm, P., 2011. Essential role of tryptophan residues in toxicity of binary toxin from *Bacillus sphaericus*. BMB Rep. 44, 674-679.

Limpanawat, S., Promdonkoy, B., Boonserm, P., 2009. The C-terminal domain of BinA is responsible for *Bacillus sphaericus* binary toxin BinA-BinB interaction. Curr. Microbiol. 59**,** 509-513.

Moonsom, S., Chaisri, U., Kasinrerk, W., Angsuthanasombat, C., 2007. Binding characteristics to mosquito-larval midgut proteins of the cloned domain II-III fragment from the *Bacillus thuringiensis* Cry4Ba toxin. J. Biochem. Mol. Biol. 40, 783-790.

Nicolas, L., Lecroisey, A., Charles, J.F., 1990. Role of the gut proteinases from mosquito larvae in the mechanism of action and the specificity of the *Bacillus sphaericus* toxin. Can. J. Microbiol. 36, 804-807.

Nicolas, L., Nielsen-Leroux, C., Charles, J.F., Delecluse, A., 1993. Respective role of the 42- and 51-kDa components of the *Bacillus sphaericus* toxin overexpressed in *Bacillus thuringiensis*. FEMS Microbiol. Lett. 106**,** 275-280.

Oei, C., Hindley, J., Berry, C., 1990. An analysis of the genes encoding the 51.4- and 41.9-kDa toxins of *Bacillus sphaericus* 2297 by deletion mutagenesis: the construction of fusion proteins. FEMS Microbiol. Lett. 60**,** 265-273.

Oei, C., Hindley, J., Berry, C., 1992. Binding of purified *Bacillus sphaericus* binary toxin and its deletion derivatives to *Culex quinquefasciatus* gut: elucidation of functional binding domains. J. Gen. Microbiol. 138**,** 1515-1526.

Promdonkoy, B., Promdonkoy, P., Panyim, S., 2008. High-level expression in *Escherichia coli*, purification and mosquito-larvicidal activity of the binary toxin from *Bacillus sphaericus*. Curr. Microbiol. 57**,** 626-630.

Romao, T.P., de-Melo-Neto, O.P., Silva-Filha, M.H., 2011. The N-terminal third of the BinB subunit from the *Bacillus sphaericus* binary toxin is sufficient for its interaction with midgut receptors in *Culex quinquefasciatus*. FEMS Microbiol. Lett. 321, 167-174.

Shanmugavelu, M., Rajamohan, F., Kathirvel, M., Elangovan, G., Dean, D.H., Jayaraman, K., 1998. Functional complementation of nontoxic mutant binary toxins of *Bacillus sphaericus* 1593M generated by site-directed mutagenesis. Appl. Environ. Microbiol. 64**,** 756-759.

Silva-Filha, M.H., Nielsen-Leroux, C. Charles, J.F., 1997. Binding kinetics of *Bacillus sphaericus* binary toxin to midgut brush-border membranes of *Anopheles* and *Culex* sp. mosquito larvae. Eur. J. Biochem. 247, 754-761.

Silva-Filha, M.H., Nielsen-LeRoux, C., Charles, J.F., 1999. Identification of the receptor for *Bacillus sphaericus* crystal toxin in the brush border membrane of the mosquito *Culex pipiens* (Diptera: Culicidae). Insect Biochem. Mol. Biol. 29**,** 711-721.

Singkhamanan, K., Promdonkoy, B., Chaisri, U., Boonserm, P., 2010. Identification of amino acids required for receptor binding and toxicity of the *Bacillus sphaericus* binary toxin. FEMS Microbiol. Lett. 303**,** 84-91.

Tangsongcharoen, C., Boonserm, P., Promdonkoy, B., 2011. Functional characterization of truncated fragments of *Bacillus sphaericus* binary toxin BinB. J. Invertebr. Pathol. 106, 230-235.

Tapaneeyakorn, S., Pornwiroon, W., Katzenmeier, G., Angsuthanasombat, C., 2005. Structural requirements of the unique disulphide bond and the proline-rich motif within the alpha4-alpha5 loop for larvicidal activity of the *Bacillus thuringiensis* Cry4Aa delta-endotoxin. Biochem. Biophys. Res. Commun. 330, 519-525.

Figure legends

Figure 1. 12% SDS-polyacrylamide gel of BinB wild-type and mutant proteins. *E. coli* cells harbouring the 43-kDa truncated *binB* gene (WT) or mutated plasmids were induced by 0.1 mM IPTG for 5 hours. Cells were lysed using a French Pressure cell and protein inclusions were partially purified by repeated washing and centrifugation. Panel A represents partially purified inclusion bodies of block mutants, $_{35}PEI_{37}\rightarrow{}_{35}AAA_{37}$, $_{41}FYN_{43}\rightarrow{}_{41}AAA_{43}$ and panel B represents partially purified inclusion bodies of single-point mutants, P35A, E36A, I37A, F41A, Y42A, and N43A. M represents protein standard markers. Arrows indicate the BinB protein bands.

Figure 2. BinA-BinB interaction detected by Far-Western dot blot analysis. Various amounts of BinA protein were immobilized on a membrane and then overlaid with BinB wild-type or its mutant protein at a concentration of 20 µg/ml. Negative control was BinA alone without overlaid BinB protein. BinA-BinB complexes were detected by incubating the membrane with rabbit anti-BinB followed by goat anti-rabbit IgG conjugated with alkaline phosphatase.

Figure 3. Immunohistrochemical staining of the 4th-instar *C. quinquefasciatus* larval midgut tissues. Slides were incubated with either BinB wild type (WT) or P35A, F41A, Y42A, and N43A mutants at a concentration of 20 µg/ml. Negative control was done by incubating with carbonate buffer. MV represents microvilli.

Figure 4. The insertion ability of BinB wild-type and its mutant proteins into DMPC monolayer using the Langmuir-Blodgett Trough. The degree of membrane insertion was monitored by an increase of the mean molecule area as a function of time under a constant surface pressure. All data were subtracted from the negative control (buffer only).

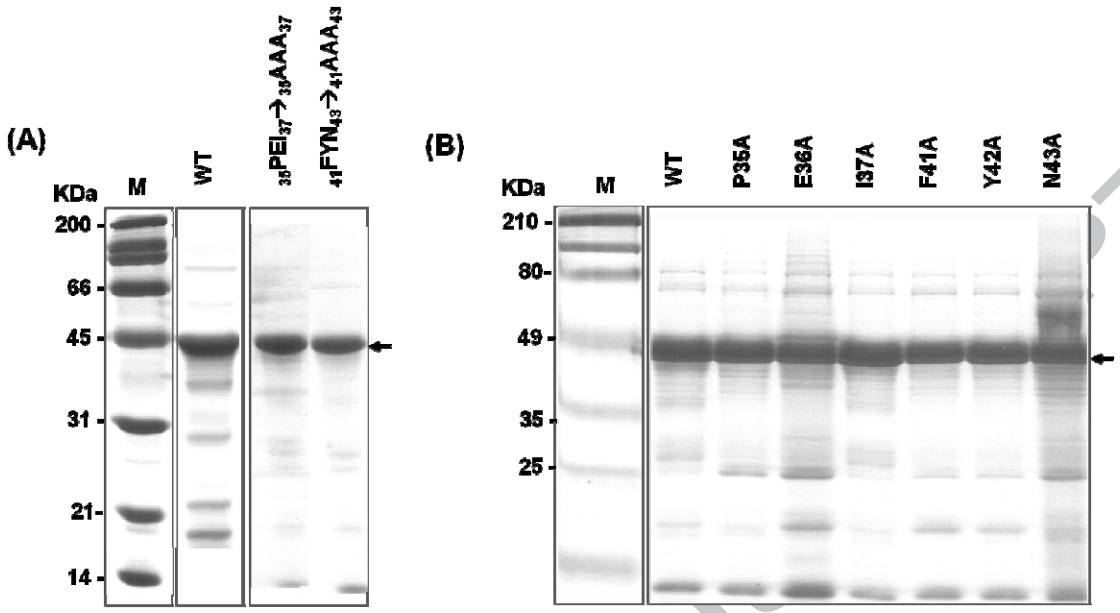

434

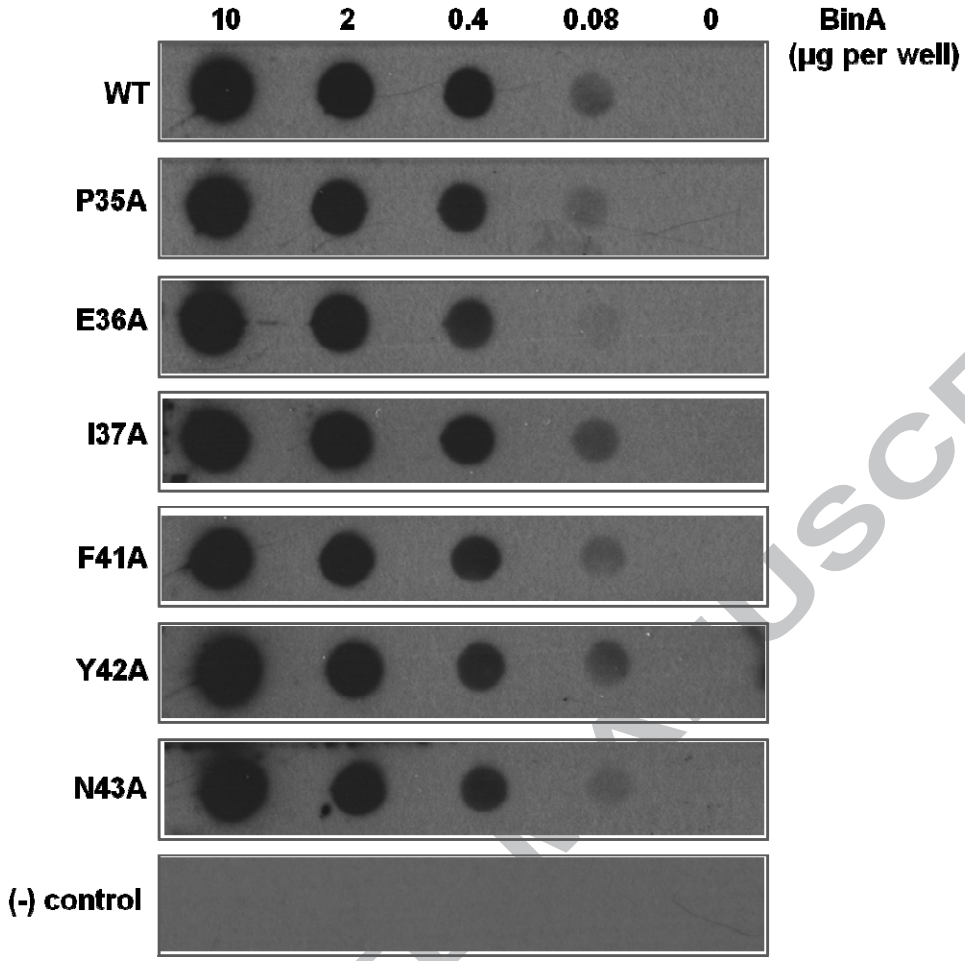

435

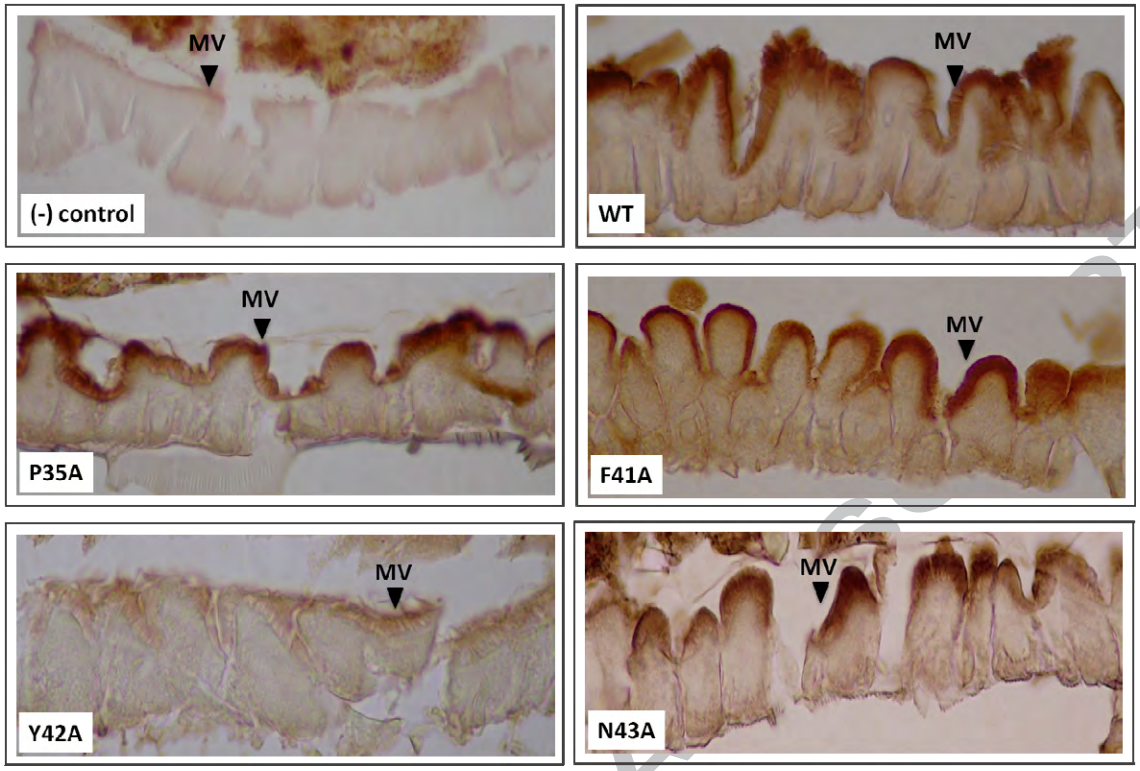

436

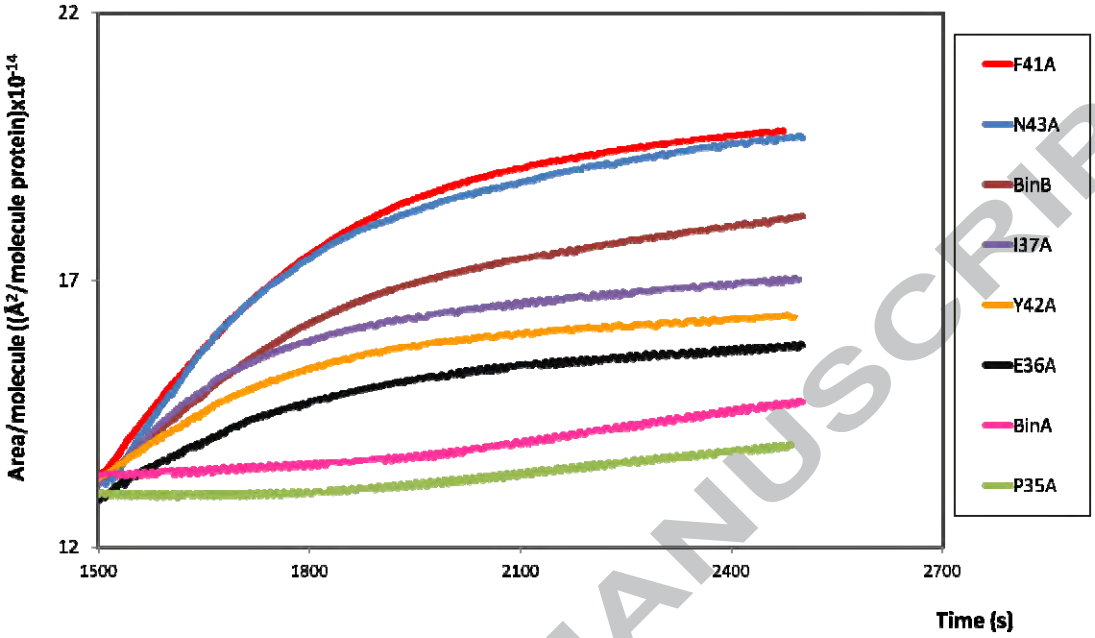

437

Table 1. Oligonucleotide primers for generation of BinB mutants

Primer	Sequence	Restriction enzyme
35PEI37f	5′TAGCAACCTT**G**CGG**CCG**CATCAAAAAAATTTTATA3′	*Eae*I
35PEI37r	5′AAAATTTTTTTGAT**GCGG**CCG**C**AAGGTTGCTAGCC3′	
41FYN43f	5′TATCAAAAAAA**GCAGCTGC**CCTTAAGAATAAATAT3′	*Pvu*II
41FYN43r	5′ATTCTTAAGG**GCAGCTGC**TTTTTTTGATATTTCTG3′	
P35Af	5′GCTAGCAACCT**GGCC**GAAATATCAAAAAAA3′	*Cfr*I
P35Ar	5′TTTTTTGATATTT**CGGCC**AGGTTGCTAGCC3′	
E36Af	5′AGCAACCTTCC**GGCC**ATATCAAAAAAATTT3′	*Cfr*I
E36Ar	5′ATTTTTTTGATAT**GG**CC**G**GAAGGTTGCTAG3′	
I37Af	5′AACCTTCCAGAA**GCTT**CAAAAAAATTTTAT3′	*Hind*III
I37Ar	5′TAAAATTTTTTTGA**AGCTT**CTGGAAGGTTG3′	
F41Af	5′ATATCAAAAAA**GGCC**TATAACCTTAAGAAT3′	*Stu*I
F41Ar	5′CCTAAGGTTATA**GGCC**TTTTTTGATATTTC3′	
Y42Af	5′TCAAAAAAATT**CGCG**AACCTTAAGAATAAA3′	*Nru*I
Y42Ar	5′TCTTAAGGTT**CGCG**AATTTTTTTGATATTT3′	
N43Af	5′ATATCAAAAAAA**TTTTA**TGCCCTTAAGAAT3′	-
N43Ar	5′CTTAAGGGC**ATAAA**ATTTTTTTGATATTTC3′	

*Recognition sites introduced in the primers for restriction endonuclease analysis are underlined. Mutated nucleotides are shown in bold; f and r represent forward and reverse primers, respectively.

Table 2. Mosquito larvicidal activity of the wild-type and mutant toxins against the 2nd-instar *C. quinquefasciatus* larvae

Protein	LC_{50} (µg/ml)
BinB	Inactive
BinA + BinB wild type	0.36 (0.31-0.42)
BinA+ $_{35}PEI_{37} \rightarrow {}_{35}AAA_{37}$	Inactive
BinA+ $_{41}FYN_{43} \rightarrow {}_{41}AAA_{43}$	Inactive
BinA + P35A	1.45 (1.24-1.68)
BinA + E36A	1.75 (1.51-2.02)
BinA + I37A	0.51 (0.43-0.60)
BinA + F41A	3.38 (2.92-3.90)
BinA + Y42A	2.43 (2.10-2.84)
BinA + N43A	0.49 (0.42-0.56)

BinA and BinB inclusions were mixed at 1:1 molar ratio. Mortality was recorded after feeding toxins for 48 h. LC_{50} was calculated using Probit analysis (Finney, 1971) from at least three independent experiments. The fiducial limits at 95% confidence are shown in parentheses. Samples with no mortality at high concentration (32 µg/ml) of toxin are regarded as inactive.

Acta Crystallographica Section F
Structural Biology and Crystallization Communications
ISSN 1744-3091

Crystallization and preliminary X-ray crystallographic analysis of the functional form of BinB binary toxin from *Bacillus sphaericus*

Kanokporn Srisucharitpanit,[a] Min Yao,[b] Sarin Chimnaronk,[a] Boonhiang Promdonkoy,[c] Isao Tanaka[b]* and Panadda Boonserm[a]*

[a]Institute of Molecular Biosciences, Mahidol University, Salaya, Phuttamonthon, Nakhon Pathom 73170, Thailand, [b]Faculty of Advanced Life Sciences, Hokkaido University, Sapporo 060-0810, Japan, and [c]National Center for Genetic Engineering and Biotechnology, National Science and Technology Development Agency, 113 Pahonyothin Road, Klong 1, Klong Luang, Pathumthani 12120, Thailand

Correspondence e-mail: tanaka@castor.sci.hokudai.ac.jp, panadda.boo@mahidol.ac.th

Received 9 November 2012
Accepted 2 January 2013

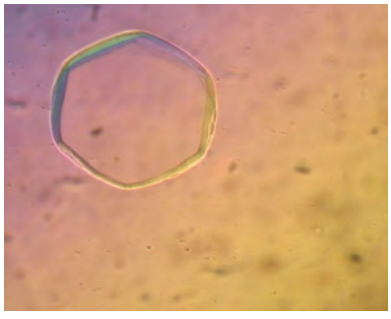

The binary toxin from *Bacillus sphaericus* consists of two proteins, BinA and BinB, which work together to exert toxicity against mosquito larvae. BinB is proposed to be a receptor-binding domain and internalizes BinA into the midgut cells, resulting in toxicity *via* an unknown mechanism. The functional form of BinB has been successfully crystallized. The crystals of BinB diffracted to a resolution of 1.75 Å and belong to space group $P6_222$, with unit-cell parameters $a = b = 95.2$, $c = 154.9$ Å. Selenomethionine-substituted BinB (SeMetBinB) was prepared and crystallized for experimental phasing. The SeMetBinB crystal data were collected at a wavelength of 0.979 Å and diffracted to a resolution of 1.85 Å.

1. Introduction

A binary toxin is produced as crystalline inclusions during sporulation by the Gram-positive bacterium *Bacillus sphaericus* (*Bs*). This toxin is highly toxic to mosquito larvae after being ingested; hence it becomes an alternative mosquito-control agent. The binary toxin consists of two polypeptides, 42 kDa BinA and 51 kDa BinB (Baumann *et al.*, 1991; Charles *et al.*, 1996), and both of them are required for maximum toxicity against the larvae of *Culex* and *Anopheles* mosquito species (Berry *et al.*, 1993). The binary toxin components are synthesized as inactive protoxins that are solubilized under alkaline conditions upon ingestion by susceptible mosquito larvae, and are subsequently converted by larval gut proteases into their active forms of 40 and 45 kDa for BinA and BinB, respectively (Broadwell & Baumann, 1987; Nicolas *et al.*, 1990). The activated BinB has been demonstrated to bind to a specific receptor on the larval gut epithelial cells and mediates the regional binding and internalization of BinA (Oei *et al.*, 1992). The receptor of binary toxin has been identified as a Cpm1-α-glucosidase (*Culex pipiens* maltase 1) (Silva-Filha *et al.*, 1999; Darboux *et al.*, 2001).

The binary toxin has been shown to induce channel and pore formation in cultured *C. quinquefasciatus* cells and in a mammalian epithelial cell line (MDCK) expressing the binary toxin Cpm1 receptor (Cokmus *et al.*, 1997; Pauchet *et al.*, 2005). The ability of the binary toxin to insert into receptor-free lipid membranes and permeabilize phospholipid vesicles has also been reported (Schwartz *et al.*, 2001; Boonserm *et al.*, 2006; Kunthic *et al.*, 2011). Moreover, several cytopathological alterations were observed on intoxicated *C. quinquefasciatus* larvae including the formation of cytoplasm vacuoles, mitochondria swelling and microvilli destruction (Silva-Filha & Peixoto, 2003). The above evidence seems to indicate a complex mechanism for binary toxin activity. In the absence of a detailed three-dimensional structure, its toxicity mechanism remains unclear. Moreover, both BinA and BinB proteins show low amino-acid sequence similarity to proteins with known structures; hence their three-dimensional structures cannot be reliably predicted. Although there are reports describing the crystallization of BinB (Chiou *et al.*, 1999) and the binary toxin from a native *Bs* strain (Smith *et al.*, 2004), their structures have not been reported. As BinB plays a key role in the specificity of binary toxin, its protein fragments and amino-acid residues involved in the receptor binding have been investigated (Singkhamanan *et al.*, 2010; Tangsongcharoen *et al.*, 2011; Romão *et al.*, 2011). However, the lack of structural information

limits the usefulness of these functional data. To gain insight into the structure–function correlation and provide guidelines for engineering the protein with higher potency, we report the crystallization and preliminary X-ray crystallographic analysis of the functional form of BinB protein.

2. Materials and methods

2.1. Expression, purification and activation of native and selenomethionine-substituted BinB

Detailed cloning, expression and purification protocols for the trypsin-activated BinB have been described previously (Srisucharitpanit *et al.*, 2012). Briefly, the *binB* gene from *B. sphaericus* strain 2297 (GenBank accession No. AJ224478) was cloned by fusion with a hexahistidine tag at the N-terminus and expressed as a soluble protein in *Escherichia coli*. BinB protein was purified by using Ni-affinity and size-exclusion chromatography. To convert BinB into its active form, purified BinB protoxin was digested with trypsin enzyme (Sigma) at a trypsin:protoxin ratio of 1:20 (*w*:*w*) at 310 K for 2 h to remove some amino acids from both the N- and C-termini. The trypsin-activated reaction was stopped by adding 10 m*M* phenylmethylsulfonyl fluoride (PMSF, Sigma). The trypsin was removed by size-exclusion chromatography which was equilibrated with 50 m*M* Tris–HCl pH 9.0 and 1 m*M* dithiothreitol (DTT). The purified activated BinB was further concentrated to 5 mg ml^{-1} with an ultracentrifugal 30 K cutoff filter (Amicon, USA) prior to crystallization.

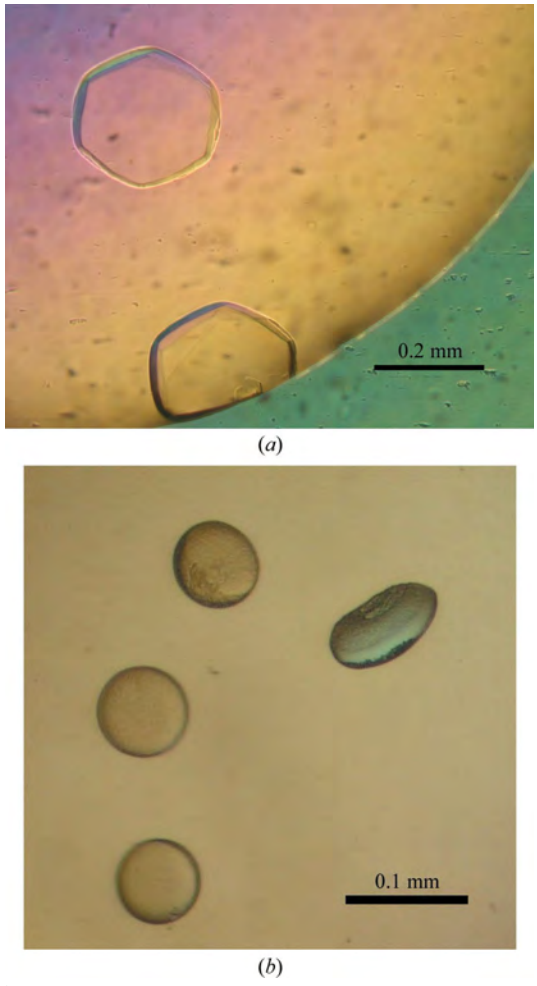

Figure 1
Crystals of native (*a*) and SeMet-substituted (*b*) BinB used for X-ray diffraction.

Table 1
Summary of crystallographic data.

Values in parentheses correspond to the highest-resolution shell.

	Native	SeMet
Wavelength (Å)	1	0.979
Radiation source	BL41XU, SPring-8	BL41XU, SPring-8
Space group	$P6_222$	$P6_222$
Unit-cell parameters (Å)	a = 95.2, b = 95.2, c = 154.9	a = 95.0, b = 95.0, c = 154.5
Resolution range (Å)	28.99–1.75 (1.84–1.75)	28.99–1.85 (1.95–1.85)
No. of unique reflections	42536 (6069)	35916 (5127)
Multiplicity	10.6 (10.7)	15 (15)
Completeness (%)	100 (100)	100 (100)
$\langle I/\sigma(I)\rangle$	4.4 (1.8)	4.7 (2.4)
$R_{\rm meas}$† (%)	12.6 (45.5)	11.9 (32.9)

† $R_{\rm meas} = \sum_{hkl}\{N(hkl)/[N(hkl)-1]\}^{1/2}\sum_i|I_i(hkl)-\langle I(hkl)\rangle|/\sum_{hkl}\sum_i I_i(hkl)$, where I_h is the mean intensity of symmetry-equivalent reflection h and N is redundancy.

The activated BinB is composed of 390 amino acids with seven methionine residues; therefore, the selenomethionine-substituted BinB (SeMetBinB) was prepared for phasing. The recombinant plasmid, pET 28b-BinB, was introduced into *E. coli* B834 (DE3) methionine (Met) auxotrophic strain (Leahy *et al.*, 1992; Wood, 1966). The transformant was pre-cultured in 100 ml Luria-Bertani (LB) broth containing 50 µg ml^{-1} kanamycin at 310 K for 18 h and cultured cells were harvested by centrifugation. The cell pellets were washed twice with PBS (phosphate-buffered saline) buffer before being resuspended in 1 l of M9 medium containing 40 µg of each amino acid except methionine, 1 µg of each vitamin mixture supplement (riboflavin, pyridoxine monohydrochloride, thiamine and nicotinamide) and 40 µg of SeMet (Sigma). Expression was induced by the addition of 1 m*M* isopropyl β-D-1-thiogalactopyranoside (IPTG) when the culture reached an OD_{600} of 0.6 and cultured cells were further grown at 303 K for 24 h. SeMetBinB was purified and activated following the same protocols as those for the native protein.

2.2. Crystallization and X-ray diffraction data collection

Crystallization was performed by hanging- and sitting-drop vapour-diffusion methods in 96- and 24-well plates at 295 K (Molecular Dimensions, UK and Qiagen, Germany). Initial screening was performed using Hampton Research Crystal Screen kits (Hampton Research, USA) and positive hits were then optimized. Drops were prepared by mixing 1 µl of 5 mg ml^{-1} protein solution (50 m*M* Tris–HCl pH 9.0, 1 m*M* DTT) with an equivalent volume of reservoir solution and were equilibrated against 500 µl of reservoir solution. For the SeMetBinB, initial screening was done using the PEGs Suite crystallization screening kit (Qiagen, Germany). Both native and SeMetBinB crystals were briefly soaked in a cryoprotecting solution consisting of 25%(*v*/*v*) glycerol dissolved in their corresponding mother liquors before being cryocooled in a nitrogen steam at 100 K.

Preliminary diffraction data were collected in-house (SLRI Thailand) using a Cu rotating-anode generator (λ = 1.54 Å; Microstar, Bruker). Higher resolution data were collected on the BL41XU beamline of the SPring-8 synchrotron (Hyogo, Japan). The diffraction data set of the native crystal was collected at 1 Å wavelength. The single-wavelength anomalous dispersion (SAD) data of the SeMetBinB crystal were collected at 0.979 Å based on the fluorescence spectrum of the Se *K* absorption edge (Rice *et al.*, 2000). A total of 180 frames of native and SAD data were collected with an oscillation angle of 0.5° and an exposure time of 0.3 s for each image. The diffraction images of both crystals were recorded on the Rayonix MX-225HE CCD detector. All diffraction data were indexed and integrated using *iMOSFLM* software (Battye *et al.*, 2011), and scaled

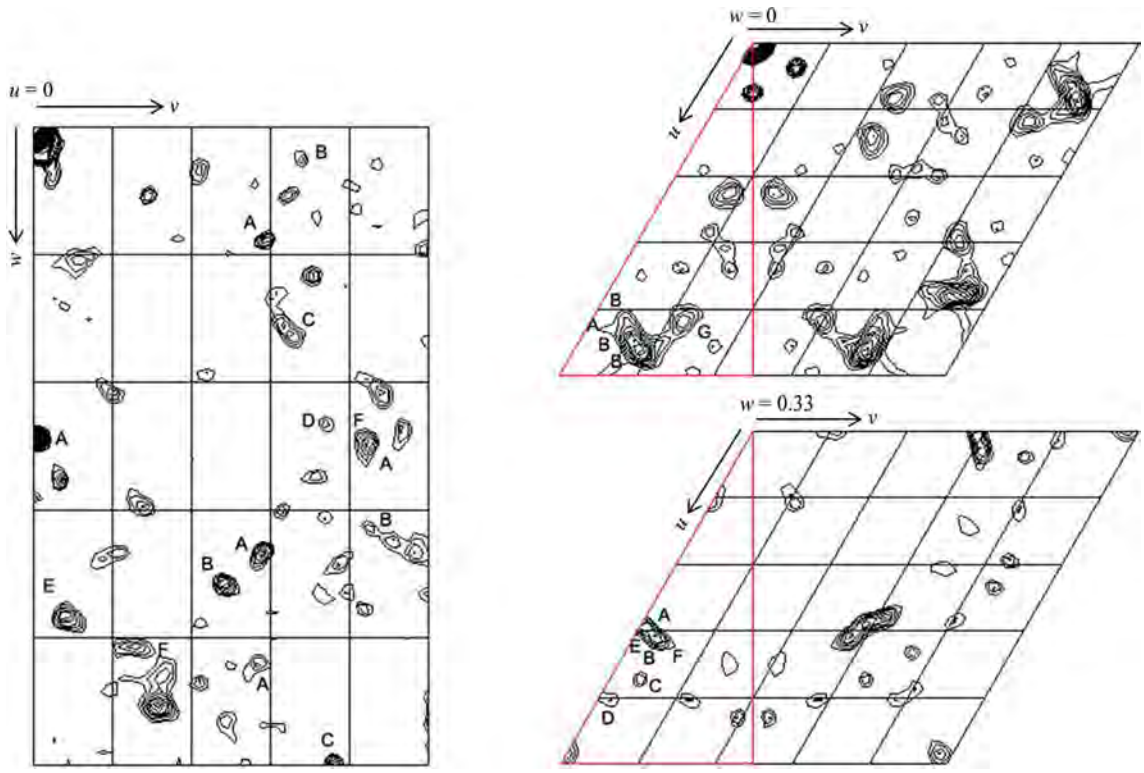

Figure 2
Harker sections ($u = 0$, $w = 0$ and $w = 0.33$) of the anomalous difference Patterson maps of SeMet-substituted BinB (space group $P6_222$), calculated at 1.9 Å resolution with data collected at $\lambda = 0.979$ Å (see Table 1). Maps are drawn with a minimum contour level of 1.0σ, with 1.0σ increments. The seven Se peaks are labelled (A–G).

and merged with *SCALA* in the *CCP*4 program suite (Winn *et al.*, 2011). Anomalous difference Patterson maps for SeMetBinB were calculated by the *CCP*4 program package.

3. Results and discussion

As reported previously, the expression of recombinant BinB protein as a soluble form in *E. coli* was achieved by fusing the protein with a hexahistidine tag at the N-terminus and modifying the strategy of cell culture by reducing temperature (Srisucharitpanit *et al.*, 2012). The *in vitro* activation of the recombinant BinB was performed by trypsin digestion to generate a resistant fragment of 45 kDa which is fully active against *C. quinquefasciatus* larvae. Hence, the trypsin-activated product is a good candidate for the atomic structural study of BinB in its functional form.

During initial crystallization screening, microcrystals appeared in conditions containing PEG 4000 and some salts with divalent cation such as magnesium chloride, lithium sulfate and calcium chloride. All favourable conditions were further optimized by adjusting the concentrations of protein, precipitants and salts, and by varying pH from 6.5 to 10. The best native BinB crystals were grown in a condition consisting of 0.1 *M* Tris–HCl pH 8.0, 0.2 *M* lithium sulfate and 12%(*w*/*v*) PEG 4000. The crystals grew to their maximal dimensions of 250 × 250 × 50 µm within 1 week (Fig. 1*a*).

Since a limited sequence identity is observed between BinB and other proteins with known structures, SeMetBinB was prepared to solve the phase problem. SeMetBinB was prepared with high purity comparable to native protein (data not shown). Furthermore, SeMetBinB still retained high toxicity against the *C. quinquefasciatus* larvae (data not shown). SeMetBinB crystals were obtained from a condition consisting of 0.1 *M* Tris–HCl pH 8.0, 0.2 *M* magnesium acetate and 16%(*w*/*v*) PEG 3350, which is very similar to that used for the native protein. The crystals grew to their maximal dimensions of 100 × 100 × 50 µm after 4 d (Fig. 1*b*).

X-ray diffraction data of the native BinB crystal were collected to 1.75 Å resolution using 25% glycerol in the mother liquor as a cryoprotectant. The crystal belongs to space group $P6_222$, with unit-cell parameters $a = b = 95.2$, $c = 154.9$ Å. The SAD data of a SeMetBinB crystal were collected to 1.85 Å resolution at the Se *K* absorption edge (wavelength 0.979 Å). The SeMetBinB crystal was found to be isomorphous with the native crystal, with unit-cell parameters $a = b = 95.0$, $c = 154.5$ Å. The Matthews coefficient (V_M) was estimated to be 2.35 $Å^3\,Da^{-1}$ with one molecule in the asymmetric unit, corresponding to a solvent content of 48% (Matthews, 1968). The seven selenium sites of SeMetBinB were found with the *SHELXD* program (Sheldrick, 2008) (Fig. 2), suggesting the usefulness of these data for phasing using the SAD method. Details of the data-collection statistics are summarized in Table 1. Structure determination and refinement are in progress.

We are grateful to the Synchrotron Light Research Institute (SLRI Public Organization, Thailand) for providing the in-house X-ray machine (MX end station) and the staff at BL41XU, SPring-8, for data collection. This work was supported by the Thailand Research Fund (TRF) and the Commission on Higher Education (CHE-PhD-SW).

References

Battye, T. G. G., Kontogiannis, L., Johnson, O., Powell, H. R. & Leslie, A. G. W. (2011). *Acta Cryst.* D**67**, 271–281.

Baumann, P., Clark, M. A., Baumann, L. & Broadwell, A. H. (1991). *Microbiol. Rev.* **55**, 425–436.

Berry, C., Hindley, J., Ehrhardt, A. F., Grounds, T., de Souza, I. & Davidson, E. W. (1993). *J. Bacteriol.* **175**, 510–518.

Boonserm, P., Moonsom, S., Boonchoy, C., Promdonkoy, B., Parthasarathy, K. & Torres, J. (2006). *Biochem. Biophys. Res. Commun.* **342**, 1273–1278.

Broadwell, A. H. & Baumann, P. (1987). *Appl. Environ. Microbiol.* **53**, 1333–1337.

Charles, J. F., Nielson-LeRoux, C. & Delécluse, A. (1996). *Annu. Rev. Entomol.* **41**, 451–472.

Chiou, C.-K., Davidson, E. W., Thanabalu, T., Porter, A. G. & Allen, J. P. (1999). *Acta Cryst.* D**55**, 1083–1085.

Cokmus, C., Davidson, E. W. & Cooper, K. (1997). *J. Invertebr. Pathol.* **69**, 197–204.

Darboux, I., Nielsen-LeRoux, C., Charles, J. F. & Pauron, D. (2001). *Insect Biochem. Mol. Biol.* **31**, 981–990.

Kunthic, T., Promdonkoy, B., Srikhirin, T. & Boonserm, P. (2011). *BMB Rep.* **44**, 674–679.

Leahy, D. J., Hendrickson, W. A., Aukhil, I. & Erickson, H. P. (1992). *Science*, **258**, 987–991.

Matthews, B. W. (1968). *J. Mol. Biol.* **33**, 491–497.

Nicolas, L., Lecroisey, A. & Charles, J. F. (1990). *Can. J. Microbiol.* **36**, 804–807.

Oei, C., Hindley, J. & Berry, C. (1992). *J. Gen. Microbiol.* **138**, 1515–1526.

Pauchet, Y., Luton, F., Castella, C., Charles, J. F., Romey, G. & Pauron, D. (2005). *Cell. Microbiol.* **7**, 1335–1344.

Rice, L. M., Earnest, T. N. & Brunger, A. T. (2000). *Acta Cryst.* D**56**, 1413–1420.

Romão, T. P., de-Melo-Neto, O. P. & Silva-Filha, M. H. (2011). *FEMS Microbiol. Lett.* **321**, 167–174.

Schwartz, J. L., Potvin, L., Coux, F., Charles, J. F., Berry, C., Humphreys, M. J., Jones, A. F., Bernhart, I., Dalla Serra, M. & Menestrina, G. (2001). *J. Membr. Biol.* **184**, 171–183.

Sheldrick, G. M. (2008). *Acta Cryst.* A**64**, 112–122.

Silva-Filha, M. H., Nielsen-LeRoux, C. & Charles, J. F. (1999). *Insect Biochem. Mol. Biol.* **29**, 711–721.

Silva-Filha, M. H. N. & Peixoto, C. A. (2003). *Pestic. Biochem. Physiol.* **77**, 138–146.

Singkhamanan, K., Promdonkoy, B., Chaisri, U. & Boonserm, P. (2010). *FEMS Microbiol. Lett.* **303**, 84–91.

Smith, A. W., Camara-Artigas, A. & Allen, J. P. (2004). *Acta Cryst.* D**60**, 952–953.

Srisucharitpanit, K., Inchana, P., Rungrod, A., Promdonkoy, B. & Boonserm, P. (2012). *Protein Expr. Purif.* **82**, 368–372.

Tangsongcharoen, C., Boonserm, P. & Promdonkoy, B. (2011). *J. Invertebr. Pathol.* **106**, 230–235.

Winn, M. D. *et al.* (2011). *Acta Cryst.* D**67**, 235–242.

Wood, W. B. (1966). *J. Mol. Biol.* **16**, 118–133.

Protein Expression and Purification 82 (2012) 368–372

Contents lists available at SciVerse ScienceDirect

Protein Expression and Purification

journal homepage: www.elsevier.com/locate/yprep

Expression and purification of the active soluble form of *Bacillus sphaericus* binary toxin for structural analysis

Kanokporn Srisucharitpanit [a], Pattarapong Inchana [a], Amporn Rungrod [b], Boonhiang Promdonkoy [b], Panadda Boonserm [a,*]

[a] Institute of Molecular Biosciences, Mahidol University, Salaya, Phuttamonthon, Nakhon Pathom 73170, Thailand
[b] National Center for Genetic Engineering and Biotechnology, National Science and Technology Development Agency, 113 Pahonyothin Road, Klong 1, Klong Luang, Pathumthani 12120, Thailand

ARTICLE INFO

Article history:
Received 22 December 2011
and in revised form 8 February 2012
Available online 20 February 2012

Keywords:
Binary toxin
Bacillus sphaericus
Proteolytic activation
Mosquito-larvicidal activity
Culex quinquefasciatus

ABSTRACT

The binary toxin produced from *Bacillus sphaericus* is highly toxic against larvae of *Culex* and *Anopheles* mosquitoes. The two major components of the binary toxin are 42-kDa BinA and 51-kDa BinB, which are produced as crystalline inclusions during sporulation. Currently, there is no detailed knowledge of the molecular mechanism of the binary toxin, mainly due to the lack of structural information. Herein, we describe an expression protocol with modified conditions allowing production of soluble, biologically active BinA and BinB for further structural analysis. The *binA* and *binB* genes from *B. sphaericus* 2297 strain were independently cloned and fused with a polyhistidine tag at their N-termini. Both $(His)_6$-tagged BinA and $(His)_6$-tagged BinB were expressed as soluble forms at low temperature. Highly pure proteins were obtained after two-step purification by Ni–NTA affinity and size exclusion chromatography. *In vitro* activation by trypsin digestion generated a resistant fragment, of 40 kDa for BinA, and of 45 kDa for BinB, and an oligomeric complex of BinA and BinB in solution was observed after proteolytic activation. Their functional and structural properties were confirmed by a biological assay and far-UV circular dichroism, respectively. The mixture of BinA and BinB, either as a protoxin or as a trypsin-activated form, exhibited high mosquito-larvicidal activity against *Culex quinquefasciatus* larvae with LC_{50} of about 10 ng/ml, while no toxicity was observed from the single binary toxin component. Results from far-UV circular dichroism of BinA and BinB suggest the presence of mainly β-structure. The expression and purification protocols reported here will be useful for the production of the active and homogeneous binary toxin to allow further detailed structural investigation.

Introduction

During sporulation, the Gram-positive bacterium *Bacillus sphaericus* (*Bs*) produces crystalline inclusions known as binary toxin, which is highly pathogenic to certain mosquito larvae. Hence, *B. sphaericus* has been used in recent years as a biopesticide to control mosquito populations. The latter are vectors of several human diseases such as malaria, filariasis, dengue, Japanese encephalitis, West Nile fever, and chikungunya. Two major toxins produced by *Bs* are mosquitocidal toxins (Mtx) and binary toxin (Bin). During the sporulation phase, binary toxin is produced as parasporal crystalline inclusions. The binary toxin, consisting of BinA (42 kDa) and BinB (51 kDa) components, is highly toxic against the larvae of *Culex* and *Anopheles* mosquitoes, but mildly toxic or non toxic to *Aedes* species [1–4]. BinA is proposed to function as a toxic subunit, as observed from its larvicidal activity when used at high concentration, whereas BinB is responsible for receptor binding [5,6]. However, both BinA and BinB are required in equimolar amounts to exert the maximum toxicity [2]. After ingestion of the crystal toxins by the susceptible larvae, the BinA and BinB protoxin inclusions are dissolved under alkaline conditions inside the larval midgut, accompanied by proteolytic activation by gut proteases to produce the active proteins of approximately 40 and 45 kDa, respectively [7,8]. The activated BinB then binds to a specific receptor, identified as a 60-kDa α-glucosidase (Cpm1), on the surface of midgut epithelium cell of susceptible larvae [9–12]. Upon binding, the binary toxin is thought to internalize into the target cells, eventually causing larval death via unknown mechanism [5,13].

To date, the knowledge of mechanism of action leading to larvicidal activity of the binary toxin is still insufficient, and a major reason is the lack of structural information. The problem is compounded by the fact that the amino acid sequences of BinA and BinB are not sufficiently similar to any other protein with known structure, which makes homology modeling very difficult. BinA and

* Corresponding author. Fax: +66 2 4419906.
E-mail address: mbpbs@mahidol.ac.th (P. Boonserm).

1046-5928/$ - see front matter © 2012 Elsevier Inc. All rights reserved.
doi:10.1016/j.pep.2012.02.009

BinB, however, are similar to each other, with 25% identity and 40% similarity, suggesting that their structures are also similar [14].

The binary toxin genes have been cloned and expressed in several host cells such as *Escherichia coli*, *Bacillus thuringiensis* and *Bacillus subtilis* [15–18], but in most cases expression only occurs as inclusion bodies. Consequently, several subsequent steps of protein preparation, i.e., inclusion solubilization in highly alkaline condition, dialysis against a normal alkaline buffer, and soluble protein purification are required for further structural and functional analyses. Moreover, both binary toxin components tend to be easily degraded and form large oligomers in solution after being solubilized in alkaline condition [18,19], which affects the homogeneity and purity desired for structural studies. In the present study, we expressed the individual BinA and BinB proteins with a hexahistidine tag at their N-termini to induce the expression of soluble proteins and facilitate their protein purification. The soluble binary toxin components were properly folded, as assessed by the far-UV circular dichroism spectroscopy. This is confirmed by the fact that these recombinant soluble proteins, when fed together to *Culex quinquefasciatus* mosquito larvae, showed high larvicidal activity, indicating that their conformations are in the active form. The expression and purification protocols reported here are particularly useful for further structural and functional investigation of the binary toxin.

Materials and methods

Bacterial strains and plasmids

E. coli K-12 JM109 was used as a host strain for cloning, whereas *E. coli* BL21 (DE3)pLysS (Novagen, USA) was used as a host strain for protein expression. The binary toxin genes, *binA* and *binB*, were isolated from *B. sphaericus* strain 2297 (GenBank accession No. AJ224478) as previously described [17]. The plasmid pRSET C (Invitrogen) was used as a cloning vector for *binA* gene, whereas the plasmid pET-28b(+) (Novagen) was used as a cloning vector for *binB* gene. Both plasmids contain the N-terminal tag coding sequences.

Construction of recombinant plasmids to express histidine-tagged BinA and BinB proteins

The *binA* and *binB* genes were separately cloned in-frame with the hexahistidine tags at their 5′ ends. The genes encoding BinA and BinB were amplified by polymerase chain reaction from the recombinant plasmid pET42f and pET51f, respectively [17]. The forward and reverse primers for *binA* amplification were 5′-CCG TGG ATC CGA AAT TTG GAT TTT ATT GAT TCT-3′ and 5′-GCG AAG CTT TTA GTT TTG ATC ATC TGT AAT AAT-3′, respectively (Underlined bases indicate restriction sites.). The forward and reverse primers for *binB* amplification were 5′-GCG CCA TAT GTG CGA TTC AAA AGA CAA TTT C-3′ and 5′-GCG CGG ATC CTC ACT GGT TAA TTT TAG GTA ATT C-3′, respectively (BioDesign, Thailand). The PCR product of *binA* gene was digested with *Bam*HI and *Hind*III and ligated in-frame into pRSET C vector between the same restriction sites to create the recombinant vector pRSETC-BinA with a hexahistidine tag at the 5′ end of the cloned gene. While, the PCR product of *binB* gene was digested with *Nde*I and *Bam*HI and ligated in-frame into pET28b(+) vector between the same restriction sites to create the recombinant vector pET28b-BinB with a hexahistidine tag at the 5′ end of the cloned gene.

BinA and BinB protein expression and purification

E. coli BL21(DE3)pLysS cells harboring pRSETC-BinA or pET28b-BinB were grown in Luria–Bertani (LB) medium containing appropriate antibiotics (100 μg/ml ampicillin and 34 μg/ml chloramphenicol for BinA and 50 μg/ml kanamycin and 34 μg/ml chloramphenicol for BinB). The culture cells were induced with 0.2 mM isopropyl β-D thiogalactopyranoside (IPTG) when OD_{600} reached 0.7 and further grown at 18 °C for 5 h. The culture cells were harvested by centrifugation at 7000*g* for 10 min. The cell pellets were suspended in buffer A (50 mM Tris–HCl pH8.0 and 200 mM NaCl), and subsequently subjected to ultra-sonication to completely break the cells. Crude extracts were separated by centrifugation in order to collect supernatant containing the expressed $(His)_6$-tagged BinA and $(His)_6$-tagged BinB proteins for further purification step. The supernatant fraction was loaded into a HiTrap™ Chelating HP 5-ml column prepacked with a precharged Ni^{2+} (GE Healthcare Life Sciences) that had been pre-equilibrated with buffer A. Non-specific bound proteins were washed twice with buffer A containing 25 mM imidazole and 50 mM imidazole, respectively. The bound $(His)_6$-tagged BinA was eluted with buffer A containing 100 mM imidazole, whereas the bound $(His)_6$-tagged BinB was eluted with buffer A containing 250 mM imidazole. The protein-containing fractions were pooled and concentrated by ultrafiltration at 4 °C using a Centriprep column (30-kDa cutoff, Amicon), followed by applying the concentrated fraction into a Superdex 200 HR 10/30 column (GE Healthcare Life Sciences) which was equilibrated with 50 mM Tris–HCl pH 9.0 and 1 mM DTT. The BinA and BinB proteins eluted from the size exclusion column were examined their molecular sizes and homogeneity by comparing with standard proteins (gel filtration LMW calibration kit, GE Healthcare Life Sciences). The proteins collected at every step were analyzed by 12% sodium dodecyl sulfate–polyacrylamide (SDS) gel. The concentration of protein was determined by Bradford's assay using BSA as a standard protein.

Trypsin activation of BinA and BinB

Purified BinA and BinB recombinant protoxins were mixed with trypsin (L-1-tosylamide-2-phenylethyl chloromethyl ketone treated, Sigma) at a trypsin:protoxin ratio of 1:20 (w/w) and incubated at 37 °C for 2 h. The proteolytic reaction was stopped by adding 10 mM Phenylmathylsulfonyl fluoride (PMSF, Sigma). Trypsin-activated BinA (40 kDa) and BinB (45 kDa) were purified by size exclusion chromatography using the Superdex 200 HR 10/30 column, which was equilibrated with 50 mM Tris–HCl pH 9.0 and 1 mM DTT. Eluted fractions were concentrated by ultrafiltration as described above.

Mosquito-larvicidal activity assay

Toxicity assays against the second-instar *C. quinquefasciatus* larvae were conducted following the protocol as previously described [18]. Purified BinA and BinB, either $(His)_6$-tagged protoxins or trypsin-activated forms, were mixed at 1:1 M ratio, followed by 2-fold serially diluted with distilled water in different concentrations. Then, 1 ml of each protein dilution was added to each well of a 24-well tissue culture plate containing 10 larvae/well in 1 ml water. The $(His)_6$-tagged BinB was used as a negative control. Mortality was recorded after incubation at room temperature for 48 h. All of the data from three independent experiments were used to calculate the median lethal concentration (LC_{50}) by using GWbasic program Probit analysis [20].

Secondary structure analysis

The secondary structures of the recombinant BinA and BinB, both protoxins and activated forms, were determined by using a Jasco J-715 CD spectropolarimeter (Jasco Inc., USA). The purified protein of 1 mg/ml in a quartz cuvette (0.2 mm optical path length)

was measured the CD spectra from 200 to 260 nm with scanning speed of 50 nm/min. Each spectrum was averaged from three scans and subtracted from a baseline.

Results and discussion

Expression and purification of BinA and BinB proteins

As mentioned previously, both BinA and BinB have been cloned and expressed in various host strains, but expressed proteins tended to accumulate as inclusion bodies. Although those expressed proteins are in a similar form as the native binary toxin, solubilization in highly alkaline pH results in several additional steps of protein preparation. To facilitate the soluble protein expression and protein purification , both *binA* and *binB* genes from *Bs* strain 2297 were independently cloned and expressed with $(His)_6$-tags at their N-termini. The nucleotide sequences of recombinant plasmids were confirmed by DNA sequencing (data not shown). The recombinant BinA and BinB proteins were expressed in *E.coli* BL21 (DE3)pLysS with modified conditions to provide an optimum yield of soluble products. Both recombinant BinA and BinB fused with polyhistidine tags at their N-termini were expressed mainly in soluble form after induction with 0.2 mM IPTG at lower temperature of 18 °C for 5 h. Crude extract was released by sonication and the supernatant fraction containing either expressed BinA or BinB was initially loaded into the Ni–NTA affinity chromatography. The collected BinA and BinB proteins after elution from the Ni–NTA column were subsequently loaded to a size exclusion column to improve purity. Purified proteins were analysed by SDS–PAGE (Fig. 1). The BinA and BinB proteins appeared as bands with apparent molecular masses of 42 and 51 kDa, and showed high purity.

BinA and BinB toxin activation and their complex formation in solution

The native BinA and BinB proteins are produced as protoxins that are subsequently digested by larval proteases and converted to active toxins [7]. Here, *in vitro* toxin activation was performed by incubating $(His)_6$-tagged BinA and BinB with trypsin, followed by purification of the native proteins by size exclusion chromatography. The molecular sizes of the trypsin-activated BinA and BinB were checked by SDS–PAGE and MALDI-TOF mass spectrometry. As observed by SDS–PAGE, digestion with trypsin appeared to generate a resistant-fragment of about 40 and 45 kDa for BinA and BinB, respectively (Fig. 2). MALDI-TOF mass spectra of trypsin-digested BinA and BinB showed peaks at 40,823 Da and 45,028 Da for BinA and BinB, respectively (data not shown) that agree well with the predicted molecular masses from their deduced amino acid sequences (40,985 Da for BinA and 44,884 Da for BinB).

To demonstrate a complex formation of activated BinA and BinB in solution, their trypsin-activated products were mixed at a 1:1 M ratio before applying size exclusion chromatography (HiLoad 16/60 Superdex 200). Both trypsin-activated BinA and BinB co-eluted before the individual proteins, indicating formation of a BinA–BinB complex in solution after trypsin activation (Fig. 3). The gel-filtration elution volume of the binary toxin complex was between IgG (158 kDa) and albumin (66 kDa). According to the estimation based on this elution volume, the molecular mass of the binary toxin complex was about 140 kDa. MALDI-TOF mass spectra of the binary toxin complex showed peaks corresponding to the 40,823 Da BinA and 45,028 Da BinB (data not shown), confirming the presence of both activated components in the complex. It has been demonstrated that native BinA and BinB protoxins form an oligomer in solution that contains two copies of each BinA and BinB [21]. However, in that report, the trypsin-digested binary toxin was not found in an oligomeric form. Our result, in contrast, provides evidence of the formation of a BinA–BinB complex in solution after trypsin activation. This oligomeric complex may play a role in toxin insertion into the membranes of the target cells, probably via pore formation, causing pathological effects inside the cells.

Secondary structures of recombinant BinA and BinB

The conformations of purified $(His)_6$-tagged BinA, BinB and their trypsin-digested products were characterized by circular dichroism (CD) spectroscopy. CD spectra (either with or without polyhistidine tag) showed similar features, with negative bands around 202 and 210 nm and positive bands around 231 and 239 nm (Fig. 4). This result indicates that the polyhistidine tag does not interfere with protein folding and no major structural changes are induced by trypsin activation. Analysis of the secondary structure content using both K2D2 and PSIPRED program tools [22,23] also conclude that BinA and BinB proteins adopt mainly a β-strand structure (data not shown), consistent with the previous report

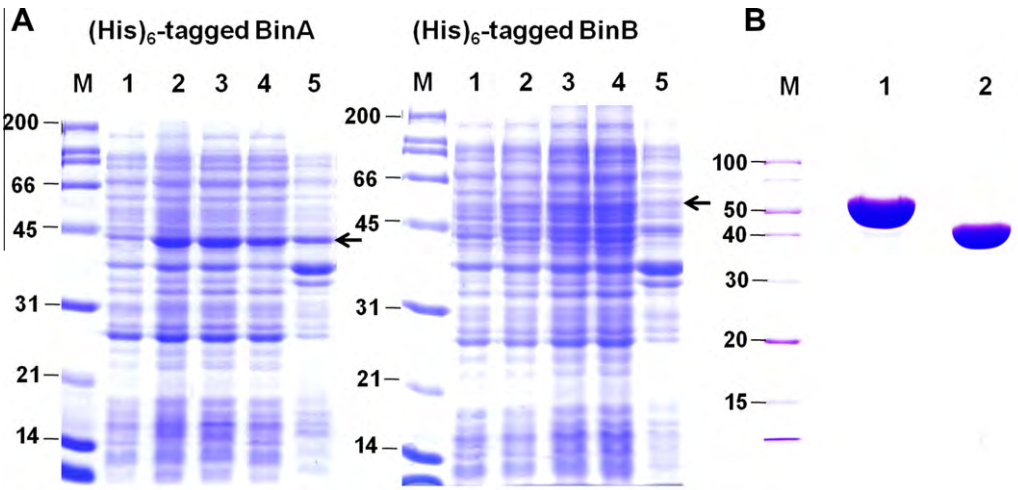

Fig. 1. Coomassie-stained SDS–PAGE (12% gel) showing the protein expression and purification of the recombinant BinA and BinB. (A) Expression profiles of $(His)_6$-tagged BinA and $(His)_6$-tagged BinB. Lanes 1 and 2, uninduced and IPTG-induced cell cultures, respectively; lanes 3, 4, and 5 cell lysate, supernatant and pellet fractions after ultrasonication, respectively; M, molecular mass standards. Arrows indicate the expressed proteins at their predicted MW. (B) Purity assessment of $(His)_6$-tagged BinB (lane 1) and $(His)_6$-tagged BinA (lane 2) after Ni–NTA affinity and size exclusion chromatography.

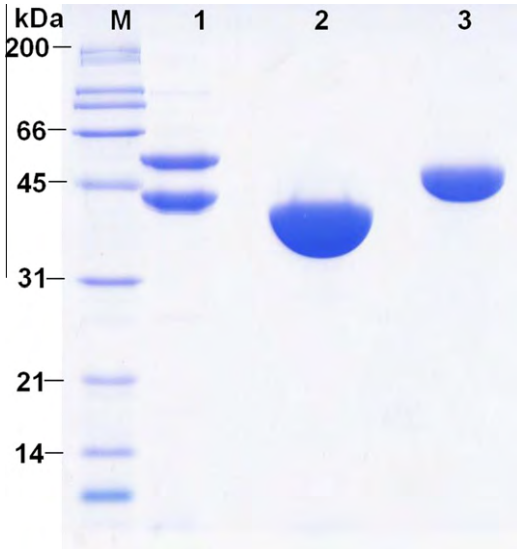

Fig. 2. Coomassie-stained SDS–PAGE (12% gel) showing proteolytic activation of recombinant BinA and BinB. Lane 1, mixture of undigested BinA (lower band) and undigested BinB (upper band); lanes 2, trypsin-activated BinA (40 kDa); lane 3, trypsin-activated BinB (45 kDa); M, molecular mass standards.

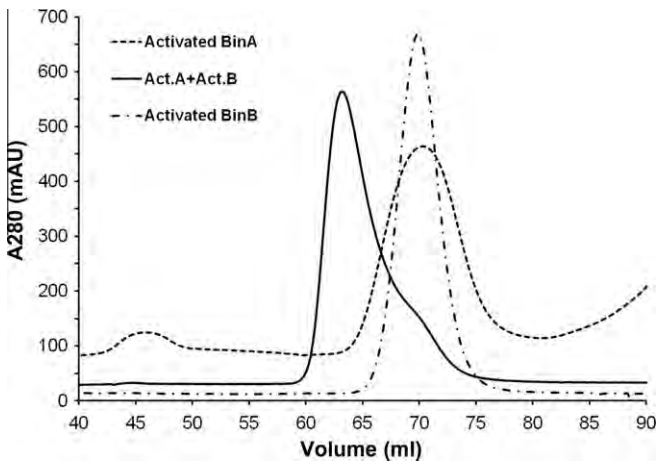

Fig. 3. Elution profile from a size-exclusion chromatographic column (Hiload 16/60 Superdex 200) of the 40-kDa trypsin-activated BinA, 45-kDa trypsin-activated BinB and their mixture at equal concentration.

and the prediction based on their amino acid sequences [24,25]. This conformational analysis suggests that the purified binary toxin components are properly folded. In addition, an equimolar mixture of BinA and BinB, either protoxin or trypsin-activated form, showed a CD spectrum intermediate between that of pure BinA and pure BinB, suggesting that no alteration of protein secondary structure was occurred when two proteins were mixed in aqueous solution (Fig. 4).

Larvicidal activity of recombinant BinA and BinB

Larvicidal activity of recombinant BinA and BinB against *C. quinquefasciatus* larvae was tested, either as protoxins or as trypsin-activated proteins. Neither BinA nor BinB alone was toxic to *C. quinquefasciatus* larvae, even using a concentration of 50 μg/ml. However, high toxicity was achieved when BinA and BinB were combined at 1:1 M ratio (Table 1). Both protoxin and trypsin-activated BinA–BinB mixtures showed comparable toxicity, indicating

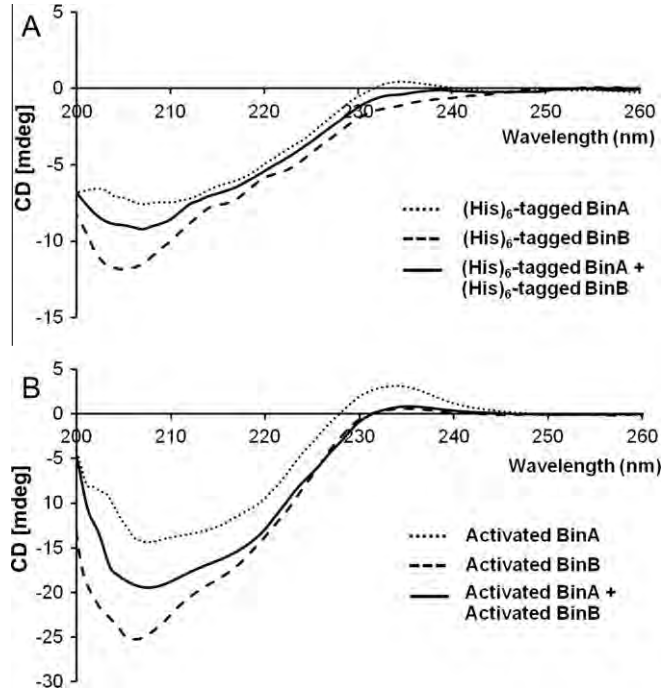

Fig. 4. Circular dichroism spectra of BinA, BinB and a mixture of BinA and BinB, either protoxins (A) or trypsin-digested forms (B), in a far-UV region of 200–260 nm.

that both larval gut proteases and trypsin could convert the protoxins into their active forms.

It has been reported previously that $(His)_6$-tagged BinA from *Bs* strain ISPC-8 in a soluble form showed high toxicity to *Culex* larvae without the requirement of the BinB counterpart [24]. These contradictory results may be explained by the different protein purification steps performed. For example, we have noted that the complete removal of imidazole after Ni–NTA affinity chromatography is critical because residual imidazole in solution was toxic to mosquito larvae (Supplement 1). Nevertheless, our results are in agreement with a previous report that showed that neither inclusions of BinA nor BinB alone were toxic to the mosquito larvae [17], which suggests that complementation is necessary for toxicity. The requirement of both BinA and BinB subunits is reminiscent of other toxins that function as A–B toxins, such as *Clostridium perfringens* Iota-toxin, *Bacillus cereus* VIP2 and *B. sphaericus* Mtx1 [26–28]. Moreover, the soluble BinA and BinB expressed from this polyhistidine tag expression system showed about 2 times higher toxicity when compared with the GST-BinA and GST-BinB fusion proteins expressed as inclusions [18]. This suggests that the protein

Table 1
Mosquito-larvicidal activity of the purified BinA and BinB with histidine tags and after trypsin activation against *Culex quinquefasciatus* larvae.

Sample	LC_{50} (ng/ml)[a]
$(His)_6$-tagged BinA	Not toxic
$(His)_6$-tagged BinB	Not toxic
Activated BinA	Not toxic
Activated BinB	Not toxic
$(His)_6$-tagged BinA + $(His)_6$-tagged BinB	8.0 (5.7–10.4)
Activated BinA + Activated BinB	10.0 (7.4–14.6)

[a] The mortality was recorded after feeding the toxin for 48 h. The LC_{50} (median lethal concentration) was calculated from three independent experiments by using Probit analysis. Numbers in parenthesis indicate the fiducial limits at 95% confidence. Mortality was not detected from either BinA or BinB alone when used at high concentration of 50 μg/ml.

solubility inside the larval gut is one of the key factors in determining the level of toxicity.

In conclusion, BinA and BinB were separately expressed with modified conditions to produce the soluble proteins. Both proteins could be purified with high purity and showed high larvicidal activity when fed together to larvae. The proteins are properly folded and form a complex in solution after proteolytic activation. The exceptional purity of the proteins may facilitate protein crystallization and detailed structural investigations in the future.

Acknowledgments

We would like to thank Prof. Isao Tanaka and Assoc. Prof. Min Yao, Graduate School of Life Sciences, Hokkaido University, Japan, for MALDI-TOF/MS analysis of the protein and great advice. This work was supported by the Thailand Research Fund (TRF), the Commission on Higher Education (CHE), Thailand, and the National Science and Technology Development Agency, Thailand.

Appendix A. Supplementary data

Supplementary data associated with this article can be found, in the online version, at doi:10.1016/j.pep.2012.02.009.

References

[1] J.F. Charles, C. Nielson-LeRoux, A. Delecluse, *Bacillus sphaericus* toxins: molecular biology and mode of action, Annu. Rev. Entomol. 41 (1996) 451–472.
[2] P. Baumann, M.A. Clark, L. Baumann, A.H. Broadwell, *Bacillus sphaericus* as a mosquito pathogen: properties of the organism and its toxins, Microbiol. Rev. 55 (1991) 425–436.
[3] C. Berry, J. Hindley, A.F. Ehrhardt, T. Grounds, I. de Souza, E.W. Davidson, Genetic determinants of host ranges of *Bacillus sphaericus* mosquito larvicidal toxins, J. Bacteriol. 175 (1993) 510–518.
[4] L. Baumann, A.H. Broadwell, P. Baumann, Sequence analysis of the mosquitocidal toxin genes encoding 51.4- and 41.9-kilodalton proteins from *Bacillus sphaericus* 2362 and 2297, J. Bacteriol. 170 (1988) 2045–2050.
[5] C. Oei, J. Hindley, C. Berry, Binding of purified *Bacillus sphaericus* binary toxin and its deletion derivatives to *Culex quinquefasciatus* gut: elucidation of functional binding domains, J. Gen. Microbiol. 138 (1992) 1515–1526.
[6] J.F. Charles, M.H. Silva-Filha, C. Nielsen-LeRoux, M.J. Humphreys, C. Berry, Binding of the 51- and 42-kDa individual components from the *Bacillus sphaericus* crystal toxin to mosquito larval midgut membranes from *Culex* and *Anopheles* sp. (Diptera: Culicidae), FEMS Microbiol. Lett. 156 (1997) 153–159.
[7] A.H. Broadwell, P. Baumann, Proteolysis in the gut of mosquito larvae results in further activation of the *Bacillus sphaericus* toxin, Appl. Environ. Microbiol. 53 (1987) 1333–1337.
[8] L. Nicolas, A. Lecroisey, J.F. Charles, Role of the gut proteinases from mosquito larvae in the mechanism of action and the specificity of the *Bacillus sphaericus* toxin, Can. J. Microbiol. 36 (1990) 804–807.
[9] E.W. Davidson, Binding of the *Bacillus sphaericus* (Eubacteriales: Bacillaceae) toxin to midgut cells of mosquito (Diptera: Culicidae) larvae: relationship to host range, J. Med. Entomol. 25 (1988) 151–157.
[10] M.H. Silva-Filha, C. Nielsen-Leroux, J.F. Charles, Binding kinetics of *Bacillus sphaericus* binary toxin to midgut brush-border membranes of *Anopheles* and *Culex* sp. mosquito larvae, Eur. J. Biochem. 247 (1997) 754–761.
[11] M.H. Silva-Filha, C. Nielsen-LeRoux, J.F. Charles, Identification of the receptor for *Bacillus sphaericus* crystal toxin in the brush border membrane of the mosquito *Culex pipiens* (Diptera: Culicidae), Insect Biochem. Molec. 29 (1999) 711–721.
[12] I. Darboux, C. Nielsen-LeRoux, J.F. Charles, D. Pauron, The receptor of *Bacillus sphaericus* binary toxin in *Culex pipiens* (Diptera: Culicidae) midgut: molecular cloning and expression, Insect Biochem. Molec. 31 (2001) 981–990.
[13] O. Opota, N.C. Gauthier, A. Doye, C. Berry, P. Gounon, E. Lemichez, D. Pauron, *Bacillus sphaericus* binary toxin elicits host cell autophagy as a response to intoxication, PLoS One 6 (2011) e14682.
[14] B. Promdonkoy, P. Promdonkoy, B. Wongtawan, P. Boonserm, S. Panyim, Cys31, Cys47, and Cys195 in BinA are essential for toxicity of a binary toxin from *Bacillus sphaericus*, Curr. Microbiol. 56 (2008) 334–338.
[15] L. Baumann, P. Baumann, Expression in *Bacillus subtilis* of the 51- and 42-kilodalton mosquitocidal toxin genes of *Bacillus sphaericus*, Appl. Environ. Microbiol. 55 (1989) 252–253.
[16] C. Bourgouin, A. Delecluse, F. de la Torre, J. Szulmajster, Transfer of the toxin protein genes of *Bacillus sphaericus* into *Bacillus thuringiensis* subsp. *israelensis* and their expression, Appl. Environ. Microbiol. 56 (1990) 340–344.
[17] B. Promdonkoy, P. Promdonkoy, M. Audtho, S. Tanapongpipat, N. Chewawiwat, P. Luxananil, S. Panyim, Efficient expression of the mosquito larvicidal binary toxin gene from *Bacillus sphaericus* in *Escherichia coli*, Curr. Microbiol. 47 (2003) 383–387.
[18] B. Promdonkoy, P. Promdonkoy, S. Panyim, High-level expression in *Escherichia coli*, purification and mosquito-larvicidal activity of the binary toxin from *Bacillus sphaericus*, Curr. Microbiol. 57 (2008) 626–630.
[19] P. Baumann, B.M. Unterman, L. Baumann, A.H. Broadwell, S.J. Abbene, R.D. Bowditch, Purification of the larvicidal toxin of *Bacillus sphaericus* and evidence for high-molecular-weight precursors, J. Bacteriol. 163 (1985) 738–747.
[20] D.J. Finney, Probit analysis, Cambridge University Press, Cambridge, 1971.
[21] A.W. Smith, A. Camara-Artigas, D.C. Brune, J.P. Allen, Implications of high-molecular-weight oligomers of the binary toxin from *Bacillus sphaericus*, J. Invertebr. Pathol. 88 (2005) 27–33.
[22] D.T. Jones, Protein secondary structure prediction based on position-specific scoring matrices, J. Mol. Biol. 292 (1999) 195–202.
[23] C. Perez-Iratxeta, M.A. Andrade-Navarro, K2D2: estimation of protein secondary structure from circular dichroism spectra, BMC Struct. Biol. 8 (2008) 25.
[24] R.S. Hire, A.B. Hadapad, T.K. Dongre, V. Kumar, Purification and characterization of mosquitocidal *Bacillus sphaericus* BinA protein, J. Invertebr. Pathol. 101 (2009) 106–111.
[25] Z. Yuan, C. Rang, R.C. Maroun, V. Juarez-Perez, R. Frutos, N. Pasteur, C. Vendrely, J.F. Charles, C. Nielsen-Leroux, Identification and molecular structural prediction analysis of a toxicity determinant in the *Bacillus sphaericus* crystal larvicidal toxin, Eur. J. Biochem. 268 (2001) 2751–2760.
[26] S. Han, J.A. Craig, C.D. Putnam, N.B. Carozzi, J.A. Tainer, Evolution and mechanism from structures of an ADP-ribosylating toxin and NAD complex, Nat. Struct. Biol. 6 (1999) 932–936.
[27] I. Carpusca, T. Jank, K. Aktories, *Bacillus sphaericus* mosquitocidal toxin (MTX) and pierisin: the enigmatic offspring from the family of ADP-ribosyltransferases, Mol. Microbiol. 62 (2006) 621–630.
[28] H. Tsuge, M. Nagahama, H. Nishimura, J. Hisatsune, Y. Sakaguchi, Y. Itogawa, N. Katunuma, J. Sakurai, Crystal structure and site-directed mutagenesis of enzymatic components from *Clostridium perfringens* iota-toxin, J. Mol. Biol. 325 (2003) 471–483.

BMB
reports

Essential role of tryptophan residues in toxicity of binary toxin from *Bacillus sphaericus*

Thittaya Kunthic[1], Boonhiang Promdonkoy[2], Toemsak Srikhirin[3] & Panadda Boonserm[1,]*

[1]Institute of Molecular Biosciences, Mahidol University, Salaya Campus, Nakhon Pathom 73170, [2]National Center for Genetic Engineering and Biotechnology, National Science and Technology Development Agency, 113 Pahonyothin Road, Klong Luang, Pathumthani 12120, [3]Department of Physics, Faculty of Sciences, Mahidol University, Rama 6 Road, Bangkok 10400, Thailand

***Bacillus sphaericus* produces mosquito-larvicidal binary toxin composed of BinA and BinB. While BinB is expected to bind to a specific receptor on the cell membrane, BinA interacts to BinB or BinB receptor complex and translocates into the cytosol to exert its activity via unknown mechanism. To investigate functional roles of aromatic cluster in BinA, amino acids at positions Y213, Y214, Y215, W222 and W226 were substituted by leucine. All mutant proteins were highly produced and their secondary structures were not affected by these substitutions. All mutants are able to insert into lipid monolayers as observed by Langmuir-Blodgett trough and could permeabilize the liposomes in a similar manner as the wild type. However, mosquito-larvicidal activity was abolished for W222L and W226L mutants suggesting that tryptophan residues at both positions play an important role in the toxicity of BinA, possibly involved in the cytopathological process after toxin entry into the cells. [BMB reports 2011; 44(10): 674-679]**

INTRODUCTION

Bacillus sphaericus produces a binary toxin, in the form of crystalline inclusion, during the sporulation phase. The binary toxin is composed of two crystal proteins, BinA (42 kDa) and BinB (51 kDa), and both of them are required at equimolar amounts to exhibit the maximal larvicidal activity (1, 2). The susceptible mosquito species of the binary toxin are limited to *Culex* and *Anopheles*, but not *Aedes* species (3). Upon ingestion by susceptible mosquito larvae, these crystal proteins are solubilized and subsequently activated by proteases in the larval midgut to generate the active-core fragments of 39-kDa BinA and 43-kDa BinB (2). The activated toxins then target on the midgut epithelial cells by receptor mediated mechanism. The activated BinB has been identified as a specificity determinant that binds to a specific receptor, known as α-glucosidase which is attached to the midgut membrane via glycosylphosphatidylinositol (GPI) anchor (4, 5). Upon receptor binding of BinB, BinA binds to BinB or BinB-receptor complex, and followed by the translocation of the binary toxin into the cells. To date, the mechanism underlying the cellular intoxication of the binary toxin remains unclear.

Several cytopathological alterations were observed in the *Culex quinquefasciatus* larvae intoxicated by the binary toxin which included the formation of large cytoplasma vacuoles, disruption of the rough endoplasmic reticulums, epithelial swelling, microvilli destruction, and eventual cell lysis and epithelial destruction in gastric caeca and posterior stomach (6). Recently, the cellular response by vacuolation of the binary toxin-treated mammalian epithelial cell line (MDCK) expressing the binary toxin Cpm1 (*Culex pipiens* maltase 1) receptor was reported to associate with the induction of autophagy process (7). Although direct evidence to support the pore-forming activity of the binary toxin on epithelial midgut cells is unavailable, membrane permeabilization using a receptor-free planar lipid bilayer and large unilamellar phospholipid vesicles has been shown as the *in vitro* effects of the binary toxin components (8). Also, the ability of the binary toxin to insert into the model neutral lipid monolayers has been demonstrated (9). In addition, dramatic conformational changes accompanying the lipid membrane association of the BinA, BinB, or their complex were observed (9).

Since the interaction of the binary toxin with target lipid membrane is one of the key steps in eliciting cytopathological effects on mosquito larvae, molecular insights into the interaction of the binary toxin with lipid membranes is required to gain a better understanding of the mechanism of toxicity. Due to the lack of three dimensional structure of the binary toxin, functional characterization has been based mainly on its amino acid sequence analysis and secondary structure prediction (10-15). Aromatic residues, especially tyrosine and tryptophan, conceivably play a key role in membrane anchoring of many membrane proteins and are mainly found at the membrane-water interface (16). Based on the amino acid sequence of BinA, a toxic component of the binary toxin, a cluster of ar-

*Corresponding author. Tel: 662-4419003-7; Fax: 662-4419906; E-mail: mbpbs@mahidol.ac.th
http://dx.doi.org/10.5483/BMBRep.2011.44.10.674

Received 16 June 2011, Accepted 19 August 2011

Keywords: *Bacillus sphaericus*, Binary toxin, Calcein release, Langmuir–blodgett, Membrane insertion

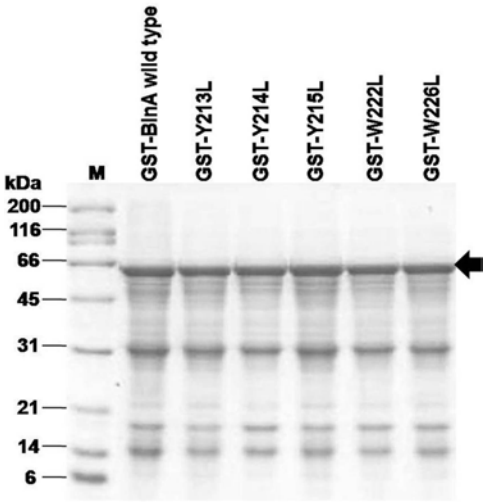

Fig. 1. Partially purified inclusions of GST- BinA and its mutants were analyzed on 12% SDS-PAGE. M represents the molecular mass standards. Position of GST-BinA fusion protein is indicated by an arrow.

omatic amino acids is found in the positions encompassing amino acids 213 to 226 (Supplement 1). In this study, aromatic residues, particularly tyrosine and tryptophan, in this region were selected for site-directed mutagenesis in search of crucial residues for the membrane interaction and biological activity. Within this region, tryptophan residues at positions 222 and 226 are found to have functional significance towards *C. quinquefasciatus* larvae.

RESULTS AND DISCUSSION

Aromatic amino acid replacements did not affect protein expression and folding of BinA

The mechanism by which the binary toxin kills the mosquito larvae remains unclear, however, it has been shown that the binary toxin is internalized in both mosquito midgut cells and MDCK cells expressing the Cpm1 receptor, possibly via endocytosis (7, 17). Hence, interaction of the binary toxin with the lipid membrane is a key step during the intoxication process. Previous study has shown that the aromaticity of F149 and Y150 of BinB is a prerequisite for larvicidal activity, possibly by playing a crucial role in membrane interaction and receptor binding (18). According to amino acid sequence of BinA protein, the aromatic residues especially tryptophan and tyrosine are clustered at the positions 213 to 226. We expected that this region could be essential for membrane interaction. To investigate the functional importance of aromatic amino acids of BinA, site-directed mutagenesis was performed by replacements of aromatic amino acids (Y213, Y214, Y215, W222, and W226) in this region by leucine residues. The replacements of aromatic residues, however, could affect the structure or function of binary toxin. Here, both structural and functional analyses were performed.

Table 1. Mosquito-larvicidal activity of the wild-type and mutant toxins against *Culex quinquefasciatus* larvae. The mortality was recorded after feeding the mixture of GST-BinB and GST-BinA or its mutant inclusions at a 1:1 molar ratio for 48 h. The LC_{50} (median lethal concentration) was calculated from three independent experiments by using Probit analysis. Numbers in parenthesis indicate the fiducial limits at 95% confidence. Mortality was not detected for W222L and W226L mutants when used the toxin up to 32 μg ml^{-1}

Protein	LC_{50} (μg ml^{-1})
GST-BinB + GST-BinA wild type	0.20 (0.14-0.32)
GST-BinB + GST-Y213L	0.45 (0.31-0.76)
GST-BinB + GST-Y214L	0.57 (0.41-0.89)
GST-BinB + GST-Y215L	0.45 (0.33-0.94)
GST-BinB + GST-W222L	Not toxic
GST-BinB + GST-W226L	Not toxic

After obtaining the mutant plasmids, automated DNA sequencing analysis revealed that all selected aromatic residues were replaced by leucines (data not shown). Upon IPTG induction, all mutant proteins were expressed as inclusions with expression levels comparable to that of the wild type (Fig. 1), suggesting that the mutations of these aromatic residues did not affect protein production and inclusion formation of the BinA. Given that the BinA proteins, both wild type and mutants, were fused with the GST tag, the mobility of GST-BinA fusion proteins as assessed by SDS-PAGE was slightly faster than expected from their predicted molecular weight (Fig. 1). This deviation could be due to the tightly-packed protein inclusions that were not completely disrupted by SDS, resulting in the faster mobility than expected in a SDS-gel. Protein solubilization of inclusions was subsequently determined by dissolving inclusions in 25 mM NaOH, followed by dialysis against 50 mM Na_2CO_3 buffer, pH 10. All mutant proteins were solubilized in such an alkaline condition, yielding the stable fragments with similar amounts as that of the wild type (data not shown).

Any change of protein conformation as a result of point mutations was monitored by using the Circular Dichroism (CD) spectroscopy. CD spectra in a far UV region (190-260 nm) of all mutants were apparently similar to that of the wild-type protein (Supplement 3), suggesting that the mutations at these selected positions did not affect the structural folding of the BinA protein.

W222 and W226 of BinA play a crucial role in larvicidal activity

The effect of the mutations of selected aromatic residues of BinA on the toxicity was further examined by biological activity assay. The inclusions of GST-BinA wild type or its mutants were mixed with GST-BinB at a 1:1 molar ratio and fed to the second-instar *C. quinquefasciatus* larvae. After incubating at room temperature for 48 h, the mortality was recorded and presented as LC_{50}. Results showed that the single mutations of

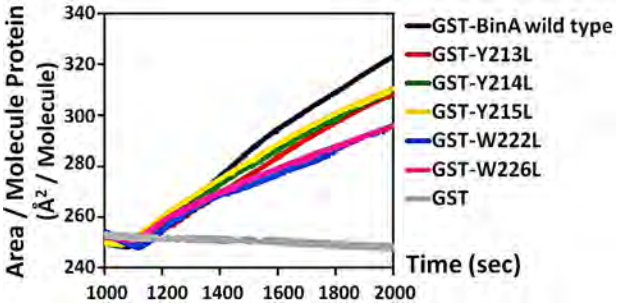

Fig. 2. The insertion ability of wild-type GST-BinA and its mutant proteins into DMPC monolayer. The data were obtained by measuring the change of lipid surface area under a constant surface pressure. Only GST protein was used as a negative control. Upon the injection, the increase of area per molecule protein was observed in all mutant proteins.

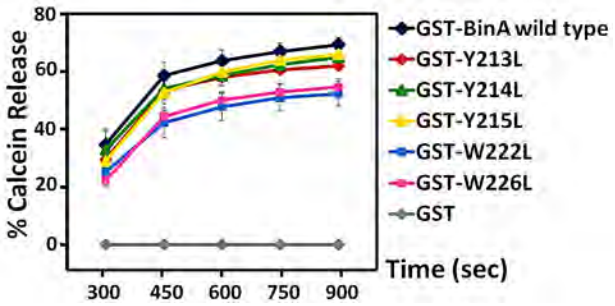

Fig. 3. The calcein release from LUVs treated with wild-type GST-BinA and its mutant proteins. Only GST protein was used as a negative control. The error bars represent the standard deviation of the measurements from three independent experiments.

three consecutive tyrosines (Y213L, Y214L and Y215L) conferred the comparable toxicity to that of the wild type, whereas the mutations of two tryptophans, W222L and W226L, rendered toxin inactive. Even though the concentration of inclusions was increased up to 32 μg ml^{-1}, no significant mortality was observed in those tryptophan mutations (Table 1), suggesting that tryptophan residues at positions 222 and 226 play a crucial role in larvicidal activity. Previous studies demonstrated the importance of tryptophan residues in the structural folding and biological activity of *B. thuringiensis* Cyt2Aa2, Cry1Ac and Cry1Ab toxins (19). The considerably reduced toxicity of W222L and W226L mutants, however, was not associated with the structural alterations as described earlier. Both W222 and W226 of BinA, therefore, seem to have functional significance in the toxication process of the binary toxin.

Effects of W222 and W226 mutations on membrane insertion and permeability

In order to study the membrane insertion ability of BinA and its mutants, the DMPC lipid monolayers were generated and the Langmuir-Blodgett (LB) trough technique was used. These DMPC lipid monolayers were previously used as model lipid monolayers for the study of interaction of BinA and BinB with receptor-free lipid membranes (9). As the liquid condensed phase, which is a fluid stage of DMPC monolayer being relevant to biological membranes, was observed when the surface pressure reached about 15-25 mN m^{-1}, the surface pressure was subsequently kept constant at 18 mN m^{-1} throughout this experiment. It was observed that the lipid packing at surface pressures 20 and 25 mN m^{-1} was more condensed although high protein concentration (50 nmol) was injected. No increase of area per molecule at both surface pressures was observed, therefore, lower pressure was required to provide more fluidity of lipid packing that allowed the protein insertion. Nevertheless, the stability of lipid monolayers, creep test, was performed to monitor the percent area reduction at constant surface pressure (20). After compressing until reaching to constant pressure and then left for 15 min at room temperature, the decrease of area per molecule of lipid was around 5% indicating that the property of the lipid monolayers still maintained after prolonged incubation time. Upon injection of the protein sample in the subphase of the trough, the degree of membrane insertion was monitored by the mean molecular area expansion. The results showed an increase in area expansion as a function of time in all protein samples, indicating the ability of these proteins to insert into DMPC monolayer. Therefore, the insertion of protein molecule into lipid monolayers was calculated and shown in term of area per molecule protein versus time (Fig. 2). No insertion was observed in the GST alone, indicating that the membrane insertion was only mediated by BinA molecules. This result shows as a single experiment. However, three independent experiments were performed and showed the correlated of those results. It should be noted that BinA, as opposed to BinB protein, was unable to insert into the lipid monolayers from the previous study (9). The discrepancies of these two observations could be explained by the different forms of proteins used for the assays. In this study, the GST-BinA fusion proteins were used, while the protoxins were used in the former study. Thus the differences of protein structure or folding possibly affect the membrane insertion ability. In this study, however, the extents of membrane insertion were somewhat different among BinA mutant proteins. Three active mutant proteins; GST-Y213L, GST-Y214L and GST-Y215L, were able to insert into the DMPC monolayer to the same extent as that of the wild-type BinA which also correlated well with their larvicidal activity. For the tryptophan mutations; GST-W222L and GST-W226L, however, less extent of membrane insertion was observed compared with that of the wild type (Fig. 2). Although the larvicidal activity of the GST-W222L and GST-W226L mutants was abolished, membrane insertion was only slightly compromised, suggesting that these two tryptophans may not directly involve in the membrane insertion.

Calcein release assay was used to investigate the effect of BinA mutations on large unilamella vesicles (LUVs) permea-

bility. The fluorescence intensity was observed after adding the wild-type GST-BinA and its mutants, indicating that all these proteins could perturb the lipid vesicles, resulting in the leakage of encapsulated calceins to the solution. In contrast, no leakage of calceins was observed in GST alone, suggesting that calcein release was solely induced by BinA protein. By comparing the degree of membrane permeability among BinA mutants, interestingly, both W222L and W226L showed less membrane permeability than that of tyrosine mutations (Fig. 3). This result is in agreement with the membrane insertion assay, providing a clue that these tryptophans may partially participate in the membrane perturbation. Since the localization of W222 and W226 in BinA molecule cannot be easily predicted with the absence of structural information of the binary toxin, it is hard to make a conclusive assumption of how these tryptophans participate in the membrane insertion and permeability. Moreover, conformational changes of the BinA/BinB complex accompanying the receptor binding to transform the water-soluble form into the membrane-translocation structure may take place inside the larval midgut. Therefore, upon the receptor-mediated conformational changes, the membrane insertion and permeability of W222L and W226L mutants may be severely affected, leading to the loss of larvicidal activity.

Taken together, the *in vivo* effects of the W222 and W226 mutations seem to be complicated. Both tryptophan residues are unlikely to participate in BinA-BinB interaction since W222L and W226L mutants could interact normally to BinB (Supplement 4). The involvement of W222 and W226 residues in subsequent steps after membrane insertion thus cannot be ruled out. It is possible that the lipid composition may be a key determinant in the membrane insertion and permeability of BinA toxin; hence, using the larval midgut membrane incorporated into the model lipid membranes would be more biologically relevant. This remains to be determined, and structural analysis of the binary toxin is essential to gain insights into its functional mechanism.

MATERIALS AND METHODS

Bacterial strains and oligonucleotides

Both *binA* and *binB* genes used in this study were derived from *B. sphaericus* strain 2297 (Genbank accession no. AJ224478). *Escherichia coli* strain JM109 was used as a host strain to express the GST-BinA and GST-BinB proteins from pGEX-BinA and pGEX-BinB, respectively (21). The recombinant plasmid pGEX-BinA encoding the GST-BinA fusion protein was used as a template for mutagenesis. All mutant plasmids were generated using QuikChange™ site-directed mutagenesis method (Stratagene). The aromatic amino acids Y213, Y214, Y215, W222, and W226 were substituted with leucine using the mutagenic oligonucleotides as shown in supplement 2. The mutant plasmids were selected by using restriction endonuclease digestion and verified by automated DNA sequencing (Macrogen Inc., Korea).

Protein expression and purification

The *E. coli* JM109 harbouring GST-BinB or GST-BinA wild type and its mutants were grown in LB broth containing 100 μg ml^{-1} ampicillin at 37°C until OD_{600} of the culture reached 0.5. Then 0.1 mM isopropyl-β-D-thiogalactopyranoside (IPTG) was added to induce protein expression. Toxin inclusions were released from host cells by French Pressure Cell and then partially purified as described previously (13). Protein inclusions were solubilized in 25 mM NaOH for 15 min and then dialyzed against 50 mM Na_2CO_3 buffer, pH 10 at 4°C for overnight. The soluble protein was subsequently purified by size-exclusion chromatography using a Superdex 200, 10/300 column (GE Healthcare Life Sciences). Protein concentration was determined by Bradford's method using bovine serum albumin (BSA) as a standard.

GST (Glutathione S-transferase) purification

E. coli cultured cells containing plasmid pGEX-4T-2 were grown in LB broth containing 100 μg ml^{-1} ampicillin at 37°C until OD_{600} reached to 0.5 and then induced by 0.1 mM IPTG for 5 h. GST protein was purified by using a GSTrap™ FF column and then HiTrap™ desalting column following the manufacturer's instructions (GE Healthcare Life Sciences).

Mosquito larvicidal assays

The second-instar *C. quinquefasciatus* larvae were obtained from the mosquito rearing facility, Institute of Molecular Biosciences, Mahidol University. The inclusions of GST-BinB and GST-BinA wild type or its mutants were mixed at a 1:1 molar ratio in 1 ml of water to the final concentration of 32 μg ml^{-1}, and further diluted as a 2-fold serial dilution. Then serial-diluted toxin mixtures were added to 1 ml of water containing 10 larvae in each well of a 24-well tissue culture plate (1.5 cm well diameter). Only GST-BinB inclusions were used as a negative control. After incubation at room temperature for 48 h, the mortality of larvae was recorded. Each experiment was done in duplicate, and at least three independent experiments were performed. The LC_{50} was analysed by Probit analysis (22).

Circular Dichroism (CD) analysis

The purified protein at 0.5 mg ml^{-1} in 50 mM Na_2CO_3 buffer, pH 10 was loaded in a rectangular quartz cuvette with 0.2 mm optical path-length. The CD spectra of proteins were observed in far-UV wavelengths of 190-260 nm by using Jasco J-715 CD spectropolarimeter at 25°C. The experiment was performed by scanning three averaged spectra using a speed at 50 nm min^{-1} with 2 nm of spectral bandwidth, 1 nm of the resolution and 2 s of response time. All spectra were subtracted from the baseline.

Membrane perturbation assay by calcein release method

Large unilamellar vesicles (LUVs) were prepared from 2 mg ml^{-1} of a lipid mixture of phosphatidylcholine (PC)/phosphatidic acid (PA) in ratio 1:1 (w/w) dissolved in chloroform as de-

scribed previously (8). The lipid mixture was evaporated under a nitrogen stream and the lipid film was resuspended in 200 µl of 60 mM calcein (pre-dissolved in 500 mM Na_2CO_3 buffer, pH 10) in 50 mM Na_2CO_3 buffer, pH 10. The mixture was subjected to 5 repeated cycles of freezing and thawing. Then the suspension was passed through a polycarbonate membrane (0.1-µm pore size, Avanti Polar Lipid) for at least 20 passes using a two-syringe extruder (Avanti Polar Lipid). The untrapped calceins were removed by using a HiTrap™ desalting column (GE Healthcare Life Sciences). Liposome concentrations were estimated by measuring the lipid phosphorus content (23). The calcein-encapsulated lipid vesicle solution was placed into a 0.5-cm light-path quartz SUPRASIL cell at a final concentration of 1.25 µM. Protein at concentration of 0.016-0.25 µM was added at time 250 s and then incubated for 10 min. The fluorescence signals were detected by using the Jasco FP-6300 spectrofluorometer at the emission and excitation wavelengths of 520 and 485 nm, respectively, with a slit width of 5 nm. Finally, 0.1% (v/v) Triton X-100 was added at time 900 s to totally release entrapped calceins. The degree of LUVs perturbation was determined as the percentage of calcein release as described previously (8).

Membrane insertion assay by Langmuir-Blodgett method

The interaction of BinA and its mutants with 2-Dimyristoyl-rac-glycero-3-phosphocholine (DMPC) monolayer was monitored by using a KSV 2,000 Langmuir-Blodgett trough (KSV, Finland). The 0.175 mg ml^{-1} of DMPC in chloroform and 50 mM Na_2CO_3 buffer, pH 10 were used as a surfactant and a subphase, respectively. To characterize the DMPC monolayer, the 60 µl of 0.175 mg ml^{-1} of lipid were spread on the subphase. The lipid monolayer was left standing for 5 min to ensure the complete evaporation of the solvent. The lipid was symmetrically compressed by barriers at a constant speed of 10 mm min^{-1} until the surface pressure reached 18 mN m^{-1} and the monolayer was kept constant at this surface pressure by using the constant surface pressure mode. The film was normally allowed to stand for 5 min prior to the injection of the protein to reach the stability. After that, the sample containing the protein (5 nmol) was injected at 1,000 s by L-shaped syringe right underneath the monolayer forming area, between barriers. Special care must be taken to avoid the formation of bubble during the injection process. All experiments were performed at room temperature.

Acknowledgements

Authors would like to thank Assoc. Prof. Chartchai Krittanai and also my colleague for their assistance. This work was supported by the National Center for Genetic Engineering and Biotechnology, National Science and Technology Development Agency, Thailand, the Thailand Research Fund and the Mahidol University Research Grant, Thailand. T.K. was supported by the Cooperation on Science and Technology Researcher Development Project (Co-STRD), Ministry of Science and Technology, Thailand.

REFERENCES

1. Davidson, E. W., Oei, C., Meyer, M., Bieber, A. L., Hindley, J. and Berry, C. (1990) Interaction of the *Bacillus sphaericus* mosquito larvicidal proteins. *Can J. Microbiol*. **36**, 870-878.
2. Baumann, P., Clark, M. A., Baumann, L. and Broadwell, A. H. (1991) *Bacillus sphaericus* as a mosquito pathogen: properties of the organism and its toxins. *Microbiol. Rev*. **55**, 425-436.
3. Charles, J. F., Nielson-LeRoux, C. and Delecluse, A. (1996) *Bacillus sphaericus* toxins: molecular biology and mode of action. *Annu. Rev. Entomol*. **41**, 451-472.
4. Silva-Filha, M. H., Nielsen-LeRoux, C. and Charles, J. F. (1999) Identification of the receptor for *Bacillus sphaericus* crystal toxin in the brush border membrane of the mosquito *Culex pipiens* (Diptera: Culicidae). *Insect Biochem. Mol. Biol*. **29**, 711-721.
5. Darboux, I., Nielsen-LeRoux, C., Charles, J. F. and Pauron, D. (2001) The receptor of *Bacillus sphaericus* binary toxin in *Culex pipiens* (Diptera: Culicidae) midgut: molecular cloning and expression. *Insect Biochem. Mol. Biol*. **31**, 981-990.
6. Silva-Filha, M. H. N. L. and Peixoto, C. A. (2003) Immunocytochemical localization of the *Bacillus sphaericus* binary toxin components in *Culex quinquefasciatus* (Diptera: Culicidae) larvae midgut. *Pesticide Biochemistry and Physiology* **77**, 138-146.
7. Opota, O., Gauthier, N. C., Doye, A., Berry, C., Gounon, P., Lemichez, E. and Pauron, D. (2011) *Bacillus sphaericus* binary toxin elicits host cell autophagy as a response to intoxication. *PLoS One* **6**, e14682.
8. Schwartz, J. L., Potvin, L., Coux, F., Charles, J. F., Berry, C., Humphreys, M. J., Jones, A. F., Bernhart, I., Dalla Serra, M. and Menestrina, G. (2001) Permeabilization of model lipid membranes by *Bacillus sphaericus* mosquitocidal binary toxin and its individual components. *J. Membr Biol*. **184**, 171-183.
9. Boonserm, P., Moonsom, S., Boonchoy, C., Promdonkoy, B., Parthasarathy, K. and Torres, J. (2006) Association of the components of the binary toxin from *Bacillus sphaericus* in solution and with model lipid bilayers. *Biochem. Biophys. Res. Commun*. **342**, 1273-1278.
10. Boonyos, P., Soonsanga, S., Boonserm, P. and Promdonkoy, B. (2009) Role of cysteine at positions 67, 161 and 241 of a *Bacillus sphaericus* binary toxin BinB. *BMB Rep*. **43**, 23-28.
11. Broadwell, A. H., Baumann, L. and Baumann, P. (1990) The 42- and 51-kilodalton mosquitocidal proteins of *Bacillus sphaericus* 2362: construction of recombinants with enhanced expression and *in vivo* studies of processing and toxicity. *J. Bacteriol*. **172**, 2217-2223.
12. Elangovan, G., Shanmugavelu, M., Rajamohan, F., Dean, D. H. and Jayaraman, K. (2000) Identification of the functional site in the mosquito larvicidal binary toxin of *Bacillus sphaericus* 1593M by site-directed mutagenesis. *Biochem. Biophys. Res. Commun*. **276**, 1048-1055.
13. Promdonkoy, B., Promdonkoy, P., Audtho, M., Tanapongpipat, S., Chewawiwat, N., Luxananil, P. and Panyim, S.

(2003) Efficient expression of the mosquito larvicidal binary toxin gene from *Bacillus sphaericus* in *Escherichia coli*. *Curr. Microbiol*. **47**, 383-387.
14. Sanitt, P., Promdonkoy, B. and Boonserm, P. (2008) Targeted mutagenesis at charged residues in *Bacillus sphaericus* BinA toxin affects mosquito-larvicidal activity. *Curr. Microbiol*. **57**, 230-234.
15. Yuan, Z., Rang, C., Maroun, R. C., Juarez-Perez, V., Frutos, R., Pasteur, N., Vendrely, C., Charles, J. F. and Nielsen-Leroux, C. (2001) Identification and molecular structural prediction analysis of a toxicity determinant in the *Bacillus sphaericus* crystal larvicidal toxin. *Eur. J. Biochem*. **268**, 2751-2760.
16. Reithmeier, R. A. (1995) Characterization and modeling of membrane proteins using sequence analysis. *Curr. Opin. Struct. Biol*. **5**, 491-500.
17. Oei, C., Hindley, J. and Berry, C. (1992) Binding of purified *Bacillus sphaericus* binary toxin and its deletion derivatives to *Culex quinquefasciatus* gut: elucidation of functional binding domains. *J. Gen. Microbiol*. **138**, 1515-1526.
18. Singkhamanan, K., Promdonkoy, B., Chaisri, U. and Boonserm, P. (2010) Identification of amino acids required for receptor binding and toxicity of the *Bacillus sphaericus* binary toxin. *FEMS Microbiol. Lett*. **303**, 84-91.
19. Promdonkoy, B., Pathaichindachote, W., Krittanai, C., Audtho, M. Chewawiwat, N. and Panyim, S. (2004) Trp132, Trp154, and Trp157 are essential for folding and activity of a Cyt toxin from *Bacillus thuringiensis*. *Biochem. Biophys. Res. Commun*. **317**, 744-748.
20. Kanintronkul, Y., Srikhirin, T., Angsuthanasombat, C., and Kerdcharoen, T. (2005) Insertion behavior of the *Bacillus thuringiensis* Cry4Ba insecticidal protein into lipid monolayers. *Arch. Biochem. Biophys*. **442**, 180-186.
21. Promdonkoy, B., Promdonkoy, P. and Panyim, S. (2008) High-level expression in *Escherichia coli*, purification and mosquito-larvicidal activity of the binary toxin from *Bacillus sphaericus*. *Curr. Microbiol*. **57**, 626-630.
22. Finney, D. J. (1971) Probit analysis. pp.50-80, Cambridge University Press, Cambridge, UK.
23. Mrsny, R. J., Volwerk, J. J. and Griffith, O. H. (1986) A simplified procedure for lipid phosphorus analysis shows that digestion rates vary with phospholipid structure. *Chem. Phys. Lipids*. **39**, 185-191.

Journal of Invertebrate Pathology 106 (2011) 230–235

Contents lists available at ScienceDirect

Journal of Invertebrate Pathology

journal homepage: www.elsevier.com/locate/jip

Functional characterization of truncated fragments of *Bacillus sphaericus* binary toxin BinB

Chontida Tangsongcharoen [a], Panadda Boonserm [a], Boonhiang Promdonkoy [b,*]

[a] Institute of Molecular Biosciences, Mahidol University, Salaya Campus, Nakhonpathom 73170, Thailand
[b] National Center for Genetic Engineering and Biotechnology, National Science and Technology Development Agency, 113 Phahonyothin Road, Klong 1, Klong Luang, Pathumthani 12120, Thailand

ARTICLE INFO

Article history:
Received 30 March 2010
Accepted 13 October 2010
Available online 20 October 2010

Keywords:
Bacillus sphaericus
Binary toxin
BinA–BinB interaction
Larvicidal activity
Receptor binding
Truncated protein

ABSTRACT

Bacillus sphaericus produces a mosquitocidal binary toxin composed of two subunits, BinA (42 kDa) and BinB (51 kDa). Both components are required for maximum toxicity against mosquito larvae. BinB has been proposed to provide specificity by binding to the epithelial gut cell membrane, while BinA may be responsible for toxicity. To identify regions in BinB responsible for receptor binding and for interaction to BinA, we used six BinB shorter constructs derived from both the N-terminal and the C-terminal halves of the protein. All constructs expressed as inclusion bodies in *Escherichia coli*, similarly to the wild-type protein. A marked decrease in larvicidal activity was observed when BinA was used in combination with these BinB constructs, used either individually or in pairs from both N and C-halves of BinB. Nevertheless, immunohistochemistry analyses demonstrate that these constructs are able to bind to the epithelium gut cell membrane, and *in vitro* protein–protein interaction assays revealed that these constructs can bind to BinA. These results show that fragments corresponding to both halves of BinB are able to bind the receptor and to interact with BinA, but both halves are required by the toxin to exhibit full larvicidal activity.

1. Introduction

Bacillus sphaericus is a Gram-positive spore-forming aerobic bacterium. During sporulation, it produces a parasporal crystal protein specifically toxic to *Culex* and *Anopheles* mosquito larvae (Berry et al., 1993). These crystal proteins have been used as a biological insecticide to control disease vectors (Mulla et al., 2001), and are composed of two proteins with molecular mass of 42 kDa (BinA) and 51 kDa (BinB). Both proteins are required for full larvicidal activity, hence the name "binary toxin" (Baumann et al., 1991). Evidence so far indicates that the activated BinB toxin (43 kDa) binds to a receptor located in epithelial cells (Silva-Filha et al., 1999). It has been demonstrated that the regional binding of BinB localized to the posterior midgut and gastric caecum (Oei et al., 1992). The activated BinA toxin (39 kDa) binds to either BinB or to a BinB-receptor complex. This is followed by internalization of both components, resulting in cell death mediated by an unknown mechanism (Oei et al., 1992). Previous studies have suggested that BinB is a two-domain protein in which the N-terminal half would play a role in receptor binding, whereas the C-terminal half would be responsible for interaction with BinA (Elangovan et al., 2000; Oei et al., 1992).

The 3D structure of the toxin is not available, although crystals of BinB (Chiou et al., 1999) and binary toxin (Smith et al., 2004) have been reported. Using EMBOSS pairwise alignment (http://www.ebi.ac.uk) it was found that amino acid sequences of BinA and BinB share high homology (25% identity and 40% similarity); therefore they are likely to have a similar 3D structure. Comparison to sequences of proteins with known 3D structure, however, shows little similarity.

BinA is degraded into three fragments, with proteolytic cleavage sites identified at Met-103 and Arg-207 (Promdonkoy et al., 2008). It has been demonstrated that the BinA C-terminal half, from Met-208 to Phe-353, is responsible for interaction with BinB (Limpanawat et al., 2009). Similar to BinA, BinB also showed some degradation fragments about 30–32 kDa (Promdonkoy et al., 2003) but the proteolytic cleavage site in BinB has not been identified. However, based on their amino acid sequence alignment, BinB may have similar cleavage sites. To investigate receptor binding and ability of BinB fragments to interact to BinA, six constructs from the N-terminal and C-terminal halves of BinB were used. Biological activity, receptor binding to the larval gut cell membrane and interaction of these constructs to BinA were investigated.

2. Materials and methods

2.1. Construction of N- and C-terminal BinB constructs

The recombinant plasmid pET-tBinB (Boonyos et al., 2010) encoding the 43 kDa active fragment of BinB wild-type toxin amino

* Corresponding author. Fax: +66 2 564 6707.
E-mail address: boonhiang@biotec.or.th (B. Promdonkoy).

0022-2011/$ - see front matter © 2010 Elsevier Inc. All rights reserved.
doi:10.1016/j.jip.2010.10.004

acid positions Asn33–Lys408, which was cloned from *B. sphaericus* 2297 into *Nhe*I and *Xho*I sites of pET-17b was used as a template for PCR with appropriate primers shown in Table 1. This truncated BinB still retained full activity similar to that of the full-length BinB (Boonyos et al., 2010). Plasmids encoding BinB N-terminal constructs, N–11K (N33–F132), N–25K (N33–K254) and N–32K (N33–R318), were generated based on Stratagene QuikChange™ Site-directed mutagenesis by substitutions of codons encoding E133, M255 and S319 with stop codons, respectively. The PCR products were treated with *Dpn*I and transformed into *Escherichia coli* JM109. Selected clones were screened by restriction endonuclease digestion and then verified by automated DNA sequencer at Macrogen Inc., Korea. Plasmids encoding the respective C-terminal fragments were constructed by PCR. The plasmid pET-tBinB (Boonyos et al., 2010) was used as a template together with T7 terminator primer and appropriate forward primers (Table 1) designed for encoding different C-terminal BinB constructs, C–32K (E133 to K408), C–18K (M255 to K408) and C–11K (S319 to K408). PCR products were digested with *Nde*I and *Xho*I and cloned into pET-17b that was digested with the same enzymes.

2.2. Protein preparation

Each recombinant plasmid was extracted from *E. coli* JM109 and re-transformed into *E. coli* BL21(DE3)pLysS for expression. The transformant clones were grown in LB broth containing ampicillin 100 μg/ml and chloramphenicol 34 μg/ml at 37 °C until OD_{600} reached 0.3–0.4. The cultures were induced with 1 mM IPTG (isopropyl-β-D-thiogalactopyranoside) and further grown at 37 °C for 5 h. Protein inclusions were released from host cells using French Pressure Cell at 10,000 psi and partially purified using differential centrifugation as described earlier (Promdonkoy et al., 2003). The partially purified inclusions were analyzed by SDS–PAGE and immunoblotting. Protein inclusions were solubilized in 25 mM NaOH and then dialyzed in 50 mM Na_2CO_3 pH 10 at 4 °C. The dialyzed proteins were further purified by size-exclusion liquid chromatography using Superdex 200 HR 10/300 column with carbonate buffer (pH 10). Protein concentrations were determined by Bradford-based protein assay (Bio-RAD), and bovine serum albumin (BSA) was used as a standard.

2.3. Mosquito-larvicidal activity assays

Larvicidal activity assays were performed against 2nd-instar *Culex quinquefasciatus* larvae as described previously (Promdonkoy et al., 2008). BinA and BinB inclusions were mixed at 1:1 molar ratio and the concentration of total protein was adjusted to 50 μg/ml. One ml of the protein mixture was added to each well of a 24-well tissue culture plate containing 10 larvae in 1 ml water (the final concentration of the protein mixture was 25 μg/ml). Mortality was recorded after 48 h incubation at room temperature.

Table 1
Nucleotide primers used for construction of truncated BinB constructs. Primers E133stop, M255stop and S319stop were used for site-directed mutagenesis to change codons at positions E133, M255 and S319 to stop codons in order to generate N-terminal truncated constructs N–11K, N25K and N32K, respectively. Forward primers E133, M255 and S319 were used in combination with T7 terminator primer in PCR reactions to generate DNA constructs encoding C-terminal truncated BinB proteins C–32K, C–18K and C–11K, respectively. The recognition sites of restriction enzymes are underlined.

Primer name	Sequence (5′ → 3′)	Enzyme
E133stop_f	AGACAAAAGTTTTGACGCGTAGGTAGTGGA	*Mlu*I
E133stop_r	TCCACTACCTACGCGTCAAAACTTTTGTCTC	*Mlu*I
M255stop_f	TTCCGATAAATAGCGCTTTAATACCTACTA	*Eco*47III
M255stop_r	TAGTAGGTATTAAAGCGCTATTTATCGGAAT	*Eco*47III
S319stop_f	TTTTATTTGAGATAATCCGGATTTTAAGGAA	*Kpn*2I
S319stop_r	CTTAAATCCGGATTATCTCAAATAAAAATA	*Kpn*2I
E133_forward	GGATCCCATATGGAGCAGGTAGGTAGTGGA	*Nde*I
M255_forward	GGATCCCATATGAAATTTAATACCTACTAT	*Nde*I
S319_forward	GGATCCCATATGTCTAGCGGATTTAAGGAA	*Nde*I
T7 terminator	TGCTAGTTATTGCTCAGCGG	–

2.4. Secondary structure analysis

Circular dichroism (CD) spectrum of the purified protein (0.45 mg/ml) prepared in the carbonate buffer, pH 10, was measured using a Jasco J-715 CD spectropolarimeter (Jasco Inc., USA) as described earlier (Leetachewa et al., 2006). CD spectra were recorded by using a 1 nm spectral bandwidth for three scans at a rate 20 nm/min and all spectra were subtracted from a baseline.

2.5. In vitro receptor binding assays via immunohistochemical staining

Paraffin-embedded histological sections of 4th-instar *C. quinquefasciatus* larval gut tissue were prepared as described previously (Chayaratanasin et al., 2007). Immunohistochemical staining was performed following the method described previously (Chayaratanasin et al., 2007; Singkhamanan et al., 2010) by using 20 μg/ml of the 43-kDa BinB wild-type or the purified truncated constructs and subsequently probed with rabbit anti-BinB polyclonal antibody (1:10,000 dilution), biotinated goat anti-rabbit IgGs (1:200 dilution) and HRP-labeled streptavidins (1:500 dilution). DAB (3,3-Diaminobenzidine) substrate solution was added and the signal was visualized under light microscope.

2.6. In vitro BinA–BinB interaction assays via dot blot analysis

Various amounts of BinB wild-type and each truncated BinB fragment ranging from 1, 0.2, 0.04 and 0.008 μmole were immobilized on the nitrocellulose membrane using dot blot apparatus. The membrane was blocked with 5% skim milk in PBS buffer at 25 °C for 1 h. The membrane was overlaid for 1 h at 25 °C with 5% skim milk in PBS containing 20 μg/ml of a fusion protein between glutathione S-transferase and the full-length BinA (GST-BinA) (Promdonkoy et al., 2008). Unbound proteins were removed by washing three times with PBS. The bound protein was detected by probing with rabbit anti-GST antibody (1:2500 dilution) and goat anti-rabbit IgGs conjugated HRP (1:5000 dilution). The signals were developed using Enhanced chemiluminescence (ECL) substrate.

3. Results and discussion

3.1. Production and conformation of the BinB constructs

Amino acid sequence analysis revealed that BinA and BinB share no significant homology to any protein with known 3D structure. However, both proteins show high homology to each other which may suggest their similar 3D structures. Previous reports suggested that BinB is a 2-domain protein. The receptor binding domain should be in the N-terminal part whereas the C-terminal part should interact to BinA (Elangovan et al., 2000;Oei et al., 1992). SDS–PAGE and immunoblot analyses revealed proteolytic degradation products of BinB about 30–32 kDa (Promdonkoy et al., 2003). Since the internal proteolytic cleavage site in BinB has not been identified, six BinB constructs were generated based on amino acid sequence alignment and proteolytic processing sites in BinA (Limpanawat et al., 2009;Promdonkoy et al., 2008). The possible processing sites in BinB should be at carboxyl terminal residues F132, K254 and R318. Therefore three N-terminal

constructs named N–11K (N33–F132), N–25K (N33–K254), N–32K (N33–R318), and three C-terminal constructs C–32K (E133–K408), C–18K (M255–K408) and C–11K (S319–K408) were generated (Fig. 1).

All constructs expressed as inclusion bodies inside *E. coli* similar to the wild-type protein. The protein inclusions were released from the host cells and partially purified before analysis on SDS–PAGE (Fig. 2A). Some protein degradation was detected in N–25K, N–32K and C–32K constructs. Most of the constructs migrated normally in SDS–polyacrylamide gel except N–11K, which showed a smear pattern, with bands with higher molecular weight than expected.

Most of the constructs were successfully detected by Western blot and immunodetection analysis with anti-BinB polyclonal antibody, except the C–11K (Fig. 2B). However, the identity of the C–11K was confirmed by N-terminal amino acid sequencing. Failure to detect this fragment by immunoblotting might be due to the loss of the antigenic recognition sequence from amino acid deletion. In addition, the immunological signal of N–11K was weaker than that of the wild type, suggesting that antibody binding epitopes were affected. N–25K, C–32K and C–18K showed a strong immunological signal, comparable to the wild type indicating that most antibody binding epitopes are located between E133 and R318.

The secondary structure content of the constructs was determined by CD. Whereas spectra of N–32K and C–32K were similar to that of the wild type, those corresponding to N–11K, N–25K, C–18K and C–11K were dramatically different (Fig. 3). All constructs contain a high percentage of α-helix, and some β-sheet as demonstrated by the far-UV CD spectra (190–250 nm). Interestingly, Boonserm et al. reported that the secondary structure of BinB in aqueous solution was likely random coil using attenuated total reflection Fourier transform infrared spectroscopy (ATR-FTIR), observing only one intense band in the infrared amide I region at ~1670 cm^{-1} (Boonserm et al., 2006). These results were confirmed using CD spectroscopy, which showed that BinB in solution is likely to be in a random coil conformation. Further, these authors observed extensive changes in secondary structure after interaction of either BinA or BinB or both subunits with a lipid bilayer. Thus, deletion at either N- or C-termini may equally induce a dramatic conformational change. The secondary structure prediction of wild-type BinB using Profile network prediction Heidelberg (PROF) (Rost and Sander, 1993) show that it contains β-sheet more than α-helix (7% α-helix, 37% β-sheet, and 55% of either random or β-turns or loops). Prediction has shown that amino acids 1–34 are potential loop forming regions, followed by an α-helical structure up to 45 amino acids (Elangovan et al., 2000). For the secondary structure prediction of BinB, it shows rather similar prediction as that of BinA which contains 2% α-helix, 48% β-sheet and 50% of either random or β-turns or loops (Boonserm et al., 2006).

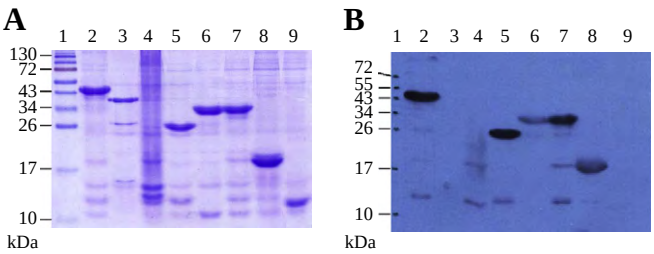

Fig. 2. Coomassie blue-stained SDS–polyacrylamide gel (A) and immunoblot (B). Protein inclusions were extracted from *E. coli* and partially purified by repeated washing and centrifugations. The inclusions were mixed with protein sample buffer and applied to SDS–PAGE (A). Proteins in SDS–polyacrylamide gel were transferred to nitrocellulose membrane and detected by rabbit polyclonal anti-BinB and goat anti-rabbit IgG conjugated with HRP. Lane 1 is broad-range protein standard marker. Lanes 2–9 are partially purified inclusions of BinB, BinA, N–11K, N–25K, N–32K, C–32K, C–18K and C–11K, respectively. (For interpretation of the references to color in this figure legend, the reader is referred to the web version of this article.)

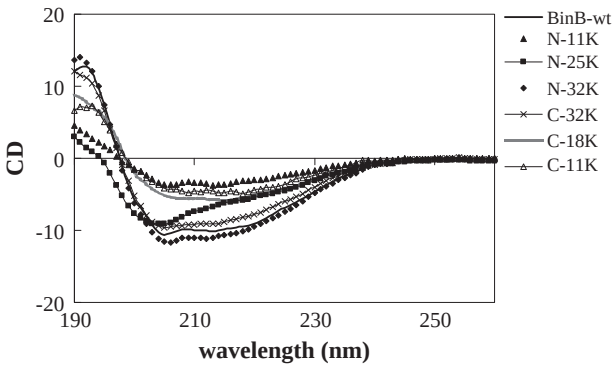

Fig. 3. CD spectra of the BinB wild type and N- and C-terminal BinB constructs. The figure shows far-UV CD spectra of the 43-kDa purified BinB toxin in comparison with that of the N- and C-terminal BinB constructs, N–11K, N–25K, N–32K, C–32K, C–18K and C–11K in 50 mM carbonate buffer, pH 10.

3.2. Larvicidal activity of truncated constructs

Both subunits, BinA and BinB, are required to exhibit maximum toxicity to mosquito larvae (Broadwell et al., 1990; Nicolas et al., 1993; Oei et al., 1990). However, BinA alone at high concentration was also toxic to mosquito larvae, suggesting that the toxic domain is located in BinA (Berry et al., 1993; Nicolas et al., 1993; Yuan et al., 2001). In the present study, BinB, inclusion bodies of each BinB construct, and combinations of N- and C-terminal BinB constructs, were mixed with BinA and fed to mosquito larvae at high concentration (25 μg/ml). Whereas all larvae were killed (100% mortality) when fed with mixture of wild-type BinA and BinB, toxicity was

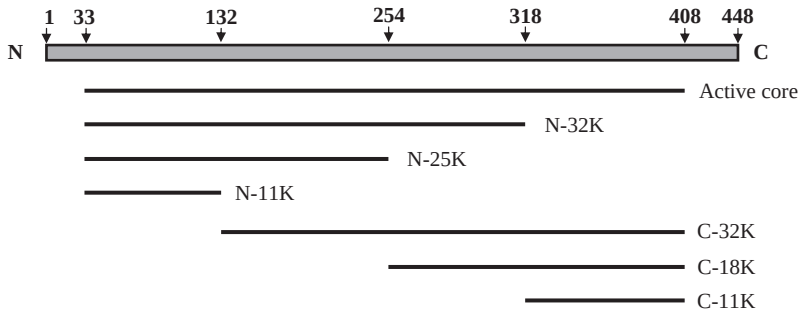

Fig. 1. Schematic diagram representing six truncated BinB constructs. N–32K, N–25K and N–11K represent the N-terminal BinB constructs while C–32K, C–18K and C–11K represent the respective C-terminal BinB constructs. Numbers above the diagram indicate positions of the predicted proteolytic cleavage sites in BinB. The active core (N33–K408) retains full biological activities similar to the full-length toxin.

significantly reduced when BinB was replaced by individual BinB constructs (Table 2). LC_{50} (concentration of toxin that cause 50% mortality) of the mixture of BinA and BinB inclusions is normally in the range of 10–100 ng/ml when using the full-length or active truncated toxin (Boonyos et al., 2010; Singkhamanan et al., 2010). No mortality was observed when the larvae were fed with mixtures of BinA and individual BinB constructs at 1000 ng/ml. Therefore all BinB fragments are considered non-toxic at this concentration. However, mixtures of BinA and some BinB fragments such as N–32K, C–18K and C–32K at high concentration could significantly improve toxicity (Table 2). This suggests that the above fragments can exhibit biological activity but at much lower level compared to the full-length BinB. Toxicity was not improved after mixing BinA with a mixture of N- and C-terminal BinB constructs, suggesting that they cannot complement each other. In fact, the toxicity was lowered when mixtures of N- and C-terminal BinB constructs were used compared to that of BinA alone or mixtures of BinA and individual BinB construct. One explanation is that the conformation of these constructs is not the same as in the wild-type protein. These alterations could affect receptor binding (Davidson, 1988), oligomerization (Smith et al., 2005), membrane insertion (Boonserm et al., 2006; Schwartz et al., 2001) or internalization of the toxic component into cytosol (Cokmus et al., 1997; Oei et al., 1992). Improper folding could also make the protein more susceptible to be degraded by larval gut proteases. Indeed, previous reports found that deletions of some amino acids from N- and C-termini of BinA and BinB proteins dramatically reduced or abolished toxicity (Baumann et al., 1991; Oei et al., 1992). Earlier studies also showed that deletion of 41 amino acids from the N-terminal region of BinB disrupted its biological activity (Clark and Baumann, 1990). In addition, mutations in the C-terminal region of BinB resulted in a total loss of activity as observed with mutants $^{387}YRL^{389} \rightarrow AAA$ and $^{392}IQ^{393} \rightarrow AA$ (Elangovan et al., 2000). Therefore both N- and C-terminal halves are required for full activity albeit both of them are correctly folded.

Previous reports have shown that the mixtures of two non-toxic mutants of either BinA (42N2: $C_{47} \rightarrow A$ and 42C2: $R_{312} \rightarrow A$) or BinB (51N4: $S_{38}KK_{40} \rightarrow AAA$ and 51C2: $I_{392}Q_{393} \rightarrow AA$) could restore the toxicity possibly via functional complementation (Elangovan et al., 2000; Shanmugavelu et al., 1998). Functional complementation of two non-toxic mutants also suggested that oligomerization of the binary toxin subunits takes place in the midgut of mosquito larvae and the mutation at one site can be complemented by another mutation at different sites. However in our experiment, combination of each N- and the respective C-terminal fragment could not restore the larvicidal activity. This indicated that these truncated proteins could not functionally complement each other in the same way as the mutant proteins.

Table 2
Mosquito larvicidal assays against *Culex quinquefasciatus* larvae. Larvae were fed with 25 μg/ml of mixture of inclusions BinA and BinB or BinB truncated constructs (1:1 molar ratio). The wild-type BinA and BinB inclusions alone were used as controls. Mortality was recorded after feeding the mixture for 48 h. Data represent means ± SEM (standard error of the mean) based on three independent experiments.

Protein mixture	% Mortality ± SEM
BinA	28 ± 7
BinB	11 ± 3
BinA + BinB	100 ± 0
BinA + N–11K	20 ± 7
BinA + N–25K	31 ± 17
BinA + N–32K	40 ± 10
BinA + C–11K	28 ± 12
BinA + C–18K	40 ± 12
BinA + C–32K	37 ± 12
BinA + N–11K + C–32K	17 ± 3
BinA + N–25K + C–18K	13 ± 3
BinA + N–32K + C–11K	17 ± 3

3.3. N- and C-terminal BinB constructs bind to mosquito gut cell membrane

Previous deletion studies suggest that BinB may have two domains, one that binds a receptor on the target membrane and the other interacts with BinA (Oei et al., 1992). In order to determine receptor binding activity of the BinB constructs, immunohistochemistry was performed on the midgut epithelial membrane of *C. quinquefasciatus* larvae. The susceptible midgut incubated with BinB wild type (positive control) showed a strong signal intensity which was in contrast with the non overlay with BinB as the negative control that showed only a faint signal. Constructs N–25K, N–32K, C–32K and C–18K were able to bind the gut cell membrane in a similar manner as BinB wild type (Fig. 4). This is consistent with a previous report that showed specific binding of BinB in regional areas of gastric caecum and posterior stomach in susceptible *Culex* species (Davidson, 1988; Davidson et al., 1990; Oei et al., 1992). The fact that all these constructs could bind to the membrane on their own, indicate that a receptor binding motif is present in these constructs (N–25K, N–32K, C–32K and C–18K). N–11K showed the binding insignificantly different from the negative control, although this may be due to a lower immunological reactivity of N–11K to anti-BinB (Fig. 2). Finally, the binding of C–11K was not tested since it cannot react to anti-BinB polyclonal antibody. Thus, the smallest constructs used from the N- and the

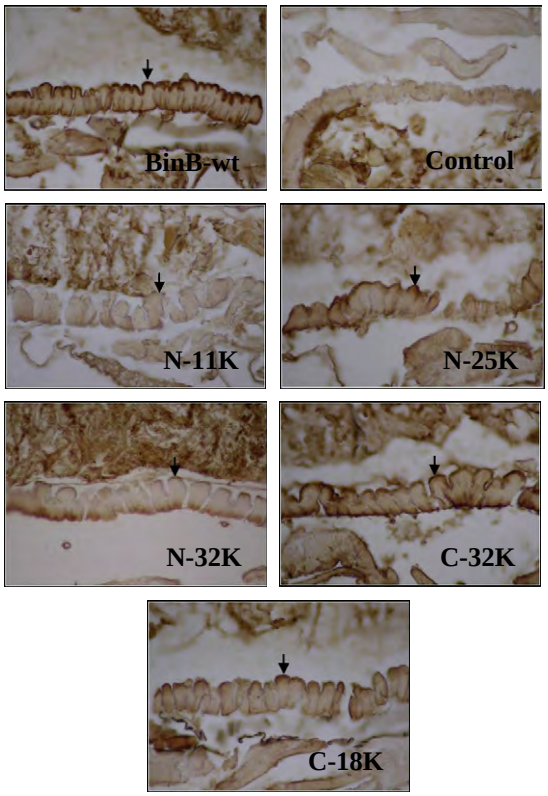

Fig. 4. Binding of N- and C-terminal BinB constructs on larval gut sections prepared from 4th-instar *C. quinquefasciatus* larvae *via* immunohistochemistry technique. The sections were blocked for non-specific protein binding and were then overlaid with 20 μg/ml of purified BinB wild type, N–11K, N–25K, N–32K, C–32K and C–18K. Section overlaid with carbonate buffer was used as negative control. The bound proteins were probed with anti-BinB polyclonal antibody followed by HRP-labeled streptavidin. Arrows indicate toxin binding regions on the larval gut cells.

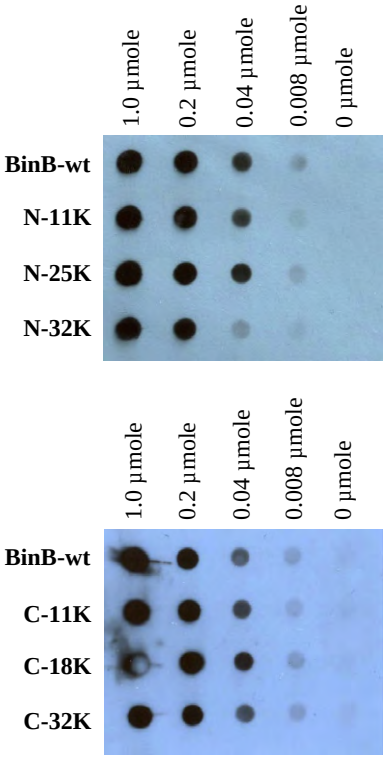

Fig. 5. BinA–BinB interactions by dot blot analysis. Various amounts of purified N- and C-terminal constructs of BinB were immobilized on the nitrocellulose membrane. The membrane was blocked with skim milk and then overlaid with purified GST-BinA. The presence of GST was detected by rabbit anti-GST and goat anti-rabbit conjugated with HRP.

C-terminal regions that showed strong binding were N–25K and C–18K, therefore the residues involved with receptor binding should be located in both regions: N33–K254 and M255–K408. This result is in agreement to previous examination of the deletion derivatives that found the N-terminal region of BinB is required for binding to the larval gut (Oei et al., 1992). The importance of specific amino acids in these regions has not been investigated, although F149 and Y150 were recently identified to play a critical role during membrane interaction and receptor binding (Singkhamanan et al., 2010).

3.4. N- and C-terminal constructs of BinB interact with BinA

Previous *in vivo* binding studies suggested that the BinB N-terminal region is crucial for specific binding to certain regions of the larval gut, while BinB C-terminal region could be responsible for interacting with BinA (Baumann et al., 1991; Broadwell et al., 1990; Oei et al., 1992). To test whether the decrease in toxicity of the BinB constructs is due to their inability to form BinA–BinB complex, *in vitro* BinA–BinB interaction was analyzed using a dot blot assay. BinB constructs were immobilized on a nitrocellulose membrane and overlaid with GST-BinA fusion protein. Results in Fig. 5 demonstrate that all BinB constructs can interact with GST-BinA. No signal was observed when immobilized BinB constructs were overlaid with GST, indicating that the interaction is specific. We observe that even the smallest constructs, N–11K and C–11K were able to bind BinA at a level comparable to that of the wild-type BinB (Fig. 5). This clearly suggests that the two N- and C-terminal BinB regions that can interact to BinA are located within constructs N33–F132 (N-terminal part) and S319–K408 (C-terminal part). However, it should be noted that not only the relative binding affinity of the constructs could not be determined from these assays but also the binding assays were carried out under non-physiological conditions.

In conclusion, our results demonstrate that both N- and C-terminal BinB constructs can independently bind mosquito larval gut cell membrane and interact to BinA without the requirement of their counterparts in the other half of the molecule. It is possible that BinB might have some regions of similar structure distributed in both N- and C-terminal halves. These regions could independently interact with BinA and bind to the gut cell membrane. However, for full activity both N- and C-terminal regions must be present.

Acknowledgments

The authors would like to thank Dr. Jaume Torres for critical reading of the manuscript, Dr. Chartchai Krittanai for assistance with CD and Ms. Chaweewan Chimwai for supplying mosquito larvae. This work was supported by the Thailand Research Fund, the National Center for Genetic Engineering and Biotechnology, National Science and Technology Development Agency, Thailand and a scholarship from the Ministry of Science and Technology under the Cooperation on Science and Technology Researcher Development Project (Co-STRD), Thailand.

Appendix A. Supplementary material

Supplementary data associated with this article can be found, in the online version, at doi:10.1016/j.jip.2010.10.004.

References

Baumann, P., Clark, M.A., Baumann, L., Broadwell, A.H., 1991. *Bacillus sphaericus* as a mosquito pathogen: properties of the organism and its toxins. Microbiol. Rev. 55, 425–436.

Berry, C., Hindley, J., Ehrhardt, A.F., Grounds, T., de Souza, I., Davidson, E.W., 1993. Genetic determinants of host ranges of *Bacillus sphaericus* mosquito larvicidal toxins. J. Bacteriol. 175, 510–518.

Boonserm, P., Moonsom, S., Boonchoy, C., Promdonkoy, B., Parthasarathy, K., Torres, J., 2006. Association of the components of the binary toxin from *Bacillus sphaericus* in solution and with model lipid bilayers. Biochem. Biophys. Res. Commun. 342, 1273–1278.

Boonyos, P., Soonsanga, S., Boonserm, P., Promdonkoy, B., 2010. Role of cysteine at positions 67, 161 and 241 of a *Bacillus sphaericus* binary toxin BinB. BMB. Rep. 43, 23–28.

Broadwell, A.H., Baumann, L., Baumann, P., 1990. The 42- and 51-kilodalton mosquitocidal proteins of *Bacillus sphaericus* 2362: construction of recombinants with enhanced expression and *in vivo* studies of processing and toxicity. J. Bacteriol. 172, 2217–2223.

Chayaratanasin, P., Moonsom, S., Sakdee, S., Chaisri, U., Katzenmeier, G., Angsuthanasombat, C., 2007. High level of soluble expression in *Escherichia coli* and characterisation of the cloned *Bacillus thuringiensis* Cry4Ba domain III fragment. J. Biochem. Mol. Biol. 40, 58–64.

Chiou, C., Davidson, E.W., Thanabalu, T., Porter, A.G., Allen, J.P., 1999. Crystallization and preliminary X-ray diffraction studies of the 51 kDa protein of the mosquito-larvicidal binary toxin from *Bacillus sphaericus*. Acta Crystallogr. D Biol. Crystallogr. 55, 1083–1085.

Clark, M.A., Baumann, P., 1990. Deletion analysis of the 51-kilodalton protein of the *Bacillus sphaericus* 2362 binary mosquitocidal toxin: construction of derivatives equivalent to the larva-processed toxin. J. Bacteriol. 172, 6759–6763.

Cokmus, C., Davidson, E.W., Cooper, K., 1997. Electrophysiological effects of *Bacillus sphaericus* binary toxin on cultured mosquito cells. J. Invertebr. Pathol. 69, 197–204.

Davidson, E.W., 1988. Binding of the *Bacillus sphaericus* (Eubacteriales: Bacillaceae) toxin to midgut cells of mosquito (Diptera: Culicidae) larvae: relationship to host range. J. Med. Entomol. 25, 151–157.

Davidson, E.W., Oei, C., Meyer, M., Bieber, A.L., Hindley, J., Berry, C., 1990. Interaction of the *Bacillus sphaericus* mosquito larvicidal proteins. Can. J. Microbiol. 36, 870–878.

Elangovan, G., Shanmugavelu, M., Rajamohan, F., Dean, D.H., Jayaraman, K., 2000. Identification of the functional site in the mosquito larvicidal binary toxin of *Bacillus sphaericus* 1593M by site-directed mutagenesis. Biochem. Biophys. Res. Commun. 276, 1048–1055.

Leetachewa, S., Katzenmeier, G., Angsuthanasombat, C., 2006. Novel preparation and characterization of the alpha4-loop-alpha5 membrane-perturbing peptide from the *Bacillus thuringiensis* Cry4Ba delta-endotoxin. J. Biochem. Mol. Biol. 39, 270–277.

Limpanawat, S., Promdonkoy, B., Boonserm, P., 2009. The C-terminal domain of BinA is responsible for *Bacillus sphaericus* binary toxin BinA–BinB interaction. Curr. Microbiol. 59, 509–513.

Mulla, M.S., Thavara, U., Tawatsin, A., Kong-ngamsuk, W., Chompoosri, J., Su, T., 2001. Mosquito larval control with *Bacillus sphaericus*: reduction in adult populations in low-income communities in Nonthaburi Province, Thailand. J. Vector Ecol. 26, 221–231.

Nicolas, L., Nielsen-Leroux, C., Charles, J.F., Delecluse, A., 1993. Respective role of the 42- and 51-kDa components of the *Bacillus sphaericus* toxin overexpressed in *Bacillus thuringiensis*. FEMS Microbiol. Lett. 106, 275–280.

Oei, C., Hindley, J., Berry, C., 1990. An analysis of the genes encoding the 51.4- and 41.9-kDa toxins of *Bacillus sphaericus* 2297 by deletion mutagenesis: the construction of fusion proteins. FEMS Microbiol. Lett. 60, 265–273.

Oei, C., Hindley, J., Berry, C., 1992. Binding of purified *Bacillus sphaericus* binary toxin and its deletion derivatives to *Culex quinquefasciatus* gut: elucidation of functional binding domains. J. Gen. Microbiol. 138, 1515–1526.

Promdonkoy, B., Promdonkoy, P., Audtho, M., Tanapongpipat, S., Chewawiwat, N., Luxananil, P., Panyim, S., 2003. Efficient expression of the mosquito larvicidal binary toxin gene from *Bacillus sphaericus* in *Escherichia coli*. Curr. Microbiol. 47, 383–387.

Promdonkoy, B., Promdonkoy, P., Panyim, S., 2008. High-level expression in *Escherichia coli*, purification and mosquito-larvicidal activity of the binary toxin from *Bacillus sphaericus*. Curr. Microbiol. 57, 626–630.

Rost, B., Sander, C., 1993. Prediction of protein secondary structure at better than 70% accuracy. J. Mol. Biol. 232, 584–599.

Schwartz, J.L., Potvin, L., Coux, F., Charles, J.F., Berry, C., Humphreys, M.J., Jones, A.F., Bernhart, I., Dalla, S.M., Menestrina, G., 2001. Permeabilization of model lipid membranes by *Bacillus sphaericus* mosquitocidal binary toxin and its individual components. J. Membr. Biol. 184, 171–183.

Shanmugavelu, M., Rajamohan, F., Kathirvel, M., Elangovan, G., Dean, D.H., Jayaraman, K., 1998. Functional complementation of nontoxic mutant binary toxins of *Bacillus sphaericus* 1593M generated by site-directed mutagenesis. Appl. Environ. Microbiol. 64, 756–759.

Silva-Filha, M.H., Nielsen-LeRoux, C., Charles, J.F., 1999. Identification of the receptor for *Bacillus sphaericus* crystal toxin in the brush border membrane of the mosquito *Culex pipiens* (Diptera: Culicidae). Insect Biochem. Mol. Biol. 29, 711–721.

Singkhamanan, K., Promdonkoy, B., Chaisri, U., Boonserm, P., 2010. Identification of amino acids required for receptor binding and toxicity of the *Bacillus sphaericus* binary toxin. FEMS Microbiol. Lett. 303, 84–91.

Smith, A.W., Camara-Artigas, A., Allen, J.P., 2004. Crystallization of the mosquito-larvicidal binary toxin produced by *Bacillus sphaericus*. Acta Crystallogr. D Biol. Crystallogr. 60, 952–953.

Smith, A.W., Camara-Artigas, A., Brune, D.C., Allen, J.P., 2005. Implications of high-molecular-weight oligomers of the binary toxin from *Bacillus sphaericus*. J. Invertebr. Pathol. 88, 27–33.

Yuan, Z., Rang, C., Maroun, R.C., Juarez-Perez, V., Frutos, R., Pasteur, N., Vendrely, C., Charles, J.F., Nielsen-Leroux, C., 2001. Identification and molecular structural prediction analysis of a toxicity determinant in the *Bacillus sphaericus* crystal larvicidal toxin. Eur. J. Biochem. 268, 2751–2760.